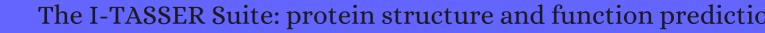
CITATION REPORT List of articles citing



DOI: 10.1038/nmeth.3213 Nature Methods, 2015, 12, 7-8.

Source: https://exaly.com/paper-pdf/61748678/citation-report.pdf

Version: 2024-04-28

This report has been generated based on the citations recorded by exaly.com for the above article. For the latest version of this publication list, visit the link given above.

The third column is the impact factor (IF) of the journal, and the fourth column is the number of citations of the article.

#	Paper	IF	Citations
2244	Classification of the Molecular Defects Associated with Pathogenic Variants of the SLC6A8 Creatine Transporter.		
2243	Comparative Proteomics Enables Identification of Nonannotated Cold Shock Proteins in E. coli.		
2242	StructureStabilityFunction Mechanistic Links in the Anti-Measles Virus Action of Tocopherol-Derivatized Peptide Nanoparticles.		
2241	In Operando Observation of Neuropeptide Capture and Release on Graphene Field-Effect Transistor Biosensors with Picomolar Sensitivity.		
2240	Fast-Acting Small Molecules Targeting Malarial Aspartyl Proteases, Plasmepsins, Inhibit Malaria Infection at Multiple Life Stages.		
2239	•		
2238	Use of a Tyrosine Analogue To Modulate the Two Activities of a Nonheme Iron Enzyme OvoA in Ovothiol Biosynthesis, Cysteine Oxidation versus Oxidative CS Bond Formation.		
2237	Investigation of Solvent Hydron Exchange in the Reaction Catalyzed by the Antibiotic Resistance Protein Cfr.		
2236			
2235	Mutations in the heat-shock protein A9 (HSPA9) gene cause the EVEN-PLUS syndrome of congenital malformations and skeletal dysplasia. 2015 , 5, 17154		45
2234	The C-terminal region of the non-structural protein 2B from Hepatitis A Virus demonstrates lipid-specific viroporin-like activity. 2015 , 5, 15884		15
2233	Substitute sweeteners: diverse bacterial oligosaccharyltransferases with unique N-glycosylation site preferences. 2015 , 5, 15237		31
2232	Antitumor potential of a synthetic interferon-alpha/PLGF-2 positive charge peptide hybrid molecule in pancreatic cancer cells. 2015 , 5, 16975		10
2231	Communication: Entropic measure to prevent energy over-minimization in molecular dynamics simulations. 2015 , 143, 171103		6
2230	Computational and functional analysis of biopharmaceutical drugs in zebrafish: Erythropoietin as a test model. 2015 , 102, 12-21		7
2229	In silico characterisation, homology modelling and structure-based functional annotation of blunt snout bream (Megalobrama amblycephala) Hsp70 and Hsc70 proteins. 2015 , 57, 44		4
2228	Protein Structure and Function Prediction Using I-TASSER. 2015 , 52, 5.8.1-5.8.15		214

(2015-2015)

2227	Direct Measurement of the Radical Translocation Distance in the Class I Ribonucleotide Reductase from Chlamydia trachomatis. 2015 , 119, 13777-84	9
2226	Adult-onset autosomal dominant spastic paraplegia linked to a GTPase-effector domain mutation of dynamin 2. 2015 , 15, 223	30
2225	Comparative studies on manual and automatic backbone chemical shift assignments of 2H/13C/15N-labeled Ube2g1. 2015 , 6,	1
2224	Expression, purification, and functional characterization of the insulin-responsive facilitative glucose transporter GLUT4. 2015 , 24, 2008-19	18
2223	Structure of Ctk3, a subunit of the RNA polymerase II CTD kinase complex, reveals a noncanonical CTD-interacting domain fold. 2015 , 83, 1849-58	4
2222	Characterization of myosin II regulatory light chain isoforms in HeLa cells. 2015 , 72, 609-20	6
2221	The Road to Metagenomics: From Microbiology to DNA Sequencing Technologies and Bioinformatics. 2015 , 6, 348	168
2220	Architecture and roles of periplasmic adaptor proteins in tripartite ellx assemblies. 2015 , 6, 513	41
2219	Giardia fatty acyl-CoA synthetases as potential drug targets. 2015 , 6, 753	5
2218	Diversity of laccase-coding genes in Fusarium oxysporum genomes. 2015 , 6, 933	10
2217	The Ty1 Retrotransposon Restriction Factor p22 Targets Gag. 2015 , 11, e1005571	21
2216	Structural Studies of the HIV-1 Integrase Protein: Compound Screening and Characterization of a DNA-Binding Inhibitor. 2015 , 10, e0128310	14
2215	The Zinc Concentration in the Diet and the Length of the Feeding Period Affect the Methylation Status of the ZIP4 Zinc Transporter Gene in Piglets. 2015 , 10, e0143098	9
2214	Identification and Structural Analysis of Amino Acid Substitutions that Increase the Stability and Activity of Aspergillus niger Glucose Oxidase. 2015 , 10, e0144289	13
2213	VapD in Xylella fastidiosa Is a Thermostable Protein with Ribonuclease Activity. 2015 , 10, e0145765	6
2212	A 14-3-3 Family Protein from Wild Soybean (Glycine Soja) Regulates ABA Sensitivity in Arabidopsis. 2015 , 10, e0146163	15
2211	Identification of B6T173 (ZmPrx35) as the prevailing peroxidase in highly insect-resistant maize (Zea mays, p84C3) kernels by activity-directed purification. 2015 , 6, 670	7
2210	Hydrodynamic Modeling and Its Application in AUC. 2015 , 562, 81-108	5

2209	VP6-SUMO Self-Assembly as Nanocarriers for Gastrointestinal Delivery. 2015 , 2015, 1-7	6
2208	Ltc1 is an ER-localized sterol transporter and a component of ER-mitochondria and ER-vacuole contacts. 2015 , 209, 539-48	177
2207	A recessive homozygous p.Asp92Gly SDHD mutation causes prenatal cardiomyopathy and a severe mitochondrial complex II deficiency. 2015 , 134, 869-79	40
2206	Structure of the voltage-gated calcium channel Cav1.1 complex. 2015 , 350, aad2395	208
2205	Structure of a lectin from the sea mussel Crenomytilus grayanus (CGL). 2015 , 71, 1429-36	12
2204	Acetylation of an NB-LRR Plant Immune-Effector Complex Suppresses Immunity. 2015 , 13, 1670-82	46
2203	Interactions of signaling proteins, growth factors and other proteins with heparan sulfate: mechanisms and mysteries. 2015 , 56, 272-80	92
2202	The barber's pole worm CAP protein superfamilyA basis for fundamental discovery and biotechnology advances. 2015 , 33, 1744-54	12
2201	Functional characterization of two single nucleotide polymorphisms of acyl-coenzyme A:cholesterol acyltransferase 2. 2015 , 566, 236-41	1
2200	Bioinformatical analysis of the sequences, structures and functions of fungal polyketide synthase product template domains. 2015 , 5, 10463	27
2199	ATP-dependent Conformational Changes Trigger Substrate Capture and Release by an ECF-type Biotin Transporter. 2015 , 290, 16929-42	20
2198	Comparative study of the mechanism of action of the antimicrobial peptide gomesin and its linear analogue: The role of the Ehairpin structure. 2015 , 1848, 2414-21	22
2197	Heat Shock Protein 90 Associates with the Per-Arnt-Sim Domain of Heme-free Soluble Guanylate Cyclase: IMplications for Enzyme Maturation. 2015 , 290, 21615-28	18
2196	GPCR-I-TASSER: A Hybrid Approach to G Protein-Coupled Receptor Structure Modeling and the Application to the Human Genome. 2015 , 23, 1538-1549	121
2195	I-TASSER server: new development for protein structure and function predictions. 2015 , 43, W174-81	1059
2194	Molecular properties of diacylglycerol kinase-epsilon in relation to function. 2015 , 192, 100-108	8
2193	Biochemical and Structural Basis for Controlling Chemical Modularity in Fungal Polyketide Biosynthesis. 2015 , 137, 9885-93	44
2192	Structural characterization and evolutionary analysis of fish-specific TLR27. 2015 , 45, 940-5	33

(2015-2015)

2191	GmHs1-1, encoding a calcineurin-like protein, controls hard-seededness in soybean. 2015 , 47, 939-43	51
2190	Solution structure of a soluble fragment derived from a membrane protein by shotgun proteolysis. 2015 , 28, 445-50	2
2189	The origin of specificity and insight into recognition between an aminoacyl carrier protein and its partner ligase. 2015 , 17, 19030-8	3
2188	The mitochondrial unselective channel in Saccharomyces cerevisiae. 2015 , 22, 85-90	6
2187	NMR data-driven structure determination using NMR-I-TASSER in the CASD-NMR experiment. 2015 , 62, 511-25	3
2186	Designing of Complex Multi-epitope Peptide Vaccine Based on Omps of Klebsiella pneumoniae: An In Silico Approach. 2015 , 21, 325-341	30
2185	Commercial potato protein concentrate as a novel source for thermoformed bio-based plastic films with unusual polymerisation and tensile properties. 2015 , 5, 32217-32226	26
2184	Identifying a potential receptor for the antibacterial peptide of sponge Axinella donnani endosymbiont. 2015 , 566, 166-74	3
2183	Autophagy protein Ulk1 promotes mitochondrial apoptosis through reactive oxygen species. 2015 , 89, 311-21	30
2182	Structural and evolutionary characteristics of fish-specific TLR19. 2015 , 47, 271-9	12
2181	Regulation of calreticulin-major histocompatibility complex (MHC) class I interactions by ATP. 2015 , 112, E5608-17	13
2180	Discovery of a Unique Clp Component, ClpF, in Chloroplasts: A Proposed Binary ClpF-ClpS1 Adaptor Complex Functions in Substrate Recognition and Delivery. 2015 , 27, 2677-91	52
2179	Rhizobial peptidase HrrP cleaves host-encoded signaling peptides and mediates symbiotic compatibility. 2015 , 112, 15244-9	64
2178	Mussel adhesion is dictated by time-regulated secretion and molecular conformation of mussel adhesive proteins. 2015 , 6, 8737	104
2177	Molecular Cloning and Characterization of a (Lys)6-Tagged Sulfide-Reactive Hemoglobin I from Lucina pectinata. 2015 , 57, 1050-62	7
2176	Heterozygous RTEL1 mutations are associated with familial pulmonary fibrosis. 2015 , 46, 474-85	96
2175	Glycosylation Analysis of Engineered H3N2 Influenza A Virus Hemagglutinins with Sequentially Added Historically Relevant Glycosylation Sites. 2015 , 14, 3957-69	50
2174	Long-term survival of Borrelia burgdorferi lacking the hibernation promotion factor homolog in the unfed tick vector. 2015 , 83, 4800-10	9

2173	Recombinant expression and predicted structure of parborlysin, a cytolytic protein from the Antarctic heteronemertine Parborlasia corrugatus. 2015 , 108, 32-7	4
2172	Structural and Antimicrobial Features of Peptides Related to Myticin C, a Special Defense Molecule from the Mediterranean Mussel Mytilus galloprovincialis. 2015 , 63, 9251-9	22
2171	A novel mutation in the PAX3 gene causes Waardenburg syndrome type I in an Iranian family. 2015 , 79, 1736-40	9
2170	Transient Kinetic Analysis of Hydrogen Sulfide Oxidation Catalyzed by Human Sulfide Quinone Oxidoreductase. 2015 , 290, 25072-80	44
2169	Genome-Wide Analysis of Oleosin Gene Family in 22 Tree Species: An Accelerator for Metabolic Engineering of BioFuel Crops and Agrigenomics Industrial Applications?. 2015 , 19, 521-41	2
2168	DED or alive: assembly and regulation of the death effector domain complexes. 2015 , 6, e1866	33
2167	The Structure and Interactions of Periplasmic Domains of Crucial MmpL Membrane Proteins from Mycobacterium tuberculosis. 2015 , 22, 1098-107	34
2166	Architecture of the Complex Formed by Large and Small Terminase Subunits from Bacteriophage P22. 2015 , 427, 3285-3299	17
2165	Isolation and Expression Analysis of CYP9A11 and Cytochrome P450 Reductase Gene in the Beet Armyworm (Lepidoptera: Noctuidae). 2015 , 15,	5
2164	Atomistic modeling of a KRT35/KRT85 keratin dimer: folding in aqueous solution and unfolding under tensile load. 2015 , 17, 21880-4	4
2163	Knowledge of Native Protein-Protein Interfaces Is Sufficient To Construct Predictive Models for the Selection of Binding Candidates. 2015 , 55, 2242-55	13
2162	The Glucose Transporter PfHT1 Is an Antimalarial Target of the HIV Protease Inhibitor Lopinavir. 2015 , 59, 6203-9	15
2161	Engineering degrons of yeast ornithine decarboxylase as vehicles for efficient targeted protein degradation. 2015 , 1850, 2452-63	6
2160	Staying green postharvest: how three mutations in the Arabidopsis chlorophyll b reductase gene NYC1 delay degreening by distinct mechanisms. 2015 , 66, 6849-62	23
2159	Structural Bioinformatics Inspection of neXtProt PE5 Proteins in the Human Proteome. 2015 , 14, 3750-61	11
2158	Sinorhizobium meliloti Phage M9 Defines a New Group of T4 Superfamily Phages with Unusual Genomic Features but a Common T=16 Capsid. 2015 , 89, 10945-58	11
2157	Mitochondrial gene order variation in the brachiopod Lingula anatina and its implications for mitochondrial evolution in lophotrochozoans. 2015 , 24 Pt 1, 31-40	16
2156	Fusion of field studies and the laboratory solves a puzzle in antimalarial resistance. 2015 , 112, 11432-3	1

2155	2015, 60, 35-46	42
2154	The Haemoglobins of Algae. 2015 , 67, 177-234	2
2153	Comparative analysis of the mechanisms of sulfur anion oxidation and reduction by dsr operon to maintain environmental sulfur balance. 2015 , 59 Pt A, 177-84	2
2152	Crystal structure of designed PX domain from cytokine-independent survival kinase and implications on evolution-based protein engineering. 2015 , 191, 197-206	9
2151	XLmap: an R package to visualize and score protein structure models based on sites of protein cross-linking. 2016 , 32, 306-8	10
2150	Three-Dimensional Architecture of the L-Type Calcium Channel: Structural Insights into the CaVal Auxiliary Protein. 2016 , 02,	7
2149	Fanconi Anemia Group D2 Protein Participates in Replication Origin Firing. 2016 , 5,	2
2148	A WDR Gene Is a Conserved Member of a Chitin Synthase Gene Cluster and Influences the Cell Wall in Aspergillus nidulans. 2016 , 17,	4
2147	Detection of Jaagsiekte sheep retrovirus in the peripheral blood during the pre-clinical period of ovine pulmonary adenomatosis. 2016 , 15,	6
2146	Bioinformatics analysis of the structural and evolutionary characteristics for toll-like receptor 15. 2016 , 4, e2079	5
2145	Illustrating and homology modeling the proteins of the Zika virus. 2016 , 5, 275	30
2144	Molecular mechanism of thermosensory function of human heat shock transcription factor Hsf1. 2016 , 5,	64
2143	Molecular and Phylogenetic Analysis of Bovine Papillomavirus Type 1: First Report in Iraqi Cattle. 2016 , 2016, 2143024	9
2142	Functional Characterization of the N-Terminal C2 Domain from Phospholipase D and D. 2016 , 2016, 2721719	7
2141	Predicted 3D Model of the Rabies Virus Glycoprotein Trimer. 2016 , 2016, 1674580	12
2140	In Silico Phylogenetic Analysis and Molecular Modelling Study of 2-Haloalkanoic Acid Dehalogenase Enzymes from Bacterial and Fungal Origin. 2016 , 2016, 8701201	6
2139	Extracellular Ribonuclease from (Balifase), a New Member of the N1/T1 RNase Superfamily. 2016 , 2016, 4239375	10
2138	Ribosome R elA structures reveal the mechanism of stringent response activation. 2016 , 5,	99

2137	Identification of HNF4A Mutation p.T130I and HNF1A Mutations p.I27L and p.S487N in a Han Chinese Family with Early-Onset Maternally Inherited Type 2 Diabetes. 2016 , 2016, 3582616	9
2136	A Novel Peptide Thrombopoietin Mimetic Designing and Optimization Using Computational Approach. 2016 , 4, 69	12
2135	Natural Inhibitors of Snake Venom Metalloendopeptidases: History and Current Challenges. 2016 , 8,	18
2134	Structural snapshots of Xer recombination reveal activation by synaptic complex remodeling and DNA bending. 2016 , 5,	6
2133	Dimeric and Trimeric Fusion Proteins Generated with Fimbrial Adhesins of Uropathogenic. 2016 , 6, 135	10
2132	Toll-Like Receptor 2 Mediates In Vivo Pro- and Anti-inflammatory Effects of Mycobacterium Tuberculosis and Modulates Autoimmune Encephalomyelitis. 2016 , 7, 191	13
2131	Development of Monoclonal Antibody and Diagnostic Test for Middle East Respiratory Syndrome Coronavirus Using Cell-Free Synthesized Nucleocapsid Antigen. 2016 , 7, 509	24
2130	Identification of Genes Required for Secretion of the Francisella Oxidative Burst-Inhibiting Acid Phosphatase AcpA. 2016 , 7, 605	2
2129	Phosphorylation Modulates Catalytic Activity of Mycobacterial Sirtuins. 2016 , 7, 677	6
2128	Genetic Selection of Peptide Aptamers That Interact and Inhibit Both Small Protein B and Alternative Ribosome-Rescue Factor A of Aeromonas veronii C4. 2016 , 7, 1228	12
2127	Identification of Genes Involved in Indole-3-Acetic Acid Biosynthesis by PAL5 Strain Using Transposon Mutagenesis. 2016 , 7, 1572	12
2126	EstDZ3: A New Esterolytic Enzyme Exhibiting Remarkable Thermostability. 2016 , 7, 1779	11
2125	Comparative Analysis of Type IV Pilin in. 2016 , 7, 2080	13
2124	Peptides from American alligator plasma are antimicrobial against multi-drug resistant bacterial pathogens including Acinetobacter baumannii. 2016 , 16, 189	16
2123	Limited genetic diversity in the PvK12 Kelch protein in Plasmodium vivax isolates from Southeast Asia. 2016 , 15, 537	10
2122	Alpha Helices Are More Robust to Mutations than Beta Strands. 2016 , 12, e1005242	45
2121	Immunomodulatory and Anti-Inflammatory Activities of Chicken Cathelicidin-2 Derived Peptides. 2016 , 11, e0147919	37
2120	Daboxin P, a Major Phospholipase A2 Enzyme from the Indian Daboia russelii russelii Venom Targets Factor X and Factor Xa for Its Anticoagulant Activity. 2016 , 11, e0153770	20

2119	The Quantum Nature of Drug-Receptor Interactions: Deuteration Changes Binding Affinities for Histamine Receptor Ligands. 2016 , 11, e0154002	32
2118	Predicting Ligand Binding Sites on Protein Surfaces by 3-Dimensional Probability Density Distributions of Interacting Atoms. 2016 , 11, e0160315	13
2117	Static Clathrin Assemblies at the Peripheral Vacuole-Plasma Membrane Interface of the Parasitic Protozoan Giardia lamblia. 2016 , 12, e1005756	33
2116	Functional Update of the Auxiliary Proteins PsbW, PsbY, HCF136, PsbN, TerC and ALB3 in Maintenance and Assembly of PSII. 2016 , 7, 423	30
2115	Moss Pathogenesis-Related-10 Protein Enhances Resistance to Pythium irregulare in Physcomitrella patens and Arabidopsis thaliana. 2016 , 7, 580	16
2114	Over-Expression of the Pikh Gene with a CaMV 35S Promoter Leads to Improved Blast Disease (Magnaporthe oryzae) Tolerance in Rice. 2016 , 7, 773	10
2113	Interactome Mapping Reveals the Evolutionary History of the Nuclear Pore Complex. 2016 , 14, e1002365	64
2112	Molecular Determinants of Mutant Phenotypes, Inferred from Saturation Mutagenesis Data. 2016 , 33, 2960-2975	28
2111	In silico study on anti-Chikungunya virus activity of hesperetin. 2016 , 4, e2602	18
2 110	An Amphiphysin-Like Domain in Fus2p Is Required for Rvs161p Interaction and Cortical Localization. 2015 , 6, 337-49	6
2109	A critical assessment of hidden markov model sub-optimal sampling strategies applied to the generation of peptide 3D models. 2016 , 37, 2006-16	8
2108	Computational modeling of Repeat1 region of INI1/hSNF5: An evolutionary link with ubiquitin. 2016 , 25, 1593-604	1
2107	Computational characterization of TTHA0379: A potential glycerophosphocholine binding protein of Ugp ATP-binding cassette transporter. 2016 , 592, 260-8	9
2106	Molecular basis of substrate recognition and specificity revealed in family 12 glycoside hydrolases. 2016 , 113, 2577-2586	7
2105	Connecting common genetic polymorphisms to protein function: A modular project sequence for lecture or lab. 2016 , 44, 526-536	O
2104	Template-based protein structure prediction in CASP11 and retrospect of I-TASSER in the last decade. 2016 , 84 Suppl 1, 233-46	42
2103	Integration of QUARK and I-TASSER for Ab Initio Protein Structure Prediction in CASP11. 2016 , 84 Suppl 1, 76-86	47
2102	Exploring structure and interactions of the bacterial adaptor protein YjbH by crosslinking mass spectrometry. 2016 , 84, 1234-45	4

2101	Biallelic Mutations in TMEM126B Cause Severe Complex I Deficiency with a Variable Clinical Phenotype. 2016 , 99, 217-27	45
2100	Indoleamine 2,3-dioxygenase: First evidence of expression in rainbow trout (Oncorhynchus mykiss). 2016 , 65, 73-78	18
2099	Competitive Inhibition of Lysine Acetyltransferase 2B by a Small Motif of the Adenoviral Oncoprotein E1A. 2016 , 291, 14363-14372	4
2098	X-ray structure of linalool dehydratase/isomerase from Castellaniella defragrans reveals enzymatic alkene synthesis. 2016 , 590, 1375-83	17
2097	Mapping surface residues of eIF5A that are important for binding to the ribosome using alanine scanning mutagenesis. 2016 , 48, 2363-74	3
2096	Recognizing metal and acid radical ion-binding sites by integrating ab initio modeling with template-based transferals. 2016 , 32, 3260-3269	56
2095	Dual nuclease activity of a Cas2 protein in CRISPR-Cas subtype I-B of Leptospira interrogans. 2016 , 590, 1002-16	19
2094	Design of peptides as inhibitors of human papillomavirus 16 transcriptional regulator E1-E2. 2016 , 88, 475-84	3
2093	A closed conformation of the Caenorhabditis elegans separase-securin complex. 2016 , 6, 160032	9
2092	Development of a group contribution method for estimating free energy of peptides in a dodecane-water system via molecular dynamic simulations. 2016 , 17, 522	1
2091	Succinic anhydride functionalized microcantilevers for protein immobilization and quantification. 2016 , 408, 7917-7926	10
2090	Near-atomic structural model for bacterial DNA replication initiation complex and its functional insights. 2016 , 113, E8021-E8030	25
2089	Evaluating the accuracy of protein design using native secondary sub-structures. 2016 , 17, 353	4
2088	A novel cold-adapted and highly salt-tolerant esterase from Alkalibacterium sp. SL3 from the sediment of a soda lake. 2016 , 6, 19494	37
2087	Construction of the spatial and temporal active protein interaction network for identifying protein complexes. 2016 ,	4
2086	Selective inhibition of apicoplast tryptophanyl-tRNA synthetase causes delayed death in Plasmodium falciparum. 2016 , 6, 27531	25
2085	Engineering of N-Acetyl-L-glutamate kinase from Corynebacterium glutamicum toward improved catalytic efficiency and thermostability. 2016 , 133, S360-S370	1
2084	Rapidly Progressive Frontotemporal Dementia Associated with MAPT Mutation G389R. 2017 , 55, 777-785	9

2083	Evolution of Chemosensory Gene Families in Arthropods: Insight from the First Inclusive Comparative Transcriptome Analysis across Spider Appendages. 2017 , 9, 178-196	31
2082	Geometrical assembly of ultrastable protein templates for nanomaterials. 2016 , 7, 11771	33
2081	Understanding the structural basis of substrate recognition by Plasmodium falciparum plasmepsin V to aid in the design of potent inhibitors. 2016 , 6, 31420	17
2080	An ensemble approach to protein fold classification by integration of template-based assignment and support vector machine classifier. 2017 , 33, 863-870	15
2079	SLC2A8 (GLUT8) is a mammalian trehalose transporter required for trehalose-induced autophagy. 2016 , 6, 38586	65
2078	In-silico analysis of non-synonymous-SNPs of STEAP2: To provoke the progression of prostate cancer. 2016 , 11, 402-416	12
2077	Artemisia annua mutant impaired in artemisinin synthesis demonstrates importance of nonenzymatic conversion in terpenoid metabolism. 2016 , 113, 15150-15155	42
2076	Antibodies from multiple sclerosis patients preferentially recognize hyperglucosylated adhesin of non-typeable Haemophilus influenzae. 2016 , 6, 39430	12
2075	Identification of novel X-linked gain-of-function RPGR-ORF15 mutation in Italian family with retinitis pigmentosa and pathologic myopia. 2016 , 6, 39179	12
2074	Engineering extrinsic disorder to control protein activity in living cells. 2016 , 354, 1441-1444	133
2074	Engineering extrinsic disorder to control protein activity in living cells. 2016 , 354, 1441-1444 Nanobubbles, cavitation, shock waves and traumatic brain injury. 2016 , 18, 32638-32652	133
2073		
2073	Nanobubbles, cavitation, shock waves and traumatic brain injury. 2016 , 18, 32638-32652 PEPlife: A Repository of the Half-life of Peptides. 2016 , 6, 36617	21
2073	Nanobubbles, cavitation, shock waves and traumatic brain injury. 2016 , 18, 32638-32652 PEPlife: A Repository of the Half-life of Peptides. 2016 , 6, 36617 Characterization of DWARF14 Genes in Populus. 2016 , 6, 21593 Ectodomain Architecture Affects Sequence and Functional Evolution of Vertebrate Toll-like	21 76
2073 2072 2071	Nanobubbles, cavitation, shock waves and traumatic brain injury. 2016 , 18, 32638-32652 PEPlife: A Repository of the Half-life of Peptides. 2016 , 6, 36617 Characterization of DWARF14 Genes in Populus. 2016 , 6, 21593 Ectodomain Architecture Affects Sequence and Functional Evolution of Vertebrate Toll-like	21 76 16
2073 2072 2071 2070	Nanobubbles, cavitation, shock waves and traumatic brain injury. 2016, 18, 32638-32652 PEPlife: A Repository of the Half-life of Peptides. 2016, 6, 36617 Characterization of DWARF14 Genes in Populus. 2016, 6, 21593 Ectodomain Architecture Affects Sequence and Functional Evolution of Vertebrate Toll-like Receptors. 2016, 6, 26705 Purification, biochemical characterization and structural modelling of alkali-stable £1,4-xylan	21 76 16
2073 2072 2071 2070 2069	Nanobubbles, cavitation, shock waves and traumatic brain injury. 2016, 18, 32638-32652 PEPlife: A Repository of the Half-life of Peptides. 2016, 6, 36617 Characterization of DWARF14 Genes in Populus. 2016, 6, 21593 Ectodomain Architecture Affects Sequence and Functional Evolution of Vertebrate Toll-like Receptors. 2016, 6, 26705 Purification, biochemical characterization and structural modelling of alkali-stable El,4-xylan xylanohydrolase from Aspergillus fumigatus R1 isolated from soil. 2016, 16, 11 Virus-Like Particles Displaying Recombinant Short-Chain Fragment Region and Interleukin 2 for	21 76 16 23

2065	The defective expression of gtpbp3 related to tRNA modification alters the mitochondrial function and development of zebrafish. 2016 , 77, 1-9	18
2064	WITHDRAWN: Molecular and phylogenetic analysis of bovine papillomavirus type 1: First report in Iraqi cattle. 2016 ,	1
2063	Diverse roles of assembly factors revealed by structures of late nuclear pre-60S ribosomes. 2016 , 534, 133-7	124
2062	Adefovir dipivoxil IA possible regimen for the treatment of dengue virus (DENV) infection. 2016 , 155, 120-127	2
2061	Protein architecture and core residues in unwound ⊞helices provide insights to the transport function of plant AtCHX17. 2016 , 1858, 1983-1998	12
2060	Effect of Silver Nanoparticles Against the Formation of Biofilm by Pseudomonas aeruginosa an In silico Approach. 2016 , 180, 426-437	18
2059	NANS-mediated synthesis of sialic acid is required for brain and skeletal development. 2016 , 48, 777-84	91
2058	Genome-wide mitochondrial DNA sequence variations and lower expression of OXPHOS genes predict mitochondrial dysfunction in oral cancer tissue. 2016 , 37, 11861-11871	9
2057	Cell-based and in silico evidence against quercetin and structurally-related flavonols as activators of vitamin D receptor. 2016 , 163, 59-67	4
2056	conSSert: Consensus SVM Model for Accurate Prediction of Ordered Secondary Structure. 2016 , 56, 455-61	27
2055	Assessment of the utility of contact-based restraints in accelerating the prediction of protein structure using molecular dynamics simulations. 2016 , 25, 19-29	24
2054	The Hevea brasiliensis XIP aquaporin subfamily: genomic, structural and functional characterizations with relevance to intensive latex harvesting. 2016 , 91, 375-96	13
2053	Cloning and characterization of metallothionein gene (HcMT) from Halostachys caspica and its expression in E. coli. 2016 , 585, 221-7	7
2052	Biological effect of LOXL1 coding variants associated with pseudoexfoliation syndrome. 2016 , 146, 212-223	16
2051	Characterization of a type I pullulanase from Anoxybacillus sp. SK3-4 reveals an unusual substrate hydrolysis. 2016 , 100, 6291-6307	14
2050	In-silico analysis and mRNA modulation of detoxification enzymes GST delta and kappa against various biotic and abiotic oxidative stressors. 2016 , 54, 353-63	19
2049	The development and characterization of SDF1& lastin-like-peptide nanoparticles for wound healing. 2016 , 232, 238-47	41
2048	Using iterative fragment assembly and progressive sequence truncation to facilitate phasing and crystal structure determination of distantly related proteins. 2016 , 72, 616-28	9

2047	Crystal Structure of a Two-domain Fragment of Hepatocyte Growth Factor Activator Inhibitor-1: FUNCTIONAL INTERACTIONS BETWEEN THE KUNITZ-TYPE INHIBITOR DOMAIN-1 AND THE NEIGHBORING POLYCYSTIC KIDNEY DISEASE-LIKE DOMAIN. 2016 , 291, 14340-14355	14
2046	Loss of the mitochondrial protein-only ribonuclease P complex causes aberrant tRNA processing and lethality in Drosophila. 2016 , 44, 6409-22	19
2045	The function of the two-pore channel TPC1 depends on dimerization of its carboxy-terminal helix. 2016 , 73, 2565-81	20
2044	Genome-wide identification of the mildew resistance locus O (MLO) gene family in novel cereal model species Brachypodium distachyon. 2016 , 145, 239-253	14
2043	Transcription initiation complex structures elucidate DNA opening. 2016 , 533, 353-8	181
2042	Architecture of the Human Mitochondrial Iron-Sulfur Cluster Assembly Machinery. 2016 , 291, 21296-21321	22
2041	Synthesis and transfer of galactolipids in the chloroplast envelope membranes of Arabidopsis thaliana. 2016 , 113, 10714-9	39
2040	A Recombinant Fungal Chitin Deacetylase Produces Fully Defined Chitosan Oligomers with Novel Patterns of Acetylation. 2016 , 82, 6645-6655	48
2039	A Novel Role for Progesterone Receptor Membrane Component 1 (PGRMC1): A Partner and Regulator of Ferrochelatase. 2016 , 55, 5204-17	51
2038	Proteolytic Activation of Bacillus thuringiensis Cry2Ab through a Belt-and-Braces Approach. 2016 , 64, 7195-200	12
2037	Structural and dynamic insights into the C-terminal extension of cysteine proteinase B from Leishmania amazonensis. 2016 , 70, 30-39	2
2036	Mechanism of action and in vitro activity of short hybrid antimicrobial peptide PV3 against Pseudomonas aeruginosa. 2016 , 479, 103-8	20
2035	Genetic polymorphisms of eNOS (-786T/C, Intron 4b/4a & 894G/T) and its association with asymptomatic first degree relatives of coronary heart disease patients. 2016 , 60, 40-49	9
2034	Stability of an amphipathic helix-hairpin surfactant peptide in liposomes. 2016 , 1858, 3113-3119	9
2033	Is unphosphorylated Rex, as multifunctional protein of HTLV-1, a fully intrinsically disordered protein? An in silico study. 2016 , 8, 14-22	1
2032	Roles of Tetratricopeptide Repeat Proteins in Biogenesis of the Photosynthetic Apparatus. 2016 , 324, 187-227	21
2031	Purification and properties of glycerol-3-phosphate dehydrogenase from the liver of the hibernating ground squirrel, Urocitellus richardsonii. 2016 , 202, 48-55	6
2030	Biochemical Characterization and Low-Resolution SAXS Molecular Envelope of GH1 EGlycosidase from Saccharophagus degradans. 2016 , 58, 777-788	3

2029	Asymmetric cryo-EM structure of the canonical Allolevivirus Qlreveals a single maturation protein and the genomic ssRNA in situ. 2016 , 113, 11519-11524	53
2028	The Chlamydia pneumoniae Adhesin Pmp21 Forms Oligomers with Adhesive Properties. 2016 , 291, 22806-228	3188
2027	Synaptic Vesicle Protein 2A as a Novel Pharmacological Target with Broad Potential for New Antiepileptic Drugs. 2016 , 53-81	
2026	The glycocins: in a class of their own. 2016 , 40, 112-119	37
2025	Characterization of a single-chain variable fragment specific to Cronobacter spp. from hybridoma based on outer membrane protein A. 2016 , 129, 136-143	4
2024	Lasso Peptide Biosynthetic Protein LarB1 Binds Both Leader and Core Peptide Regions of the Precursor Protein LarA. 2016 , 2, 702-709	22
2023	Molecular determinants for CRISPR RNA maturation in the Cas10-Csm complex and roles for non-Cas nucleases. 2017 , 45, 2112-2123	24
2022	In silico designing of some agonists of toll-like receptor 5 as a novel vaccine adjuvant candidates. 2016 , 5, 1	9
2021	Allelic barley MLA immune receptors recognize sequence-unrelated avirulence effectors of the powdery mildew pathogen. 2016 , 113, E6486-E6495	89
2020	Two isoforms of piscidin from Malabar grouper, Epinephelus malabaricus: Expression and functional characterization. 2016 , 57, 222-235	9
2019	Met(104) is the CO-replaceable ligand at Fe(II) heme in the CO-sensing transcription factor BxRcoM-1. 2016 , 21, 559-69	6
2018	Proteome Remodeling in Response to Sulfur Limitation in " Pelagibacter ubique". 2016 , 1,	9
2017	Phage-display screening identifies LMP1-binding peptides targeting the C-terminus region of the EBV oncoprotein. 2016 , 85, 73-79	3
2016	Structure of the catalytic domain of the colistin resistance enzyme MCR-1. 2016 , 14, 81	70
2015	From ZikV genome to vaccine: in silico approach for the epitope-based peptide vaccine against Zika virus envelope glycoprotein. 2016 , 149, 386-399	68
2014	Functional Interaction between the Cytoplasmic ABC Protein LptB and the Inner Membrane LptC Protein, Components of the Lipopolysaccharide Transport Machinery in Escherichia coli. 2016 , 198, 2192-203	15
2013	Structural basis for tRNA modification by Elp3 from Dehalococcoides mccartyi. 2016 , 23, 794-802	43
2012	Identification and functional analysis of a bacteriocin, pyocin S6, with ribonuclease activity from a Pseudomonas aeruginosa cystic fibrosis clinical isolate. 2016 , 5, 413-23	22

2011	Recent advances in sequence-based protein structure prediction. 2017 , 18, 1021-1032	16
2010	Structure-Function Profile of MmpL3, the Essential Mycolic Acid Transporter from Mycobacterium tuberculosis. 2016 , 2, 702-713	54
2009	Biallelic mutations in CYP26B1: A differential diagnosis for Pfeiffer and Antley-Bixler syndromes. 2016 , 170, 2706-10	10
2008	Coagulation Factor XIIIA Subunit Missense Mutations Affect Structure and Function at the Various Steps of Factor XIII Action. 2016 , 37, 1030-41	8
2007	Characterization of a highly toxic strain of Bacillus thuringiensis serovar kurstaki very similar to the HD-73 strain. 2016 , 363,	7
2006	Neisseria gonorrhoeae Crippled Its Peptidoglycan Fragment Permease To Facilitate Toxic Peptidoglycan Monomer Release. 2016 , 198, 3029-3040	15
2005	Deletion of loop fragment adjacent to active site diminishes the stability and activity of exo-inulinase. 2016 , 92, 1234-1241	15
2004	Structure-function relationships of archaeal Cbf5 during in vivo RNA-guided pseudouridylation. 2016 , 22, 1604-19	5
2003	Antibody Production with Synthetic Peptides. 2016 , 1474, 25-47	21
2002	Structure/Function Analysis of Recurrent Mutations in SETD2 Protein Reveals a Critical and Conserved Role for a SET Domain Residue in Maintaining Protein Stability and Histone H3 Lys-36 Trimethylation. 2016 , 291, 21283-21295	41
2001	Protein ligand-specific binding residue predictions by an ensemble classifier. 2016 , 17, 470	12
2000	Heat Shock Proteins and Plants. 2016 ,	5
1999	Down-regulated and Commonly mutated ALPK1 in Lung and Colorectal Cancers. 2016 , 6, 27350	7
1998	The Plastoglobule-Localized Metallopeptidase PGM48 Is a Positive Regulator of Senescence in Arabidopsis thaliana. 2016 , 28, 3020-3037	26
1997	Panel-Based Population Next-Generation Sequencing for Inherited Retinal Degenerations. 2016 , 6, 33248	33
1996	Bi-allelic Mutations in PKD1L1 Are Associated with Laterality Defects in Humans. 2016 , 99, 886-893	42
1995	Membranolytic anticancer peptides. 2016 , 7, 2232-2245	44
1994	Recurrent De Novo and Biallelic Variation of ATAD3A, Encoding a Mitochondrial Membrane Protein, Results in Distinct Neurological Syndromes. 2016 , 99, 831-845	113

Identification and in silico characterization of two novel genes encoding peptidases S8 found by functional screening in a metagenomic library of Yucatī underground water. 2016 , 593, 154-161	19
The NtrY-NtrX two-component system is involved in controlling nitrate assimilation in Herbaspirillum seropedicae strain SmR1. 2016 , 283, 3919-3930	11
1991 The characterization of a novel S100A1 binding site in the N-terminus of TRPM1. 2016 , 78, 186-19	3 5
1990 Quantitative proteomics in Giardia duodenalis-Achievements and challenges. 2016 , 208, 96-112	6
1989 Cryo-EM structure of the spliceosome immediately after branching. 2016 , 537, 197-201	164
1988 The C-terminal sequences of porcine thrombin are active as antimicrobial peptides. 2016 , 88, 905-	914 2
1987 Structure of a yeast activated spliceosome at 3.5 Iresolution. 2016 , 353, 904-11	193
Anin silicoapproach predicted potential therapeutics that can confer protection from maximum pathogenic Hantaviruses. 2016 , 11, 411-428	3
Structural Basis for Recombinatorial Permissiveness in the Generation of Anaplasma marginale Msp2 Antigenic Variants. 2016 , 84, 2740-7	5
1984 Purification and analysis of endogenous human RNA exosome complexes. 2016 , 22, 1467-75	11
Internalization of Heterologous Sugar Transporters by Endogenous Arrestins in the Yeast Saccharomyces cerevisiae. 2016 , 82, 7074-7085	8
1982 Vamana Couples Fat Signaling to the Hippo Pathway. 2016 , 39, 254-266	19
1981 Characterization of a DUF820 family protein Alr3200 of the cyanobacterium sp. strain PCC7120. 2016 , 41, 589-600	4
1980 Structure of the full-length TRPV2 channel by cryo-EM. 2016 , 7, 11130	138
Tuning the anticancer activity of a novel pro-apoptotic peptide using gold nanoparticle platforms. 2016 , 6, 31030	. 50
Genome-Wide Chromatin Immunoprecipitation Sequencing Analysis of the Penicillium chrysogenum Velvet Protein PcVelA Identifies Methyltransferase PcLlmA as a Novel Downstream Regulator of Fungal Development. 2016 , 1,	7
1977 Structural basis of complement membrane attack complex formation. 2016 , 7, 10587	147
1976 Tobacco methyl salicylate esterase mediates nonhost resistance. 2016 , 6, 48-55	

1975	Engineering. 2016 , 55, 12167-12172	9
1974	Application of Bioassay-Guided Fractionation Coupled with a Molecular Approach for the Dereplication of Antimicrobial Metabolites. 2016 , 79, 1625-1642	10
1973	Structural basis for specific self-incompatibility response in Brassica. 2016 , 26, 1320-1329	31
1972	Insights from molecular structure predictions of the infectious bronchitis virus S1 spike glycoprotein. 2016 , 46, 124-129	5
1971	Rangefinder: A Semisynthetic FRET Sensor Design Algorithm. 2016 , 1, 1286-1290	10
1970	Sleeping Beauty transposase structure allows rational design of hyperactive variants for genetic engineering. 2016 , 7, 11126	34
1969	Correcting mitochondrial fusion by manipulating mitofusin conformations. 2016 , 540, 74-79	136
1968	A chimeric protein-based malaria vaccine candidate induces robust T cell responses against Plasmodium vivax MSP1. 2016 , 6, 34527	14
1967	LRFragLib: an effective algorithm to identify fragments for de novo protein structure prediction. 2017 , 33, 677-684	3
1966	Peripheral motor neuropathy is associated with defective kinase regulation of the KCC3 cotransporter. 2016 , 9, ra77	37
1965	Coarse-Grained Simulations of Membrane Insertion and Folding of Small Helical Proteins Using the CABS Model. 2016 , 56, 2207-2215	12
1964	Structural insights into the assembly and regulation of distinct viral capsid complexes. 2016 , 7, 13014	26
1963	ZikaVR: An Integrated Zika Virus Resource for Genomics, Proteomics, Phylogenetic and Therapeutic Analysis. 2016 , 6, 32713	40
1962	Structure of the intact ATM/Tel1 kinase. 2016 , 7, 11655	39
1961	The major Arabidopsis thaliana apurinic/apyrimidinic endonuclease, ARP is involved in the plant nucleotide incision repair pathway. 2016 , 48, 30-42	14
1960	Structural/Functional Properties of Human NFU1, an Intermediate [4Fe-4S] Carrier in Human Mitochondrial Iron-Sulfur Cluster Biogenesis. 2016 , 24, 2080-2091	37
1959	Biochemical evidence for relaxed substrate specificity of N⊞cetyltransferase (Rv3420c/rimI) of Mycobacterium tuberculosis. 2016 , 6, 28892	12
1958	Brain phosphorylation of MeCP2 at serine 164 is developmentally regulated and globally alters its chromatin association. 2016 , 6, 28295	16

1957	Cysteine redox state plays a key role in the inter-domain movements of HMGB1: a molecular dynamics simulation study. 2016 , 6, 100804-100819	5
1956	Evaluation of a synthetic peptide from the Taenia saginata 18kDa surface/secreted oncospheral adhesion protein for serological diagnosis of bovine cysticercosis. 2016 , 164, 463-468	8
1955	Human antibody repertoire after VSV-Ebola vaccination identifies novel targets and virus-neutralizing IgM antibodies. 2016 , 22, 1439-1447	59
1954	Computational Prediction of Protein Secondary Structure from Sequence. 2016 , 86, 2.3.1-2.3.10	6
1953	Design of Heteronuclear Metalloenzymes. 2016 , 580, 501-37	3
1952	A large-scale comparative assessment of methods for residue-residue contact prediction. 2018 , 19, 219-230	20
1951	A cure for the blues: opsin duplication and subfunctionalization for short-wavelength sensitivity in jewel beetles (Coleoptera: Buprestidae). 2016 , 16, 107	28
1950	Phylogenetic distribution of extracellular guanyl-preferring ribonucleases renews taxonomic status of two Bacillus strains. 2016 , 62, 181-8	15
1949	Structural Prediction and Physicochemical Characterization for Mouse Caltrin I and Bovine Caltrin Proteins. 2016 , 10, 225-236	5
1948	CRHunter: integrating multifaceted information to predict catalytic residues in enzymes. 2016 , 6, 34044	8
1947	The C-terminal domain of TPX2 is made of alpha-helical tandem repeats. 2016 , 16, 17	4
1946	Molecular models of human visual pigments: insight into the atomic bases of spectral tuning. 2016 , 12,	
1945	Nitrobindin: An Ubiquitous Family of All Barrel Heme-proteins. 2016 , 68, 423-8	13
1944	Structural characterization of the C-terminal coiled-coil domains of wild-type and kidney disease-associated mutants of apolipoprotein L1. 2016 , 283, 1846-62	19
1943	Regulation of neuronal chloride homeostasis by neuromodulators. 2016 , 594, 2593-605	32
1942	Approaches for Studying the Subcellular Localization, Interactions, and Regulation of Histone Deacetylase 5 (HDAC5). 2016 , 1436, 47-84	3
1941	Another look at the mechanism involving trimeric dUTPases in Staphylococcus aureus pathogenicity island induction involves novel players in the party. 2016 , 44, 5457-69	16
1940	In silico analysis for prediction of degradative capacity of Pseudomonas putida SF1. 2016 , 591, 382-92	20

1939	STRUM: structure-based prediction of protein stability changes upon single-point mutation. 2016 , 32, 2936-46	190
1938	Evolution of Sulfur Binding by Hemoglobin in Siboglinidae (Annelida) with Special Reference to Bone-Eating Worms, Osedax. 2016 , 82, 219-29	2
1937	Effect of linker length and residues on the structure and stability of a fusion protein with malaria vaccine application. 2016 , 76, 24-9	47
1936	Analysis of the structure, evolution, and expression of CD24, an important regulator of cell fate. 2016 , 590, 324-37	14
1935	Conformation Transitions of Recombinant Spidroins via Integration of Time-Resolved FTIR Spectroscopy and Molecular Dynamic Simulation. 2016 , 2, 1298-1308	17
1934	Coarse-Grained Protein Models and Their Applications. 2016 , 116, 7898-936	489
1933	Multidimensional structure-function relationships in human Etardiac myosin from population-scale genetic variation. 2016 , 113, 6701-6	68
1932	Sequence identification, structure prediction and validation of tannase from Aspergillusniger N5-5. 2016 , 27, 1087-1090	3
1931	Endocrine disruption by Bisphenol A, polychlorinated biphenyls and polybrominated diphenyl ether, in zebra fish (Danio rerio) model: an in silico approach. 2016 , 42, 1541-1555	5
1930	Heme-bound SiaA from Streptococcus pyogenes: Effects of mutations and oxidation state on protein stability. 2016 , 158, 99-109	3
1929	Binding of a proline-independent hydrophobic motif by the Candida albicans Rvs167-3 SH3 domain. 2016 , 190, 27-36	6
1928	Molecular diagnosis of 65 families with mucopolysaccharidosis type II (Hunter syndrome) characterized by 16 novel mutations in the IDS gene: Genetic, pathological, and structural studies on iduronate-2-sulfatase. 2016 , 118, 190-197	37
1927	Gender differences in white matter pathology and mitochondrial dysfunction in Alzheimer's disease with cerebrovascular disease. 2016 , 9, 27	45
1926	Discovery of a tyrosine-rich sporocyst wall protein in Eimeria tenella. 2016 , 9, 124	8
1925	Novel function discovery through sequence and structural data mining. 2016 , 38, 53-61	22
1924	Illuminating structural proteins in viral "dark matter" with metaproteomics. 2016 , 113, 2436-41	49
1923	Proteome-wide covalent ligand discovery in native biological systems. 2016 , 534, 570-4	406
1922	Camphor-based CCR5 blocker lead compounds 🗈 computational and experimental approach. 2016 , 6, 56249-56259	4

1921	Molecular dynamic study of MlaC protein in Gram-negative bacteria: conformational flexibility, solvent effect and protein-phospholipid binding. 2016 , 25, 1430-7	15
1920	XacFhaB adhesin, an important Xanthomonas citri ssp. citri virulence factor, is recognized as a pathogen-associated molecular pattern. 2016 , 17, 1344-1353	7
1919	The evolution of substrate specificity-associated residues and Ca(2+) -binding motifs in EF-hand-containing type II NAD(P)H dehydrogenases. 2016 , 157, 338-51	7
1918	Hepatocyte Factor JMJD5 Regulates Hepatitis B Virus Replication through Interaction with HBx. 2016 , 90, 3530-42	22
1917	Key role of Dkk3 protein in inhibition of cancer cell proliferation: An in silico identification. 2016 , 393, 98-104	32
1916	c.376G>A mutation in WFS1 gene causes Wolfram syndrome without deafness. 2016 , 59, 65-9	6
1915	Structure-based binding between protein farnesyl transferase and PRL-PTP of malaria parasite: an interaction study of prenylation process in Plasmodium. 2016 , 34, 2667-2678	3
1914	CPPsite 2.0: a repository of experimentally validated cell-penetrating peptides. 2016 , 44, D1098-103	167
1913	Identification, characterization, and expression of diacylgylcerol acyltransferase type-1 from Chlorella vulgaris. 2016 , 13, 167-181	5
1912	Emergence of plasmid-mediated colistin resistance mechanism MCR-1 in animals and human beings in China: a microbiological and molecular biological study. 2016 , 16, 161-8	2954
1912 1911		2954 27
	in China: a microbiological and molecular biological study. 2016 , 16, 161-8 First independent replication of the involvement of LARS2 in Perrault syndrome by whole-exome sequencing of an Italian family. 2016 , 61, 295-300 The human iron exporter ferroportin. Insight into the transport mechanism by molecular modeling.	
1911	in China: a microbiological and molecular biological study. 2016 , 16, 161-8 First independent replication of the involvement of LARS2 in Perrault syndrome by whole-exome sequencing of an Italian family. 2016 , 61, 295-300 The human iron exporter ferroportin. Insight into the transport mechanism by molecular modeling. 2016 , 12, 1-7	27
1911 1910	in China: a microbiological and molecular biological study. 2016 , 16, 161-8 First independent replication of the involvement of LARS2 in Perrault syndrome by whole-exome sequencing of an Italian family. 2016 , 61, 295-300 The human iron exporter ferroportin. Insight into the transport mechanism by molecular modeling. 2016 , 12, 1-7	27
1911 1910 1909	in China: a microbiological and molecular biological study. 2016 , 16, 161-8 First independent replication of the involvement of LARS2 in Perrault syndrome by whole-exome sequencing of an Italian family. 2016 , 61, 295-300 The human iron exporter ferroportin. Insight into the transport mechanism by molecular modeling. 2016 , 12, 1-7 SATPdb: a database of structurally annotated therapeutic peptides. 2016 , 44, D1119-26 Interaction of the RcsB Response Regulator with Auxiliary Transcription Regulators in Escherichia	27 3 89
1911 1910 1909	in China: a microbiological and molecular biological study. 2016, 16, 161-8 First independent replication of the involvement of LARS2 in Perrault syndrome by whole-exome sequencing of an Italian family. 2016, 61, 295-300 The human iron exporter ferroportin. Insight into the transport mechanism by molecular modeling. 2016, 12, 1-7 SATPdb: a database of structurally annotated therapeutic peptides. 2016, 44, D1119-26 Interaction of the RcsB Response Regulator with Auxiliary Transcription Regulators in Escherichia coli. 2016, 291, 2357-70 Synthesis of rebaudioside A from stevioside and their interaction model with hTAS2R4 bitter taste receptor. 2016, 125, 106-11 The Pseudomonas aeruginosa PAO1 Two-Component Regulator CarSR Regulates Calcium	27 3 89 35
1911 1910 1909 1908	in China: a microbiological and molecular biological study. 2016 , 16, 161-8 First independent replication of the involvement of LARS2 in Perrault syndrome by whole-exome sequencing of an Italian family. 2016 , 61, 295-300 The human iron exporter ferroportin. Insight into the transport mechanism by molecular modeling. 2016 , 12, 1-7 SATPdb: a database of structurally annotated therapeutic peptides. 2016 , 44, D1119-26 Interaction of the RcsB Response Regulator with Auxiliary Transcription Regulators in Escherichia coli. 2016 , 291, 2357-70 Synthesis of rebaudioside A from stevioside and their interaction model with hTAS2R4 bitter taste receptor. 2016 , 125, 106-11 The Pseudomonas aeruginosa PAO1 Two-Component Regulator CarSR Regulates Calcium Homeostasis and Calcium-Induced Virulence Factor Production through Its Regulatory Targets	273893525

1903	Assessment of goat milk-derived potential probiotic L. lactis AMD17 and its application for preparation of dahi using honey. 2016 , 66, 1217-1228	4
1902	Characterization and Structural Insights into Selective E1-E2 Interactions in the Human and Plasmodium falciparum SUMO Conjugation Systems. 2016 , 291, 3860-70	12
1901	KRAS insertion mutations are oncogenic and exhibit distinct functional properties. 2016 , 7, 10647	10
1900	Dissecting the peripheral stalk of the mitochondrial ATP synthase of chlorophycean algae. 2016 , 1857, 1183-1190	13
1899	Vestiges of Ent3p/Ent5p function in the giardial epsin homolog. 2016 , 1863, 749-59	2
1898	Gene dosage effects and signatures of purifying selection in lateral organ boundaries domain (LBD) genes LBD1 and LBD18. 2016 , 302, 433-445	3
1897	Structural characterization of ANGPTL8 (betatrophin) with its interacting partner lipoprotein lipase. 2016 , 61, 210-20	23
1896	The Type 2 dUTPase of Bacteriophage ?NM1 Initiates Mobilization of Staphylococcus aureus Bovine Pathogenicity Island 1. 2016 , 428, 142-152	16
1895	In-silico analysis of Pasteurella multocida to identify common epitopes between fowl, goat and buffalo. 2016 , 580, 58-66	3
1894	Efficient Restoration of the Dystrophin Gene Reading Frame and Protein Structure in DMD Myoblasts Using the CinDel Method. 2016 , 5, e283	58
1893	Expression and characterization of a barley phosphatidylinositol transfer protein structurally homologous to the yeast Sec14p protein. 2016 , 246, 98-111	4
1892	Design, structure prediction and molecular dynamics simulation of a fusion construct containing malaria pre-erythrocytic vaccine candidate, PfCelTOS, and human interleukin 2 as adjuvant. 2016 , 17, 71	19
1891	Structural and Functional Significance of the N- and C-Terminal Appendages in Arabidopsis Truncated Hemoglobin. 2016 , 55, 1724-40	7
1890	Design, synthesis and activity evaluation of novel peptide fusion inhibitors targeting HIV-1 gp41. 2016 , 24, 201-6	6
1889	Dissecting the Role of E2 Protein Domains in Alphavirus Pathogenicity. 2015 , 90, 2418-33	17
1888	Hfq: a multifaceted RNA chaperone involved in virulence. 2016 , 11, 137-51	28
1887	Substrate Selectivity of Lysophospholipid Transporter LplT Involved in Membrane Phospholipid Remodeling in Escherichia coli. 2016 , 291, 2136-49	22
1886	Recurrent Mutations of Chromatin-Remodeling Genes and Kinase Receptors in Pheochromocytomas and Paragangliomas. 2016 , 22, 2301-10	94

1885	Choosing the Optimal Rigid Receptor for Docking and Scoring in the CSAR 2013/2014 Experiment. 2016 , 56, 1004-12	17
1884	Rational design of mirror-like peptides with alanine regulation. 2016 , 48, 403-17	14
1883	Modulation of Mitochondrial Antiviral Signaling by Human Herpesvirus 8 Interferon Regulatory Factor 1. 2016 , 90, 506-20	20
1882	3DRobot: automated generation of diverse and well-packed protein structure decoys. 2016 , 32, 378-87	87
1881	The complement of family M1 aminopeptidases of Haemonchus contortusBiotechnological implications. 2016 , 34, 65-76	6
1880	A novel homozygous truncating GNAT1 mutation implicated in retinal degeneration. 2016 , 100, 495-500	20
1879	Proteomic Tools for the Analysis of Cytoskeleton Proteins. 2016 , 1365, 385-413	
1878	Preface. 2016 , 1365, v-vi	3
1877	Amino acid residues adjacent to the catalytic cavity of tetramer L-asparaginase II contribute significantly to its catalytic efficiency and thermostability. 2016 , 82, 15-22	22
1876	In silico analysis suggests that PH0702 and PH0208 encode for methylthioribose-1-phosphate isomerase and ribose-1,5-bisphosphate isomerase, respectively, rather than aIF2BIand aIF2BI 2016 , 575, 118-26	6
1875	Structural Insights into KCTD Protein Assembly and Cullin3 Recognition. 2016 , 428, 92-107	28
1874	Discovery of Selective Histone Deacetylase 6 Inhibitors Using the Quinazoline as the Cap for the Treatment of Cancer. 2016 , 59, 1455-70	59
1873	Plasmodium actin is incompletely folded by heterologous protein-folding machinery and likely requires the native Plasmodium chaperonin complex to enter a mature functional state. 2016 , 30, 405-16	17
1872	ResQ: An Approach to Unified Estimation of B-Factor and Residue-Specific Error in Protein Structure Prediction. 2016 , 428, 693-701	76
1871	Functional expression and purification of Anabaena PCC 7120 XisA protein. 2016 , 118, 64-9	1
1870	FALCON@home: a high-throughput protein structure prediction server based on remote homologue recognition. 2016 , 32, 462-4	25
1869	PLD3 in Alzheimer's Disease: a Modest Effect as Revealed by Updated Association and Expression Analyses. 2016 , 53, 4034-4045	24
1868	Glutathione Is the Resolving Thiol for Thioredoxin Peroxidase Activity of 1-Cys Peroxiredoxin Without Being Consumed During the Catalytic Cycle. 2016 , 24, 115-28	34

1867	Genome-Wide Identification and Comparative Analysis of Copper Transporter Genes in Plants. 2017 , 9, 278-291	8
1866	New Insights into Cooperative Binding of Homeodomain Transcription Factors PREP1 and PBX1 to DNA. 2017 , 7, 40665	6
1865	Expression and characterization of recombinant chicken mannose binding lectin. 2017 , 222, 518-528	11
1864	Mutations in ATP6V1E1 or ATP6V1A Cause Autosomal-Recessive Cutis Laxa. 2017 , 100, 216-227	58
1863	Side chain flexibility and coupling between the S4-S5 linker and the TRP domain in thermo-sensitive TRP channels: Insights from protein modeling. 2017 , 85, 630-646	2
1862	In silico characterization of TTHA0596: A potential Zn 2+ binding protein of ATP-binding cassette transporter. 2017 , 6, 132-141	2
1861	STRUCTURE-FUNCTION STUDIES OF THE ALPHA PHEROMONE RECEPTOR FROM YEAST. 2017 , 20, 16-26	3
1860	SMCHD1 mutations associated with a rare muscular dystrophy can also cause isolated arhinia and Bosma arhinia microphthalmia syndrome. 2017 , 49, 238-248	88
1859	Kobuviral Non-structural 3A Proteins Act as Molecular Harnesses to Hijack the Host ACBD3 Protein. 2017 , 25, 219-230	28
1858	Structural pierce into molecular mechanism underlying Clostridium perfringens Epsilon toxin function. 2017 , 127, 90-99	20
1857	HAP2/GCS1 is a gamete fusion protein homologous to somatic and viral fusogens. 2017, 216, 571-581	59
1856	RNA-Puzzles Round III: 3D RNA structure prediction of five riboswitches and one ribozyme. 2017 , 23, 655-672	118
1855	Identification of a Novel Epoxyqueuosine Reductase Family by Comparative Genomics. 2017, 12, 844-851	27
1854	The expression of hypoxia-inducible factor-1 gene is not affected by low-oxygen conditions in yellow perch (Perca flavescens) juveniles. 2017 , 43, 849-862	10
1853	Cathelicidin antimicrobial peptide from Alligator mississippiensis has antibacterial activity against multi-drug resistant Acinetobacter baumanii and Klebsiella pneumoniae. 2017 , 70, 135-144	29
1852	Molecular Engineering of Enzymes. 2017 , 47-80	
1851	AKT1, LKB1, and YAP1 Revealed as MYC Interactors with NanoLuc-Based Protein-Fragment Complementation Assay. 2017 , 91, 339-347	17
1850	Genetic diagnosis and treatment of a Chinese ketosis-prone MODY 3 family with depression. 2017 , 9, 5	6

1849	Bactericidal activity of fish galectin 4 derived membrane-binding peptide tagged with oligotryptophan. 2017 , 71, 37-48	22
1848	Plasmodium malariae and P. ovale genomes provide insights into malaria parasite evolution. 2017 , 542, 101-104	99
1847	Ligand binding pocket of a novel Allatostatin receptor type C of stick insect, Carausius morosus. 2017 , 7, 41266	6
1846	A de novo deletion mutation in SOX10 in a Chinese family with Waardenburg syndrome type 4. 2017 , 7, 41513	4
1845	Proteoform Profile Mapping of the Human Serum Complement Component C9 Revealing Unexpected New Features of N-, O-, and C-Glycosylation. 2017 , 89, 3483-3491	33
1844	HIV Tat protein and amyloid-peptide form multifibrillar structures that cause neurotoxicity. 2017 , 24, 379-386	49
1843	Vicinal diaryl azole-based urea derivatives as potential cholesterol lowering agents acting through inhibition of SOAT enzymes. 2017 , 130, 107-123	8
1842	Conserved Ankyrin Repeat Proteins and Their NIMA Kinase Partners Regulate Extracellular Matrix Remodeling and Intracellular Trafficking in Caenorhabditis elegans. 2017 , 205, 273-293	10
1841	Analysis of plant UDP-arabinopyranose mutase (UAM): Role of divalent metals and structure prediction. 2017 , 1865, 510-519	2
1840	Phylogenetics: Tertiary protein structures needed. 2017 , 1, 80	2
1839	Conformational Profiling of the AT1 Angiotensin II Receptor Reflects Biased Agonism, G Protein Coupling, and Cellular Context. 2017 , 292, 5443-5456	54
1838	The importance of the non-active site and non-periodical structure located histidine residue respect to the structure and function of exo-inulinase. 2017 , 98, 542-549	12
1837	Trichoderma reesei xylanase 5 is defective in the reference strain QM6a but functional alleles are present in other wild-type strains. 2017 , 101, 4139-4149	7
1836	Myosin B of Plasmodium falciparum (PfMyoB): in silico prediction of its three-dimensional structure and its possible interaction with MTIP. 2017 , 116, 1373-1382	2
1835	A putative Toll/interleukin-1 receptor domain protein from Helicobacter pylori is dimeric in solution and interacts with human Toll-like receptor adaptor myeloid differentiation primary response 88. 2017 , 61, 85-91	2
1834	An in silico approach for characterization of encoded protein from Rdr1, a black spot resistance gene in Rosa multiflora. 2017 , 124, 319-330	1
1833	Modulation of LAT1 (SLC7A5) transporter activity and stability by membrane cholesterol. 2017 , 7, 43580	45
1832	Computational Prediction of Usutu Virus E Protein B Cell and T Cell Epitopes for Potential Vaccine Development. 2017 , 85, 350-364	5

1831	Extracellular proteasome-osteopontin circuit regulates cell migration with implications in multiple sclerosis. 2017 , 7, 43718	29
1830	Genetic variability in E6, E7 and L1 genes of Human Papillomavirus 62 and its prevalence in Mexico. 2017 , 12, 15	6
1829	A family 13 thioesterase isolated from an activated sludge metagenome: Insights into aromatic compounds metabolism. 2017 , 85, 1222-1237	5
1828	Metal ions and phosphatidylinositol 4,5-bisphosphate as interacting effectors of ⊞ype plant phospholipase D. 2017 , 138, 57-64	3
1827	Identifying different transcribed proteins in the newly described Theraphosidae Pamphobeteus verdolaga. 2017 , 129, 81-88	4
1826	In-silico screening, identification and validation of a novel vaccine candidate in the fight against Plasmodium falciparum. 2017 , 116, 1293-1305	7
1825	In silico design of an immunogen against Acinetobacter baumannii based on a novel model for native structure of Outer membrane protein A. 2017 , 105, 201-210	34
1824	The vaccinia virus DNA polymerase and its processivity factor. 2017 , 234, 193-206	22
1823	Loss-of-Function Mutations in KIF15 Underlying a Braddock-Carey Genocopy. 2017 , 38, 507-510	6
1822	Theoretical analysis of somatostatin receptor 5 with antagonists and agonists for the treatment of neuroendocrine tumors. 2017 , 21, 367-384	3
1821	The first description of a hormone-sensitive lipase from a basidiomycete: Structural insights and biochemical characterization revealed Bjerkandera adusta BaEstB as a novel esterase. 2017 , 6, e00463	11
1820	Prediction of GCRV virus-host protein interactome based on structural motif-domain interactions. 2017 , 18, 145	30
1819	Nmd3 is a structural mimic of eIF5A, and activates the cpGTPase Lsg1 during 60S ribosome biogenesis. 2017 , 36, 854-868	46
1818	Impact of ERG3 mutations and expression of ergosterol genes controlled by UPC2 and NDT80 in Candida parapsilosis azole resistance. 2017 , 23, 575.e1-575.e8	26
1817	Heme Assimilation in Requires Cell-surface-anchored Protein Shu1 and Vacuolar Transporter Abc3. 2017 , 292, 4898-4912	18
1816	Open-ringed structure of the Cdt1-Mcm2-7 complex as a precursor of the MCM double hexamer. 2017 , 24, 300-308	56
1815	Chikungunya virus nsP4 RNA-dependent RNA polymerase core domain displays detergent-sensitive primer extension and terminal adenylyltransferase activities. 2017 , 143, 38-47	31
1814	Impairment of infectious laryngotracheitis virus replication by deletion of the UL[-1] gene. 2017 , 162, 1541-1548	3

1813	Molecular dynamics simulations of early steps in RNA-mediated conversion of prions. 2017, 26, 1524-1534	7
1812	Three new piscidins from orange-spotted grouper (Epinephelus coioides): Phylogeny, expression and functional characterization. 2017 , 66, 240-253	18
1811	Lysibodies are IgG Fc fusions with lysin binding domains targeting wall carbohydrates for effective phagocytosis. 2017 , 114, 4781-4786	15
1810	In-Silico Drug discovery approach targeting receptor tyrosine kinase-like orphan receptor 1 for cancer treatment. 2017 , 7, 1029	10
1809	Mroh1, a lysosomal regulator localized by WASH-generated actin. 2017 , 130, 1785-1795	5
1808	The Lon protease-like domain in the bacterial RecA paralog RadA is required for DNA binding and repair. 2017 , 292, 9801-9814	10
1807	Two glycosaminoglycan-binding domains of the mouse cytomegalovirus-encoded chemokine MCK-2 are critical for oligomerization of the full-length protein. 2017 , 292, 9613-9626	3
1806	Single amino acid substitutions in the selectivity filter render NbXIP1;1 dquaporin water permeable. 2017 , 17, 61	7
1805	Comparative Protein Structure Modelling. 2017 , 91-134	6
1804	Derepression of SaPIbov1 Is Independent of NM1 Type 2 dUTPase Activity and Is Inhibited by dUTP and dUMP. 2017 , 429, 1570-1580	4
1803	Intermolecular Interactions Between DM\(\hat{\text{B}}\) nd DM\(\hat{\text{Proteins}}\) in BuLA-DM Complex of Water Buffalo Bubalus bubalis. 2017 , 118, 4254-4266	1
1802	COFACTOR: improved protein function prediction by combining structure, sequence and protein-protein interaction information. 2017 , 45, W291-W299	235
1801	Structures of closed and open conformations of dimeric human ATM. 2017 , 3, e1700933	63
1800	Giardia duodenalis Rad52 protein: biochemical characterization and response upon DNA damage. 2017 , 162, 123-135	3
1799	Insights in luteovirid structural biology guided by chemical cross-linking and high resolution mass spectrometry. 2017 , 241, 42-52	12
1798	A Naturally Occurring Recombinant Enterovirus Expresses a Torovirus Deubiquitinase. 2017 , 91,	29
1797	Insights into the catalysis of a lysine-tryptophan bond in bacterial peptides by a SPASM domain radical -adenosylmethionine (SAM) peptide cyclase. 2017 , 292, 10835-10844	13
1796	Expression, immunogenicity and variation of iron-regulated surface protein A from bovine isolates of Staphylococcus aureus. 2017 , 364,	6

1795	Functional differentiation of 3-ketosteroid Edehydrogenase isozymes in Rhodococcus ruber strain Chol-4. 2017 , 16, 42	19
1794	Class III Histidine Kinases: a Recently Accessorized Kinase Domain in Putative Modulators of Type IV Pilus-Based Motility. 2017 , 199,	4
1793	The myosin mesa and the basis of hypercontractility caused by hypertrophic cardiomyopathy mutations. 2017 , 24, 525-533	101
1792	Computational study of the competitive binding of valproic acid glucuronide and carbapenem antibiotics to acylpeptide hydrolase. 2017 , 32, 201-207	2
1791	Computational design of ligand-binding membrane receptors with high selectivity. 2017 , 13, 715-723	24
1790	Maintenance of neural activities in torpid Rhinolophus ferrumequinum bats revealed by 2D gel-based proteome analysis. 2017 , 1865, 1004-1019	4
1789	Evolution, structure and membrane association of NDUFAF6, an assembly factor for NADH:ubiquinone oxidoreductase (Complex I). 2017 , 35, 13-22	6
1788	Camelus dromedarius glucose transporter 4: in silico analysis, cloning, expression, purification and characterisation in E. coli. 2017 , 123, 254-264	
1787	Understanding human thiol dioxygenase enzymes: structure to function, and biology to pathology. 2017 , 98, 52-66	17
1786	Isolation, cloning, and characterization of a cuticle collagen gene, Mi-col-5, in Meloidogyne incognita. 2017 , 7, 64	3
1785	Differential Coupling of Binding, ATP Hydrolysis, and Transport of Fluorescent Probes with P-Glycoprotein in Lipid Nanodiscs. 2017 , 56, 2506-2517	14
1784	Mechanistic and structural basis of bioengineered bovine Cathelicidin-5 with optimized therapeutic activity. 2017 , 7, 44781	9
1783	The first report on transcriptome analysis of the venom gland of Iranian scorpion, Hemiscorpius lepturus. 2017 , 125, 123-130	32
1782	Biosensor-assisted transcriptional regulator engineering for Methylobacterium extorquens AM1 to improve mevalonate synthesis by increasing the acetyl-CoA supply. 2017 , 39, 159-168	31
1781	An Evolution-Based Approach to De Novo Protein Design. 2017 , 1529, 243-264	9
1780	The Shigella Virulence Factor IcsA Relieves N-WASP Autoinhibition by Displacing the Verprolin Homology/Cofilin/Acidic (VCA) Domain. 2017 , 292, 134-145	10
1779	Analysis of an ADTKD family with a novel frameshift mutation in MUC1 reveals characteristic features of mutant MUC1 protein. 2017 , 32, 2010-2017	17
1778	Identification and characterization of a biosynthetic gene cluster for tryptophan dimers in deep sea-derived Streptomyces sp. SCSIO 03032. 2017 , 101, 6123-6136	13

1777	Polymerase Enteracting Protein 2: A Multifunctional Protein. 2017, 69, 335-342	19
1776	The group II intron maturase: a reverse transcriptase and splicing factor go hand in hand. 2017 , 47, 30-39	16
1775	PSA3, a Protein on the Stromal Face of the Thylakoid Membrane, Promotes Photosystem I Accumulation in Cooperation with the Assembly Factor PYG7. 2017 , 174, 1850-1862	15
1774	A single nucleotide polymorphism in COQ9 affects mitochondrial and ovarian function and fertility in Holstein cows. 2017 , 96, 652-663	23
1773	A D53 repression motif induces oligomerization of TOPLESS corepressors and promotes assembly of a corepressor-nucleosome complex. 2017 , 3, e1601217	40
1772	A novel HIV-1 gp41 tripartite model for rational design of HIV-1 fusion inhibitors with improved antiviral activity. 2017 , 31, 885-894	24
1771	The first acidobacterial laccase-like multicopper oxidase revealed by metagenomics shows high salt and thermo-tolerance. 2017 , 101, 6261-6276	40
1770	Solution structure of human steroidogenic acute regulatory protein STARD1 studied by small-angle X-ray scattering. 2017 , 489, 445-450	6
1769	Structure of the Human Lipid Exporter ABCA1. 2017, 169, 1228-1239.e10	152
1768	Display of B. pumilus chitinase on the surface of B. subtilis spore as a potential biopesticide. 2017 , 140, 17-23	17
1767	Identification of epitopes on nonstructural protein 7 of porcine reproductive and respiratory syndrome virus recognized by monoclonal antibodies using phage-display technology. 2017 , 53, 623-635	2
1766	Systems-wide Studies Uncover Commander, a Multiprotein Complex Essential to Human Development. 2017 , 4, 483-494	23
1765	Cryo-EM structure of the activated GLP-1 receptor in complex with a G protein. 2017, 546, 248-253	344
1764	Structure-based prediction of Wnt binding affinities for Frizzled-type cysteine-rich domains. 2017 , 292, 11218-11229	21
1763	A Glycosylphosphatidylinositol-Anchored Carbonic Anhydrase-Related Protein of Is Important for Rhoptry Biogenesis and Virulence. 2017 , 2,	16
1762	Continuous fast Fourier transforms cyclic voltammetry as a new approach for investigation of skim milk k-casein proteolysis, a comparative study. 2017 , 103, 972-977	2
1761	Activity modulation of the oligopeptidase B from Serratia proteamaculans by site-directed mutagenesis of amino acid residues surrounding catalytic triad histidine. 2017 , 139, 125-136	14
1760	Design of Surfactant Protein B Peptide Mimics Based on the Saposin Fold for Synthetic Lung Surfactants. 2016 , 1,	18

1759	Whipworm kinomes reflect a unique biology and adaptation to the host animal. 2017, 47, 857-866	9
1758	Model-based structural and functional characterization of the Rice stripe tenuivirus nucleocapsid protein interacting with viral genomic RNA. 2017 , 506, 73-83	6
1757	Redesigning pH optimum of Geobacillus sp. TF16 endoxylanase through in silico designed DNA swapping strategy. 2017 , 137, 174-189	2
1756	Identification of functional SNPs in human LGALS3 gene by in silico analyses. 2017 , 18, 321-328	8
1755	Machine Learning of Global Phosphoproteomic Profiles Enables Discrimination of Direct versus Indirect Kinase Substrates. 2017 , 16, 786-798	20
1754	A newly identified amino acid substitution T123I in the 14Hdemethylase (Erg11p) of Candida albicans confers azole resistance. 2017 , 17,	14
1753	Calcium regulation of the human mitochondrial ATP-Mg/Pi carrier SLC25A24 uses a locking pin mechanism. 2017 , 7, 45383	23
1752	New advances in probing cell-extracellular matrix interactions. 2017 , 9, 383-405	40
1751	Characterization of two novel bacterial type A exo-chitobiose hydrolases having C-terminal 5/12-type carbohydrate-binding modules. 2017 , 101, 4533-4546	5
1750	Atomistic Study of Intramolecular Interactions in the Closed-State Channelrhodopsin Chimera, C1C2. 2017 , 112, 943-952	17
1749	Production of low-expressing recombinant cationic biopolymers with high purity. 2017 , 134, 11-17	5
1748	A rare case of plastid protein-coding gene duplication in the chloroplast genome of Euglena archaeoplastidiata (Euglenophyta). 2017 , 53, 493-502	4
1747	Nuclear Magnetic Resonance Structure of the Human Polyoma JC Virus Agnoprotein. 2017 , 118, 3268-3280	7
1746	Cell adhesion pattern created by OSTE polymers. 2017 , 9, 025006	5
1745	Structural modeling of human organic cation transporters. 2017 , 68, 153-163	25
1744	Optimized protocol for soluble prokaryotic expression, purification and structural analysis of human placenta specific-1(PLAC1). 2017 , 133, 139-151	10
1743	Nidovirus RNA polymerases: Complex enzymes handling exceptional RNA genomes. 2017 , 234, 58-73	69
1742	Attenuation of Phosphorylation-dependent Activation of Cystic Fibrosis Transmembrane Conductance Regulator (CFTR) by Disease-causing Mutations at the Transmission Interface. 2017 , 292, 1988-1999	6

1741	Protein Phosphatase 2Cs and Control Microtubule Stability, Plant Growth, and Drought Response. 2017 , 29, 169-191	56
1740	Interaction of E. coli Hsp90 with DnaK Involves the DnaJ Binding Region of DnaK. 2017 , 429, 858-872	22
1739	In silico analysis for predicting pathogenicity of five unclassified mitochondrial DNA mutations associated with mitochondrial cytopathies' phenotypes. 2017 , 60, 172-177	7
1738	Lipidomics Characterization of Biosynthetic and Remodeling Pathways of Cardiolipins in Genetically and Nutritionally Manipulated Yeast Cells. 2017 , 12, 265-281	16
1737	Biochemical characterization of the selenoproteome in Gallus gallus via bioinformatics analysis: structure-function relationships and interactions of binding molecules. 2017 , 9, 124-131	20
1736	Immunoinformatics analysis and in silico designing of a novel multi-epitope peptide vaccine against Staphylococcus aureus. 2017 , 48, 83-94	110
1735	Dynamics of the peptidoglycan biosynthetic machinery in the stalked budding bacterium Hyphomonas neptunium. 2017 , 103, 875-895	26
1734	The Emerging Role of MORC Family Proteins in Cancer Development and Bone Homeostasis. 2017 , 232, 928-934	21
1733	E-cadherin cleavage by MT2-MMP regulates apical junctional signaling and epithelial homeostasis in the intestine. 2017 , 130, 4013-4027	12
1732	Arabidopsis EAmylase2 Is a K-Requiring, Catalytic Tetramer with Sigmoidal Kinetics. 2017 , 175, 1525-1535	12
1731	Effect of calcium ions on structure and stability of the C1q-like domain of otolin-1 from human and zebrafish. 2017 , 284, 4278-4297	17
1730	Polyphenol oxidase from Pectobacterium atrosepticum: identification and cloning of gene and characteristics of the enzyme. 2017 , 57, 998-1009	1
1729	Structural Basis for EarP-Mediated Arginine Glycosylation of Translation Elongation Factor EF-P. 2017 , 8,	15
1728	Complete genomic characterisation of two novel poxviruses (WKPV and EKPV) from western and eastern grey kangaroos. 2017 , 242, 106-121	7
1727	Biogenic manganese oxide nanoparticle formation by a multimeric multicopper oxidase Mnx. 2017 , 8, 746	46
1726	Discovery of an O-mannosylation pathway selectively serving cadherins and protocadherins. 2017 , 114, 11163-11168	50
1725	Structures of transcription pre-initiation complex with TFIIH and Mediator. 2017 , 551, 204-209	147
1724	Allosteric inhibition of the guanine nucleotide exchange factor DOCK5 by a small molecule. 2017 , 7, 14409	19

1723	A comprehensive structural model for the human KCNQ1/KCNE1 ion channel. 2017 , 78, 26-47	6
1722	Strain-dependent neutralization reveals antigenic variation of human parechovirus 3. 2017 , 7, 12075	18
1721	Defining the Architecture of the Core Machinery for the Assembly of Fe-S Clusters in Human Mitochondria. 2017 , 595, 107-160	2
1720	Expression and Functional Characterization of Breast Cancer-Associated Cytochrome P450 4Z1 in. 2017 , 45, 1364-1371	25
1719	Isolation and expression analysis of from different finger millet genotypes shows conserved nature of the gene. 2017 , 7, 342	2
1718	Molecular docking and simulation studies of phytocompounds against structural and nucleocapsid proteins of white spot syndrome virus. 2017 , 7, 353	7
1717	Anti-Markovnikov alkene oxidation by metal-oxo-mediated enzyme catalysis. 2017, 358, 215-218	108
1716	pH-Induced interfacial properties of Chaplin E from Streptomyces coelicolor. 2017 , 160, 589-597	1
1715	Spatial transcriptomes within the Pseudomonas aeruginosa biofilm architecture. 2017 , 106, 976-985	23
1714	A structural model of flagellar filament switching across multiple bacterial species. 2017 , 8, 960	63
1713	Identification and Characterization of the Major Porin of Desulfovibrio vulgaris Hildenborough. 2017 , 199,	4
1712	The organic anion transporter SLCO2A1 constitutes the core component of the Maxi-Cl channel. 2017 , 36, 3309-3324	35
1711	Functional analyses of the interaction of chicken interleukin 23 subunit p19 with IL-12 subunit p40 to form the IL-23 complex. 2017 , 92, 54-67	13
1710	Characterization of aromatic residue-controlled protein retention in the endoplasmic reticulum of. 2017 , 292, 20707-20719	13
1709	Challenging metastatic breast cancer with the natural defensin PvD. 2017 , 9, 16887-16899	14
1708	Exome sequencing and network analysis identifies shared mechanisms underlying spinocerebellar ataxia. 2017 , 140, 2860-2878	68
1707	Increase of Bacillus badius Phenylalanine dehydrogenase specificity towards phenylalanine substrate by site-directed mutagenesis. 2017 , 635, 44-51	4
1706	Functional reconstruction of a eukaryotic-like E1/E2/(RING) E3 ubiquitylation cascade from an uncultured archaeon. 2017 , 8, 1120	13

1705	IFITM3 requires an amphipathic helix for antiviral activity. 2017 , 18, 1740-1751	57
1704	Immobilization of bacteriophage in wound-dressing nanostructure. 2017 , 13, 2475-2484	38
1703	Bioenergetics of Monoterpenoid Essential Oil Biosynthesis in Nonphotosynthetic Glandular Trichomes. 2017 , 175, 681-695	13
1702	Conformational dynamics of 1-deoxy-d-xylulose 5-phosphate synthase on ligand binding revealed by H/D exchange MS. 2017 , 114, 9355-9360	26
1701	Be positive: optimizing pramlintide from microcanonical analysis of amylin isoforms. 2017 , 19, 25617-25633	8
1700	In silico interaction analysis of cannabinoid receptor interacting protein 1b (CRIP1b) - CB1 cannabinoid receptor. 2017 , 77, 311-321	5
1699	Discovery of a proteolytic flagellin family in diverse bacterial phyla that assembles enzymatically active flagella. 2017 , 8, 521	27
1698	Two novel mutations in ZAP70 gene that result in human immunodeficiency. 2017 , 183, 278-284	3
1697	In vitro efficacy of bumped kinase inhibitors against Besnoitia besnoiti tachyzoites. 2017 , 47, 811-821	16
1696	How does the exosite of rhomboid protease affect substrate processing and inhibition?. 2017 , 26, 2355-2366	7
1696 1695	How does the exosite of rhomboid protease affect substrate processing and inhibition?. 2017 , 26, 2355-2366 A Computational Approach to Identify the Biophysical and Structural Aspects of Methylenetetrahydrofolate Reductase (MTHFR) Mutations (A222V, E429A, and R594Q) Leading to Schizophrenia. 2017 , 108, 105-125	7
	A Computational Approach to Identify the Biophysical and Structural Aspects of Methylenetetrahydrofolate Reductase (MTHFR) Mutations (A222V, E429A, and R594Q) Leading to	<i>'</i>
1695	A Computational Approach to Identify the Biophysical and Structural Aspects of Methylenetetrahydrofolate Reductase (MTHFR) Mutations (A222V, E429A, and R594Q) Leading to Schizophrenia. 2017, 108, 105-125 Exploring the Stability of Ligand Binding Modes to Proteins by Molecular Dynamics Simulations: A	10
1695 1694	A Computational Approach to Identify the Biophysical and Structural Aspects of Methylenetetrahydrofolate Reductase (MTHFR) Mutations (A222V, E429A, and R594Q) Leading to Schizophrenia. 2017, 108, 105-125 Exploring the Stability of Ligand Binding Modes to Proteins by Molecular Dynamics Simulations: A Cross-docking Study. 2017, 57, 2514-2522 A component analysis of the free energies of folding of 35 proteins: A consensus view on the	10
1695 1694 1693	A Computational Approach to Identify the Biophysical and Structural Aspects of Methylenetetrahydrofolate Reductase (MTHFR) Mutations (A222V, E429A, and R594Q) Leading to Schizophrenia. 2017, 108, 105-125 Exploring the Stability of Ligand Binding Modes to Proteins by Molecular Dynamics Simulations: A Cross-docking Study. 2017, 57, 2514-2522 A component analysis of the free energies of folding of 35 proteins: A consensus view on the thermodynamics of folding at the molecular level. 2017, 38, 2791-2801 Identification of a specific agonist of human TAS2R14 from Radix Bupleuri through virtual	10 55 8
1695 1694 1693	A Computational Approach to Identify the Biophysical and Structural Aspects of Methylenetetrahydrofolate Reductase (MTHFR) Mutations (A222V, E429A, and R594Q) Leading to Schizophrenia. 2017, 108, 105-125 Exploring the Stability of Ligand Binding Modes to Proteins by Molecular Dynamics Simulations: A Cross-docking Study. 2017, 57, 2514-2522 A component analysis of the free energies of folding of 35 proteins: A consensus view on the thermodynamics of folding at the molecular level. 2017, 38, 2791-2801 Identification of a specific agonist of human TAS2R14 from Radix Bupleuri through virtual screening, functional evaluation and binding studies. 2017, 7, 12174 Adenoviral E4 34K protein interacts with virus packaging components and may serve as the	10 55 8 19
1695 1694 1693 1692	A Computational Approach to Identify the Biophysical and Structural Aspects of Methylenetetrahydrofolate Reductase (MTHFR) Mutations (A222V, E429A, and R594Q) Leading to Schizophrenia. 2017, 108, 105-125 Exploring the Stability of Ligand Binding Modes to Proteins by Molecular Dynamics Simulations: A Cross-docking Study. 2017, 57, 2514-2522 A component analysis of the free energies of folding of 35 proteins: A consensus view on the thermodynamics of folding at the molecular level. 2017, 38, 2791-2801 Identification of a specific agonist of human TAS2R14 from Radix Bupleuri through virtual screening, functional evaluation and binding studies. 2017, 7, 12174 Adenoviral E4 34K protein interacts with virus packaging components and may serve as the putative portal. 2017, 7, 7582 Molecular details of secretory phospholipase A from flax (Linum usitatissimum L.) provide insight	10 55 8 19

1687	Towards designer organelles by subverting the peroxisomal import pathway. 2017 , 8, 454	10
1686	Molecular modeling and structure-based drug discovery approach reveals protein kinases as off-targets for novel anticancer drug RH1. 2017 , 34, 176	6
1685	Development of a luciferase-based biosensor to assess enterovirus 71 3C protease activity in living cells. 2017 , 7, 10385	3
1684	MAST-like protein kinase IREH1 from Arabidopsis thaliana co-localizes with the centrosome when expressed in animal cells. 2017 , 246, 959-969	2
1683	PxAPN5 serves as a functional receptor of Cry2Ab in Plutella xylostella (L.) and its binding domain analysis. 2017 , 105, 516-521	5
1682	Novel functions of CCM1 delimit the relationship of PTB/PH domains. 2017 , 1865, 1274-1286	14
1681	Overcoming the loss of blue sensitivity through opsin duplication in the largest animal group, beetles. 2017 , 7, 8	123
1680	The butyrophilin 3A1 intracellular domain undergoes a conformational change involving the juxtamembrane region. 2017 , 31, 4697-4706	35
1679	Aryl hydrocarbon receptor gene transitions (c742C>T; c.1661G>A) and idiopathic male infertility: a case-control study with in silico and meta-analysis. 2017 , 24, 20599-20615	6
1678	Multi-template homology based structure prediction and molecular docking studies of protein Π 0 of Zaire ebolavirus (EBOV). 2017 , 9, 68-75	8
1677	Identification and characterization of a novel recessive KCNQ1 mutation associated with Romano-Ward Long-QT syndrome in two Iranian families. 2017 , 50, 912-918	4
1676	In silico designing of therapeutic protein enriched with branched-chain amino acids for the dietary treatment of chronic liver disease. 2017 , 76, 192-204	8
1675	Structure, function and regulation of Pseudomonas aeruginosa porins. 2017 , 41, 698-722	141
1674	Pore-forming toxins in Cnidaria. 2017 , 72, 133-141	27
1673	Characterization of two peptides isolated from the venom of social wasp Chartergellus communis (Hymenoptera: Vespidae): Influence of multiple alanine residues and C-terminal amidation on biological effects. 2017 , 95, 84-93	4
1672	A Biologically-validated HCV E1E2 Heterodimer Structural Model. 2017 , 7, 214	21
1671	Inhibition of glutamate decarboxylase (GAD) by ethyl ketopentenoate (EKP) induces treatment-resistant epileptic seizures in zebrafish. 2017 , 7, 7195	16
1670	Niche-specific gene expression in a parasitic nematode; increased expression of immunomodulators in Teladorsagia circumcincta larvae derived from host mucosa. 2017 , 7, 7214	8

1669	Capturing protein communities by structural proteomics in a thermophilic eukaryote. 2017 , 13, 936	79
1668	Co-expression of lipase isozymes for enhanced expression in Pichia pastoris. 2017 , 65, 335-342	5
1667	Toward more efficient simulations of slow processes in large biomolecular systems: Comment on "Ligand diffusion in proteins via enhanced sampling in molecular dynamics" by Jakub Rydzewski and Wieslaw Nowak. 2017 , 22-23, 75-76	4
1666	ET&C Best Paper of 2016. 2017 , 36, 1693-1694	
1665	Breaking the mirror: l-Amino acid deaminase, a novel stereoselective biocatalyst. 2017 , 35, 657-668	45
1664	The functional domains for Bax aggregate-mediated caspase 8-dependent cell death. 2017, 359, 342-355	5
1663	A novel soxO gene, encoding a glutathione disulfide reductase, is essential for tetrathionate oxidation in Advenella kashmirensis. 2017 , 205, 1-7	7
1662	Predicting the helix-helix interactions from correlated residue mutations. 2017 , 85, 2162-2169	2
1661	Biological, immunological and functional properties of two novel multi-variant chimeric recombinant proteins of CSP antigens for vaccine development against Plasmodium vivax infection. 2017 , 90, 158-171	5
1660	A haplotype in CFH family genes confers high risk of rare glomerular nephropathies. 2017 , 7, 6004	4
1659	Indole Biodegradation in Acinetobacter sp. Strain O153: Genetic and Biochemical Characterization. 2017 , 83,	30
1658	Protein kinase KIN10 from Arabidopsis thaliana as a potential regulator of primary microtubule nucleation centers in plants. 2017 , 51, 415-421	3
1657	Mechanistic Insights into Autoinhibition of the Oncogenic Chromatin Remodeler ALC1. 2017 , 68, 847-859.e7	32
1656	The Kalancholgenome provides insights into convergent evolution and building blocks of crassulacean acid metabolism. 2017 , 8, 1899	77
1655	Synthesis of Isomaltooligosaccharides by Cells Expressing Educosidase. 2017 , 2, 8062-8068	15
1654	Protocol for analyzing protein ensemble structures from chemical cross-links using DynaXL. 2017 , 3, 100-108	7
1653	A Novel de novo Mutation in a Patient with Autosomal Dominant Omodysplasia. 2017, 8, 318-324	9
1652	Cox2A/Cox2B subunit interaction in Polytomella sp. cytochrome c oxidase: role of the Cox2B subunit extension. 2017 , 49, 453-461	1

1651	The structural basis of flagellin detection by NAIP5: A strategy to limit pathogen immune evasion. 2017 , 358, 888-893	123
1650	Postcatalytic spliceosome structure reveals mechanism of 3'-splice site selection. 2017 , 358, 1283-1288	70
1649	Structure of FlgK reveals the divergence of the bacterial Hook-Filament Junction of Campylobacter. 2017 , 7, 15743	6
1648	Online Tools for Teaching Large Laboratory Courses: How the GENI Website Facilitates Authentic Research. 2017 , 137-153	
1647	Unique architecture of thermophilic archaeal virus APBV1 and its genome packaging. 2017, 8, 1436	21
1646	Spectroscopic and calorimetric characterization of spermine oxidase and its association forms. 2017 , 474, 4253-4268	2
1645	A Practical Guide to Structural Aspects of Macrocycles (NMR, X-Ray, and Modeling). 2017 , 25-57	
1644	A new familial form of a late-onset, persistent hyperinsulinemic hypoglycemia of infancy caused by a novel mutation in KCNJ11. 2017 , 11, 636-647	5
1643	Mechanism of the formation of the RecA-ssDNA nucleoprotein filament structure: a coarse-grained approach. 2017 , 13, 2697-2703	2
1642	Pharmacophore modelling, virtual screening and molecular docking studies on PLD1 inhibitors. 2017 , 28, 991-1009	7
1641	Histone methyltransferase 1 regulates the encystation process in the parasite Giardia lamblia. 2017 , 284, 2396-2409	9
1640	Chicken IFN Kappa: A Novel Cytokine with Antiviral Activities. 2017 , 7, 2719	16
1639	The malate sensing two-component system MaeKR is a non-canonical class of sensory complex for C4-dicarboxylates. 2017 , 7, 2708	4
1638	Characterization of the Dihydroorotase from Methanococcus jannaschii. 2017 , 36, 361-373	2
1637	Lasso Peptide Benenodin-1 Is a Thermally Actuated [1]Rotaxane Switch. 2017, 139, 10403-10409	38
1636	Targeted DNA methylation in vivo using an engineered dCas9-MQ1 fusion protein. 2017, 8, 16026	113
1635	Involvement of FANCD2 in Energy Metabolism via ATP5 日2017 , 7, 4921	17
1634	Multimerin-2 is a ligand for group 14 family C-type lectins CLEC14A, CD93 and CD248 spanning the endothelial pericyte interface. 2017 , 36, 6097-6108	31

1633	Evolution of GSTD1 in Cactophilic Drosophila. 2017, 84, 285-294	4
1632	Structural and Functional Analysis of the Escherichia coli Acid-Sensing Histidine Kinase EvgS. 2017 , 199,	15
1631	Genome-wide identification, functional and evolutionary analysis of terpene synthases in pineapple. 2017 , 70, 40-48	5
1630	Bacterial lipid droplets bind to DNA via an intermediary protein that enhances survival under stress. 2017 , 8, 15979	49
1629	Constitutive expression of human gastric lipase in Pichia pastoris and site-directed mutagenesis of key lid-stabilizing residues. 2017 , 1862, 1025-1034	8
1628	A Novel Pathogenic Variant in the Gene Segregating with a Unique Spectrum of Ocular Findings in an Extended Iranian Waardenburg Syndrome Kindred. 2017 , 8, 195-200	12
1627	Functional characterization of 3-ketosteroid 9thydroxylases in Rhodococcus ruber strain chol-4. 2017 , 172, 176-187	11
1626	De novo RNA synthesis catalyzed by the Zika Virus RNA polymerase domain. 2017 , 7, 2697	2
1625	Supercharging SpyCatcher toward an intrinsically disordered protein with stimuli-responsive chemical reactivity. 2017 , 53, 8830-8833	21
1624	Deciphering the role of the signal- and Sty1 kinase-dependent phosphorylation of the stress-responsive transcription factor Atf1 on gene activation. 2017 , 292, 13635-13644	17
1623	Staged heterogeneity learning to identify conformational B-cell epitopes from antigen sequences. 2017 , 18, 113	5
1622	Evolution of strigolactone receptors by gradual neo-functionalization of KAI2 paralogues. 2017 , 15, 52	58
1621	Discovery and evolution of novel hemerythrin genes in annelid worms. 2017 , 17, 85	8
1620	Analysis of triglyceride synthesis unveils a green algal soluble diacylglycerol acyltransferase and provides clues to potential enzymatic components of the chloroplast pathway. 2017 , 18, 223	14
1619	A novel, complex RUNX2 gene mutation causes cleidocranial dysplasia. 2017 , 18, 13	13
1618	A bacterial negative transcription regulator binding on an inverted repeat in the promoter for epothilone biosynthesis. 2017 , 16, 92	6
1617	Lipidomics. 2017,	4
1616	A novel KCNA1 mutation in a patient with paroxysmal ataxia, myokymia, painful contractures and metabolic dysfunctions. 2017 , 83, 6-12	14

1615	Pulsed Electron Paramagnetic Resonance Insights into the Ligand Environment of Copper in Drosophila Lysyl Oxidase. 2017 , 56, 3770-3779	2
1614	Expression and integrated network analyses revealed functional divergence of NHX-type Na/H exchanger genes in poplar. 2017 , 7, 2607	23
1613	Bacterial Protein Secretion Systems. 2017,	O
1612	Computational Functional Analysis of Lipid Metabolic Enzymes. 2017 , 1609, 195-216	O
1611	Structural Analysis of Protein Complexes by Cryo Electron Microscopy. 2017 , 1615, 377-413	9
1610	Analysis of transcription factors among differentially expressed genes induced by drought stress in Populus davidiana. 2017 , 7, 209	19
1609	GH115 ⊞glucuronidase and GH11 xylanase from Paenibacillus sp. JDR-2: potential roles in processing glucuronoxylans. 2017 , 101, 1465-1476	8
1608	WDR73 missense mutation causes infantile onset intellectual disability and cerebellar hypoplasia in a consanguineous family. 2017 , 464, 24-29	5
1607	Chimeric peptide-mediated siRNA transduction to inhibit HIV-1 infection. 2017 , 25, 307-319	6
1606	Identification and characterization of nine PAT1 branch genes in poplar. 2017, 81, 355-364	2
1605	Complete mitochondrial genome and evolutionary analysis of Turritopsis dohrnii, the "immortal" jellyfish with a reversible life-cycle. 2017 , 107, 232-238	12
1604	Differences in the expression profile of endo-E(1,6)- d -galactanase in pathogenic and non-pathogenic races of Colletotrichum lindemuthianum grown in the presence of arabinogalactan, xylan or Phaseolus vulgaris cell walls. 2017 , 99, 75-86	1
1603	Cartilage acidic protein 1, a new member of the beta-propeller protein family with amyloid propensity. 2017 , 85, 242-255	12
1602	PASylation technology improves recombinant interferon-IIb solubility, stability, and biological activity. 2017 , 101, 1975-1987	23
1601	Association of SRD5A2 gene mutations with risk of hypospadias in the Iranian population. 2017 , 40, 391-396	11
1600	Balancing Inflammation: Computational Design of Small-Molecule Toll-like Receptor Modulators. 2017 , 38, 155-168	21
1599	Mapping of Functional Subdomains in the Terminal Protein Domain of Hepatitis B Virus Polymerase. 2017 , 91,	10
1598	Quantitative structure-activity relationship and molecular docking revealed a potency of anti-hepatitis C virus drugs against human corona viruses. 2017 , 89, 1040-1047	80

1597	Binding preferential of chickpea cold shock protein during nucleic acid interactions. 2017 , 26, 208-215	1
1596	Prediction of B Cell Epitopes Among Hantavirus Strains Causing Hemorragic Fever With Renal Syndrome. 2017 , 118, 1182-1188	6
1595	Identification, annotation and expression analysis of 29 Rho GTPase genes from channel catfish (Ictalurus punctatus) after bacterial infections. 2017 , 67, 445-451	8
1594	One-Dimensional Structural Properties of Proteins in the Coarse-Grained CABS Model. 2017 , 1484, 83-113	7
1593	Prediction of Protein Secondary Structure. 2017,	2
1592	The GOR Method of Protein Secondary Structure Prediction and Its Application as a Protein Aggregation Prediction Tool. 2017 , 1484, 7-24	20
1591	Protein Folding and Structure Prediction from the Ground Up II: AAWSEM for Proteins. 2017 , 121, 3473-3482	16
1590	Accurate Prediction of One-Dimensional Protein Structure Features Using SPINE-X. 2017 , 1484, 45-53	1
1589	Go it alone: four-electron oxidations by mononuclear non-heme iron enzymes. 2017 , 22, 381-394	28
1588	Multi-template homology-based structural model of L-2-haloacid dehalogenase (DehL) from Rhizobium sp. RC1. 2017 , 35, 3285-3296	12
1587	Casting the critical regions in nucleotide binding oligomerization domain 2 protein: a signature mediated structural dynamics approach. 2017 , 35, 3297-3315	6
1586	Reactive oxygen species (ROS) and the heat stress response of Daphnia pulex: ROS-mediated activation of hypoxia-inducible factor 1 (HIF-1) and heat shock factor 1 (HSF-1) and the clustered expression of stress genes. 2017 , 109, 39-64	43
1585	The use of structural modelling to infer structure and function in biocontrol agents. 2017, 142, 23-26	2
1584	Integrated Modeling and Experimental Approaches to Control Silica Modification of Design Silk-Based Biomaterials. 2017 , 3, 2877-2888	11
1583	In silico analysis of novel mutations in maple syrup urine disease patients from Iran. 2017, 32, 105-113	12
1582	CD4-gp120 interaction interface - a gateway for HIV-1 infection in human: molecular network, modeling and docking studies. 2017 , 35, 2631-2644	5
1581	Thiol oxidation of hemolymph proteins in oysters Crassostrea brasiliana as markers of oxidative damage induced by urban sewage exposure. 2017 , 36, 1833-1845	5
1580	Electrostatic potentials of the S-locus F-box proteins contribute to the pollen S specificity in self-incompatibility in Petunia hybrida. 2017 , 89, 45-57	15

1579	Design and characterization of short hybrid antimicrobial peptides from pEM-2, mastoparan-VT1, and mastoparan-B. 2017 , 89, 327-338	22
1578	Effect of natural polymorphism on structure and function of the Yersinia pestis outer membrane porin F (OmpF protein): a computational study. 2017 , 35, 2588-2603	3
1577	Conformational changes associated with L16P and T118M mutations in the membrane-embedded PMP22 protein, consequential in CMT-1A. 2017 , 35, 2880-2894	3
1576	Computational analysis unravels novel destructive single nucleotide polymorphisms in the non-synonymous region of human caveolin gene. 2017 , 6, 142-157	6
1575	Construction of Asymmetrical Hexameric Biomimetic Motors with Continuous Single-Directional Motion by Sequential Coordination. 2017 , 13, 1601600	3
1574	Assessing reproductive toxicity and antioxidant enzymes on beta asarone induced male Wistar albino rats: In vivo and computational analysis. 2017 , 173, 150-160	7
1573	Understanding protein domain-swapping using structure-based models of protein folding. 2017 , 128, 113-120	32
1572	Indole-3-acetic acid production via the indole-3-pyruvate pathway by plant growth promoter Rhizobium tropici CIAT 899 is strongly inhibited by ammonium. 2017 , 168, 283-292	23
1571	Ghand regulator of G-protein signaling (RGS) protein pairs maintain functional compatibility and conserved interaction interfaces throughout evolution despite frequent loss of RGS proteins in plants. 2017 , 216, 562-575	26
1570	Atomic modeling of the ITS2 ribosome assembly subcomplex from cryo-EM together with mass spectrometry-identified protein-protein crosslinks. 2017 , 26, 103-112	12
1569	Identification of fasciclin-like arabinogalactan proteins in textile hemp (Cannabis sativa L.): in silico analyses and gene expression patterns in different tissues. 2017 , 18, 741	27
1568	Identification of Rifampicin Resistance Mutations in Escherichia coli, Including an Unusual Deletion Mutation. 2017 , 27, 356-362	5
1567	Structure and Function of Caltrin (Calcium Transport Inhibitor) Proteins. 2017, 10, 1178626417745822	1
1566	Purification of small-size acidic proteoglycan-like domain of carbonic anhydrase IX fused with thioredoxine expressed in Escherichia coli for structural characterization. 2017 , 72, 1240-1246	
1565	Variation in the gene determines resistance against wheat stem rust race Ug99. 2017 , 358, 1604-1606	91
1564	Function of tumor necrosis factor alpha before and after mutation in gastric cancer. 2017 , 24, 1920-1924	6
1563	Genomic characterisation of environmental Pseudomonas aeruginosa isolated from dental unit waterlines revealed the insertion sequence ISPa11 as a chaotropic element. 2017 , 93,	10
1562	An improved structural model of the human iron exporter ferroportin. Insight into the role of pathogenic mutations in hereditary hemochromatosis type 4. 2017 , 13,	2

1561	Interfering with the high-affinity interaction between wheat amylase trypsin inhibitor CM3 and toll-like receptor 4: in silico and biosensor-based studies. 2017 , 7, 13169	23
1560	Evolutionary conservation of Ebola virus proteins predicts important functions at residue level. 2017 , 33, 151-154	2
1559	Ebolavirus interferon antagonists-protein interaction perspectives to combat pathogenesis. 2018 , 17, 392-401	2
1558	Recombinant Antibodies for Infectious Diseases. 2017,	1
1557	Computer-Aided Antibody Design: An Overview. 2017 , 1053, 221-243	5
1556	Broad Phylogenetic Occurrence of the Oxygen-Binding Hemerythrins in Bilaterians. 2017 , 9, 2580-2591	6
1555	Computational study of non-catalytic T-loop pocket on CDK proteins for drug development. 2017 , 26, 128702	9
1554	Brevibacillus Thermoruber 9X-GLC, Bacteria Isolated from Hot Compost, Producer of a Beta-Glucosidase Resistant to Glucose Inhibition. 2017 , 13, 157-166	1
1553	Mutation in () Adapts Barley to Drought Stress at Phenotypic and Transcriptomic Levels. 2017, 8, 942	17
1552	The Glycosyltransferases of LPS Core: A Review of Four Heptosyltransferase Enzymes in Context. 2017 , 18,	19
1551	Biochemical and Structural Insights into a Novel Thermostable 🗓 ,3-Galactosidase from Marinomonas sp. BSi20414. 2017 , 15,	15
1550	Marine Inspired 2-(5-Halo-1H-indol-3-yl)-N,N-dimethylethanamines as Modulators of Serotonin Receptors: An Example Illustrating the Power of Bromine as Part of the Uniquely Marine Chemical Space. 2017 , 15,	15
1549	Predicting and Interpreting the Structure of Type IV Pilus of Electricigens by Molecular Dynamics Simulations. 2017 , 22,	4
1548	A Comparative Genomic and Transcriptomic Survey Provides Novel Insights into N-Acetylserotonin Methyltransferase (ASMT) in Fish. 2017 , 22,	9
1547	A Large Size Chimeric Highly Immunogenic Peptide Presents Multistage Plasmodium Antigens as a Vaccine Candidate System against Malaria. 2017 , 22,	3
1546	Understanding the Mechanism of Translocation of Adenylate Cyclase Toxin across Biological Membranes. 2017 , 9,	7
1545	HCIV-1 and Other Tailless Icosahedral Internal Membrane-Containing Viruses of the Family Sphaerolipoviridae. 2017 , 9,	17
1544	DNA-Interacting Characteristics of the Archaeal Rudiviral Protein SIRV2_Gp1. 2017 , 9,	7

1543	PSN-PC: A Novel Antimicrobial and Anti-Biofilm Peptide from the Skin Secretion of Phyllomedusa-camba with Cytotoxicity on Human Lung Cancer Cell. 2017 , 22,	13
1542	A conformational switch regulates the ubiquitin ligase HUWE1. 2017 , 6,	44
1541	Net Evolutionary Loss of Residue Polarity in Drosophilid Protein Cores Indicates Ongoing Optimization of Amino Acid Composition. 2017 , 9, 2879-2892	3
1540	3D-QSAR and Molecular Docking Studies on the TcPMCA1-Mediated Detoxification of Scopoletin and Coumarin Derivatives. 2017 , 18,	8
1539	The All-Rounder Sodalis: A New Bacteriome-Associated Endosymbiont of the Lygaeoid Bug Henestaris halophilus (Heteroptera: Henestarinae) and a Critical Examination of Its Evolution. 2017 , 9, 2893-2910	33
1538	A Novel Chimeric Endolysin with Antibacterial Activity against Methicillin-Resistant. 2017 , 7, 290	38
1537	Distinct Conformational Dynamics of Three G Protein-Coupled Receptors Measured Using FlAsH-BRET Biosensors. 2017 , 8, 61	17
1536	Conservation of Three-Dimensional Helix-Loop-Helix Structure through the Vertebrate Lineage Reopens the Cold Case of Gonadotropin-Releasing Hormone-Associated Peptide. 2017 , 8, 207	10
1535	The Immune Epitope Database and Analysis Resource in Epitope Discovery and Synthetic Vaccine Design. 2017 , 8, 278	202
1534	Group 1 Capsular Polysaccharide Exportation Nanomachinary as a Plausible Antivirulence Target in the Perspective of Emerging Antimicrobial Resistance. 2017 , 8, 70	22
1533	Error-prone DnaE2 Balances the Genome Mutation Rates in DK1622. 2017 , 8, 122	7
1532	Comparative Genomics Analysis of a New Strain from Salar de Huasco Reveals a Repertoire of Stress-Related Genes and Arsenic Resistance. 2017 , 8, 456	24
1531	Targeted Modification of a Novel Amphibian Antimicrobial Peptide from to Enhance Its Activity against MRSA and Microbial Biofilm. 2017 , 8, 628	26
1530	Comparative Omics and Trait Analyses of Marine Phages Advance the Phage OTU Concept. 2017 , 8, 1241	27
1529	Ribonucleotide Reductases from Bifidobacteria Contain Multiple Conserved Indels Distinguishing Them from All Other Organisms: Analysis of the Possible Role of a 43 aa Bifidobacteria-Specific Insert in the Class III RNR Homolog. 2017 , 8, 1409	6
1528	Analysis of the Sequences, Structures, and Functions of Product-Releasing Enzyme Domains in Fungal Polyketide Synthases. 2017 , 8, 1685	10
1527	Targeting Inhibition of SmpB by Peptide Aptamer Attenuates the Virulence to Protect Zebrafish against Infection. 2017 , 8, 1766	5
1526	Acetylome of SK17 Reveals a Highly-Conserved Modification of Histone-Like Protein HU. 2017 , 4, 77	11

1525	The Biogenic Amine Tyramine and its Receptor (AmTyr1) in Olfactory Neuropils in the Honey Bee () Brain. 2017 , 11, 77	11
1524	Structure of RNA polymerase bound to ribosomal 30S subunit. 2017 , 6,	62
1523	Phage-Displayed Peptides Selected to Bind Envelope Glycoprotein Show Antiviral Activity against Dengue Virus Serotype 2. 2017 , 2017, 1827341	12
1522	Molecular Cloning and Characterization of Rhoptry Neck 2 RON2 Protein. 2017 , 2017, 7259630	6
1521	Characteristics and Lethality of a Novel Recombinant Dermonecrotic Venom Phospholipase D from Hemiscorpius lepturus. 2017 , 9,	11
1520	Chemogenomics driven discovery of endogenous polyketide anti-infective compounds from endosymbiotic Emericella variecolor CLB38 and their RNA secondary structure analysis. 2017 , 12, e0172848	5
1519	Characteristics of candidate genes associated with embryonic development in the cow: Evidence for a role for WBP1 in development to the blastocyst stage. 2017 , 12, e0178041	7
1518	Epitope determination of immunogenic proteins of Neisseria gonorrhoeae. 2017 , 12, e0180962	
1517	Whole-genome sequencing of mutants with increased resistance against the two-peptide bacteriocin plantaricin JK reveals a putative receptor and potential docking site. 2017 , 12, e0185279	14
1516	Plastid and mitochondrial genomes of Coccophora langsdorfii (Fucales, Phaeophyceae) and the utility of molecular markers. 2017 , 12, e0187104	8
1515	Sequence-based protein-Ca2+ binding site prediction using SVM classifier ensemble with random under-sampling. 2017 ,	1
1514	Identification and characterization of two linear epitope motifs in hepatitis E virus ORF2 protein. 2017 , 12, e0184947	10
1513	Directed evolution of a soluble human DR3 receptor for the inhibition of TL1A induced cytokine secretion. 2017 , 12, e0173460	6
1512	Identification of metal ion binding sites based on amino acid sequences. 2017 , 12, e0183756	23
1511	Didehydrophenylalanine, an abundant modification in the beta subunit of plant polygalacturonases. 2017 , 12, e0171990	6
1510	Rv0004 is a new essential member of the mycobacterial DNA replication machinery. 2017 , 13, e1007115	13
1509	The single cyclic nucleotide-specific phosphodiesterase of the intestinal parasite Giardia lamblia represents a potential drug target. 2017 , 11, e0005891	9
1508	A versatile papaya mosaic virus (PapMV) vaccine platform based on sortase-mediated antigen coupling. 2017 , 15, 54	28

1507	terminus of the canine distemper virus nucleoprotein and sequence analysis of the identified epitope in different CDV isolates. 2017 , 14, 187	2
1506	Mapping genetic variations to three-dimensional protein structures to enhance variant interpretation: a proposed framework. 2017 , 9, 113	31
1505	Structural and functional annotation of hypothetical proteins of human adenovirus: prioritizing the novel drug targets. 2017 , 10, 706	10
1504	Recessive VARS2 mutation underlies a novel syndrome with epilepsy, mental retardation, short stature, growth hormone deficiency, and hypogonadism. 2017 , 11, 28	7
1503	Diverse effects of distance cutoff and residue interval on the performance of distance-dependent atom-pair potential in protein structure prediction. 2017 , 18, 542	2
1502	In Silico Validation of D7 Salivary Protein-derived B- and T-cell Epitopes of Aedes aegypti as Potential Vaccine to Prevent Transmission of Flaviviruses and Togaviruses to Humans. 2017 , 13, 366-375	4
1501	The calcium binding properties and structure prediction of the Hax-1 protein. 2017 , 64, 537-542	4
1500	Structural Insights of Induced Pluripotent Stem Cell Regulatory Factors Oct4 and Its Interaction with Sox2 and Fgf4 Gene. 2017 ,	2
1499	Comparative Study on the Binding Affinity of Methimazole and Propylthiouracil to Thyroid Peroxidase as an Anti-Thyroid Drug: An Insilico Approach. 2017 , 07,	1
1498	Protein Structure Prediction and Homology Modeling. 2017 , 120-144	
1497	Dual Functioned Pegylated Phospholipid Micelles Containing Cationic Antimicrobial Decapeptide for Treating Sepsis. 2017 , 7, 3759-3767	8
1496	Species-Specificity in Myoglobin Oxygenation and Reduction Potential Properties. 2017 , 1, 1	9
1495	An overview of comparative modelling and resources dedicated to large-scale modelling of genome sequences. 2017 , 73, 628-640	31
1494	Identification of a Mycothiol-Dependent Nitroreductase from Mycobacterium tuberculosis. 2018, 4, 771-787	12
1493	Expanded diversity of microbial groups that shape the dissimilatory sulfur cycle. 2018 , 12, 1715-1728	165
1492	Functional Replacement of Histidine in Proteins To Generate Noncanonical Amino Acid Dependent Organisms. 2018 , 140, 3829-3832	23
1491	Biochemical characterization of microbial type terpene synthases in two closely related species of hornworts, Anthoceros punctatus and Anthoceros agrestis. 2018 , 149, 116-122	16
1490	An in silico argument for mitochondrial microRNA as a determinant of primary non function in liver transplantation. 2018 , 8, 3105	6

1489	Molecular docking, molecular modeling, and molecular dynamics studies of azaisoflavone as dual COX-2 inhibitors and TP receptor antagonists. 2018 , 24, 69	5
1488	Homozygous mutation in chondrodysplasia, brachydactyly, overriding digits, clino-symphalangism and synpolydactyly. 2018 , 55, 489-496	9
1487	Functional interaction of low-homology FRPs from different cyanobacteria with Synechocystis OCP. 2018 , 1859, 382-393	11
1486	An in silico structural and physicochemical characterization of TonB-dependent copper receptor in A. baumannii. 2018 , 118, 18-31	8
1485	MetaGO: Predicting Gene Ontology of Non-homologous Proteins Through Low-Resolution Protein Structure Prediction and Protein-Protein Network Mapping. 2018 , 430, 2256-2265	32
1484	Genetic and Structural Analysis of a SKIV2L Mutation Causing Tricho-hepato-enteric Syndrome. 2018 , 63, 1192-1199	5
1483	Coarse-Grained Modeling of the Interplay between Secondary Structure Propensities and Protein Fold Assembly. 2018 , 14, 2277-2287	5
1482	Novel ABCA4 mutation leads to loss of a conserved C-terminal motif: implications for predicting pathogenicity based on genetic testing. 2018 , 28, 123-126	2
1481	Genotypic effect of a mutation of the MYBPC3 gene and two phenotypes with different patterns of inheritance. 2018 , 32, e22419	4
1480	Cryo-EM Studies of Pre-mRNA Splicing: From Sample Preparation to Model Visualization. 2018 , 47, 175-199	15
1480 1479	Cryo-EM Studies of Pre-mRNA Splicing: From Sample Preparation to Model Visualization. 2018 , 47, 175-199 Complete avian malaria parasite genomes reveal features associated with lineage-specific evolution in birds and mammals. 2018 , 28, 547-560	15 53
	Complete avian malaria parasite genomes reveal features associated with lineage-specific	
1479	Complete avian malaria parasite genomes reveal features associated with lineage-specific evolution in birds and mammals. 2018 , 28, 547-560 Identification of the Nicotinamide Salvage Pathway as a New Toxification Route for	53
1479 1478	Complete avian malaria parasite genomes reveal features associated with lineage-specific evolution in birds and mammals. 2018 , 28, 547-560 Identification of the Nicotinamide Salvage Pathway as a New Toxification Route for Antimetabolites. 2018 , 25, 471-482.e7	53
1479 1478 1477	Complete avian malaria parasite genomes reveal features associated with lineage-specific evolution in birds and mammals. 2018, 28, 547-560 Identification of the Nicotinamide Salvage Pathway as a New Toxification Route for Antimetabolites. 2018, 25, 471-482.e7 Insights into gliadin supramolecular organization at digestive pH 3.0. 2018, 165, 363-370 MT4-MMP deficiency increases patrolling monocyte recruitment to early lesions and accelerates	53 40 12
1479 1478 1477	Complete avian malaria parasite genomes reveal features associated with lineage-specific evolution in birds and mammals. 2018, 28, 547-560 Identification of the Nicotinamide Salvage Pathway as a New Toxification Route for Antimetabolites. 2018, 25, 471-482.e7 Insights into gliadin supramolecular organization at digestive pH 3.0. 2018, 165, 363-370 MT4-MMP deficiency increases patrolling monocyte recruitment to early lesions and accelerates atherosclerosis. 2018, 9, 910 ETubulin has a conserved intrinsic property of self-polymerization into double stranded filaments and fibrillar networks. 2018, 1865, 734-748	53 40 12 21
1479 1478 1477 1476	Complete avian malaria parasite genomes reveal features associated with lineage-specific evolution in birds and mammals. 2018, 28, 547-560 Identification of the Nicotinamide Salvage Pathway as a New Toxification Route for Antimetabolites. 2018, 25, 471-482.e7 Insights into gliadin supramolecular organization at digestive pH 3.0. 2018, 165, 363-370 MT4-MMP deficiency increases patrolling monocyte recruitment to early lesions and accelerates atherosclerosis. 2018, 9, 910 El Tubulin has a conserved intrinsic property of self-polymerization into double stranded filaments and fibrillar networks. 2018, 1865, 734-748 A novel modelling mechanism of PAEL receptor and GABARAPL2 interaction involved in Parkinson's	53 40 12 21

1471	BBS9 gene in nonsyndromic craniosynostosis: Role of the primary cilium in the aberrant ossification of the suture osteogenic niche. 2018 , 112, 58-70	9
1470	A Legionella pneumophila amylase is essential for intracellular replication in human macrophages and amoebae. 2018 , 8, 6340	11
1469	Fused dimerization increases expression, solubility, and activity of bacterial dehydratase enzymes. 2018 , 27, 969-975	7
1468	Genome-wide identification of mildew resistance locus O (MLO) genes in tree model poplar (Populus trichocarpa): powdery mildew management in woody plants. 2018 , 152, 95-109	8
1467	Plant Endomembrane Dynamics: Studies of K/H Antiporters Provide Insights on the Effects of pH and Ion Homeostasis. 2018 , 177, 875-895	85
1466	A-to-I RNA Editing Contributes to Proteomic Diversity in Cancer. 2018 , 33, 817-828.e7	91
1465	Regulation of carbohydrate degradation pathways in Pseudomonas involves a versatile set of transcriptional regulators. 2018 , 11, 442-454	25
1464	Integrating Cross-Linking Experiments with Ab Initio Protein-Protein Docking. 2018, 430, 1814-1828	12
1463	RPAP3 provides a flexible scaffold for coupling HSP90 to the human R2TP co-chaperone complex. 2018 , 9, 1501	31
1462	Yeast aconitase mitochondrial import is modulated by interactions of its C and N terminal domains and Ssa1/2 (Hsp70). 2018 , 8, 5903	8
1461	Plasmodium falciparum Falcipain-2a Polymorphisms in Southeast Asia and Their Association With Artemisinin Resistance. 2018 , 218, 434-442	18
1460	Metschnikowia mating genomics. 2018 , 111, 1935-1953	7
1459	NGR (Asn-Gly-Arg)-targeted delivery of coagulase to tumor vasculature arrests cancer cell growth. 2018 , 37, 3967-3980	23
1458	Mutant and wild-type p53 form complexes with p73 upon phosphorylation by the kinase JNK. 2018 , 11,	17
1457	Computational Tools for the Structural Characterization of Proteins and Their Complexes from Sequence-Evolutionary Data. 2018 , 1-19	
1456	First characterization of fucosidases in spiders. 2018 , 98, e21462	5
1455	Structural and enzymatic analysis of the cytochrome b reductase domain of Ulva prolifera nitrate reductase. 2018 , 111, 1175-1182	4
1454	Recombinant protein susceptibility to proteolysis in the plant cell secretory pathway is pH-dependent. 2018 , 16, 1928-1938	10

1453	Truncation of the processive Cel5A of Thermotoga maritima results in soluble expression and several fold increase in activity. 2018 , 115, 1675-1684	11
1452	In silico characterization of broad range proteases produced by Serratia marcescens EGD-HP20. 2018 , 58, 492-500	5
1451	Identification of Four Isoforms of Esterase-5A fromCulex quinquefasciatusSay. 2018, 43, 91-107	1
1450	Venom-derived peptide Mastoparan-1 eradicates planktonic and biofilm-embedded methicillin-resistant Staphylococcus aureus isolates. 2018 , 119, 72-80	17
1449	Comprehensive Proteoform Characterization of Plasma Complement Component C8 by Hybrid Mass Spectrometry Approaches. 2018 , 29, 1099-1110	20
1448	Mutations Alter RNA-Mediated Conversion of Human Prions. 2018 , 3, 3936-3944	2
1447	Identification of new inhibitors against human Great wall kinase using in silico approaches. 2018 , 8, 4894	17
1446	Expression of Soluble Active Interferon A in Escherichia coli Periplasm by Fusion with Thermostable Lichenase Using the Domain Insertion Approach. 2018 , 83, 259-269	5
1445	Molecular characterization and expression profiling of BMP 3 gene in broiler and layer chicken. 2018 , 45, 477-495	2
1444	Structure and regulation of the human INO80-nucleosome complex. 2018, 556, 391-395	105
1444	Structure and regulation of the human INO80-nucleosome complex. 2018 , 556, 391-395 Structural basis for ATP-dependent chromatin remodelling by the INO80 complex. 2018 , 556, 386-390	105
1443		
1443	Structural basis for ATP-dependent chromatin remodelling by the INO80 complex. 2018 , 556, 386-390	121
1443 1442 1441	Structural basis for ATP-dependent chromatin remodelling by the INO80 complex. 2018 , 556, 386-390 Novel Insights for Inhibiting Mutant Heterodimer IDH1 in Cancer: An In-Silico Approach. 2018 , 22, 369-380	121
1443 1442 1441	Structural basis for ATP-dependent chromatin remodelling by the INO80 complex. 2018 , 556, 386-390 Novel Insights for Inhibiting Mutant Heterodimer IDH1 in Cancer: An In-Silico Approach. 2018 , 22, 369-380 Molecular Modeling of Chemoreceptor:Ligand Interactions. 2018 , 1729, 353-372	121
1443 1442 1441 1440	Structural basis for ATP-dependent chromatin remodelling by the INO80 complex. 2018 , 556, 386-390 Novel Insights for Inhibiting Mutant Heterodimer IDH1 in Cancer: An In-Silico Approach. 2018 , 22, 369-380 Molecular Modeling of Chemoreceptor:Ligand Interactions. 2018 , 1729, 353-372 Sertoli Cells. 2018 ,	121 1 4
1443 1442 1441 1440 1439	Structural basis for ATP-dependent chromatin remodelling by the INO80 complex. 2018, 556, 386-390 Novel Insights for Inhibiting Mutant Heterodimer IDH1 in Cancer: An In-Silico Approach. 2018, 22, 369-380 Molecular Modeling of Chemoreceptor:Ligand Interactions. 2018, 1729, 353-372 Sertoli Cells. 2018, Cadherin-26 (CDH26) regulates airway epithelial cell cytoskeletal structure and polarity. 2018, 4, 7 Enhancing protein fold determination by exploring the complementary information of chemical	121 1 4 1

1435	Genetic diversity of the Plasmodium vivax phosphatidylinositol 3-kinase gene in two regions of the China-Myanmar border. 2018 , 61, 45-52	3
1434	Dual Role for DsbA in Attacking and Targeted Bacterial Cells during Type VI Secretion System-Mediated Competition. 2018 , 22, 774-785	15
1433	The hidden lipoproteome of Staphylococcus aureus. 2018 , 308, 569-581	7
1432	Rbfox Splicing Factors Promote Neuronal Maturation and Axon Initial Segment Assembly. 2018 , 97, 853-868.6	•6 ₄₅
1431	Effects of mutations of non-catalytic aromatic residues on substrate specificity of Bacillus licheniformis endocellulase cel12A. 2018 , 67, 38-45	1
1430	Identification and molecular characterization of Dof transcription factor gene family preferentially expressed in developing spikes of L. 2018 , 8, 82	15
1429	AIMOES: Archive information assisted multi-objective evolutionary strategy for ab initio protein structure prediction. 2018 , 146, 58-72	27
1428	Genome-wide identification of barley MCs (metacaspases) and their possible roles in boron-induced programmed cell death. 2018 , 45, 211-225	16
1427	Cep120 promotes microtubule formation through a unique tubulin binding C2 domain. 2018, 203, 62-70	6
1426	Dynamics of the Interaction of RecG Protein with Stalled Replication Forks. 2018 , 57, 1967-1976	15
1425	Distinct Regulatory Role of Carbon Catabolite Protein A (CcpA) in Oral Streptococcal Expression. 2018 , 200,	16
1424	Identification of a Golgi GPI-N-acetylgalactosamine transferase with tandem transmembrane regions in the catalytic domain. 2018 , 9, 405	24
1423	Exposure of helices 4 and 5 is required for insecticidal activity of Cry2Ab by promoting assembly of a prepore oligomeric structure. 2018 , 20, e12827	4
1422	Use of Domain-Swapping to Identify Candidate Amino Acids Involved in Differential Interactions between Two Allelic Variants of Type-1 S-Locus F-Box Protein and S3-RNase in Petunia inflata. 2018 , 59, 234-247	5
1421	Co-Expression of ORF with PHB Depolymerase (PhaZ) in Escherichia coli Induces Efficient Whole-Cell Biodegradation of Polyesters. 2018 , 13, e1700560	4
1420	New facet of non-O1/non-O139 Vibrio cholerae hemolysin A: a competitive factor in the ecological niche. 2017 , 93,	6
1419	Advances on the impact of thermal processing on structure and antigenicity of chicken ovomucoid. 2018 , 98, 3119-3128	4
1418	PokMT1 from the Polyketomycin Biosynthetic Machinery of Streptomyces diastatochromogenes TB028 Belongs to the Emerging Family of C-Methyltransferases That Act on CoA-Activated Aromatic Substrates. 2018 , 57, 1003-1011	5

	MP 2.0: An algorithm to predict genotype-phenotype correlation of lysosomal storage cases. 2018 , 93, 1008-1014	8
	ecular Insights into the Roles of Rab Proteins in Intracellular Dynamics and Neurodegenerative eases. 2018 , 20, 18-36	19
	octural prediction of protein models using distance restraints derived from cross-linking mass ctrometry data. 2018 , 13, 478-494	32
	octural and Biophysical Characterization of Human EXTL3: Domain Organization, Glycosylation, Solution Structure. 2018 , 57, 1166-1177	3
	zy Logic Augmentation of Neural and Optimization Algorithms: Theoretical Aspects and Real lications. 2018 ,	1
	oulexins: A New Family of Peptides in Venom of the Emerald Jewel Wasp, Ampulex compressa. 8 , 57, 1907-1916	7
	all heat shock protein B3 (HSPB3) mutation in an axonal Charcot-Marie-Tooth disease family. 8 , 23, 60-66	8
1410 Сог	nparative Study of Computational Strategies for Protein Structure Prediction. 2018, 449-459	1
1409 WN	T10B mutations associated with isolated dental anomalies. 2018 , 93, 992-999	24
	alpha helix 1 from the first conserved region of HIV1 gp120 is reconstructed in the short NQ21 tide. 2018 , 638, 66-75	7
	octural insights into a StART-like domain in Lam4 and its interaction with sterol ligands. 2018 , , 2270-2274	12
1406 LST	-3TM12 is a member of the OATP1B family and a functional transporter. 2018 , 148, 75-87	15
1405 Des	igning a polytope for use in a broad-spectrum dengue virus vaccine. 2018 , 13, 156-161	
1404 Bin	ding of pigments to the cyanobacterial high-light-inducible protein HliC. 2018 , 137, 29-39	25
1403 Elev	vation of soybean seed oil content through selection for seed coat shininess. 2018, 4, 30-35	31
1402 S tru	octural dynamics of protein S1 on the 70S ribosome visualized by ensemble cryo-EM. 2018 , 137, 55-66	30
1401 Ide i	ntification of a novel botulinum neurotoxin gene cluster in Enterococcus. 2018, 592, 310-317	68
1400 Sig r	naling ammonium across membranes through an ammonium sensor histidine kinase. 2018 , 9, 164	22

1399	Biocatalysis of carboxylic acid reductases: phylogenesis, catalytic mechanism and potential applications. 2018 , 20, 777-792	47
1398	Involvement of interferon regulatory factor 3 from the barbel chub Squaliobarbus curriculus in the immune response against grass carp reovirus. 2018 , 648, 5-11	7
1397	Infection by the Helminth Parasite Requires Rapid Regulation of Metabolic, Virulence, and Invasive Factors to Adjust to Its Mammalian Host. 2018 , 17, 792-809	41
1396	Combined spectroscopic, molecular docking and quantum mechanics study of Etasein and p-coumaric acid interactions following thermal treatment. 2018 , 252, 163-170	36
1395	Coproheme decarboxylases - Phylogenetic prediction versus biochemical experiments. 2018 , 640, 27-36	18
1394	An integrative in silico approach to the structure of Omp33-36 in Acinetobacter baumannii. 2018 , 72, 77-86	20
1393	DmCatD, a cathepsin D-like peptidase of the hematophagous insect Dipetalogaster maxima (Hemiptera: Reduviidae): Purification, bioinformatic analyses and the significance of its interaction with lipophorin in the internalization by developing oocytes. 2018 , 105, 28-39	8
1392	Mechanism of intersubunit ketosynthase-dehydratase interaction in polyketide synthases. 2018 , 14, 270-275	23
1391	Mutation in barley ERA1 (Enhanced Response to ABA1) gene confers better photosynthesis efficiency in response to drought as revealed by transcriptomic and physiological analysis. 2018 , 148, 12-26	14
1390	Albusnodin: an acetylated lasso peptide from Streptomyces albus. 2018 , 54, 1339-1342	32
1389	Identification of potential inhibitors against nuclear Dam1 complex subunit Ask1 of Candida albicans using virtual screening and MD simulations. 2018 , 72, 33-44	7
1388	Myoglobin from common pheasant (Phasianus colchicus L.): Purification and primary structure characterization. 2018 , 42, e12477	6
1387	Isolation, purification and characterization of proteinaceous fungal the mylase inhibitor from rhizome of Cheilocostus speciosus (J.Koenig) C.D.Specht. 2018 , 111, 39-51	4
1386	Protein structure prediction. 2018 , 32,	28
1385	Identification of a novel fused gene family implicates convergent evolution in eukaryotic calcium signaling. 2018 , 19, 306	4
1384	Characterization of a novel sugar transporter involved in sugarcane bagasse degradation in. 2018 , 11, 84	18
1383	Mimicking a p53-MDM2 interaction based on a stable immunoglobulin-like domain scaffold. 2018 , 86, 802-812	1
1382	Reassignment of the human aldehyde dehydrogenase ALDH8A1 (ALDH12) to the kynurenine pathway in tryptophan catabolism. 2018 , 293, 9594-9603	17

1381	Structural insights into the molecular mechanism of mouse TRPA1 activation and inhibition. 2018 , 150, 751-762	22
1380	Genomic and biological characterization of Newcastle disease viruses isolated from migratory mallards (Anas platyrhynchos). 2018 , 163, 2179-2188	6
1379	Structure of Radical-Induced Cell Death1 Hub Domain Reveals a Common Escaffold for Disorder in Transcriptional Networks. 2018 , 26, 734-746.e7	17
1378	A novel bacteriocin BMP11 and its antibacterial mechanism on cell envelope of Listeria monocytogenes and Cronobacter sakazakii. 2018 , 91, 160-169	43
1377	Discovery and characterization of a sulfoquinovose mutarotase using kinetic analysis at equilibrium by exchange spectroscopy. 2018 , 475, 1371-1383	13
1376	In silico comparative analysis of GGDEF and EAL domain signaling proteins from the Azospirillum genomes. 2018 , 18, 20	9
1375	Improved Production of Highly Active and Pure Human Creatine Kinase MB. 2018, 28, 28-36	2
1374	The major facilitator transporter Str3 is required for low-affinity heme acquisition in. 2018, 293, 6349-6362	15
1373	Structure-Dependent Modulation of Aryl Hydrocarbon Receptor-Mediated Activities by Flavonoids. 2018 , 164, 205-217	48
1372	Mini-Review: Ergothioneine and Ovothiol Biosyntheses, an Unprecedented Trans-Sulfur Strategy in Natural Product Biosynthesis. 2018 , 57, 3309-3325	37
1371	Advances in kinome research of parasitic worms - implications for fundamental research and applied biotechnological outcomes. 2018 , 36, 915-934	6
1370	Hitting with a BAM: Selective Killing by Lectin-Like Bacteriocins. 2018 , 9,	33
1369	Ligand Binding Site Structure Influences the Evolution of Protein Complex Function and Topology. 2018 , 22, 3265-3276	10
1368	PANDA: Protein function prediction using domain architecture and affinity propagation. 2018 , 8, 3484	12
1367	A ternary complex model of Sirtuin4-NAD-Glutamate dehydrogenase. 2018 , 74, 94-104	5
1366	Clinical genetic strategies for early onset neurodegenerative diseases. 2018 , 14, 123-142	19
1365	Structural modeling identifies Plasmodium vivax 4-diphosphocytidyl-2C-methyl-d-erythritol kinase (IspE) as a plausible new antimalarial drug target. 2018 , 67, 375-385	3
1364	Elucidating the multi-targeted anti-amyloid activity and enhanced islet amyloid polypeptide binding of -wrapins. 2018 , 116, 322-332	10

1363	Lactadherin: An unappreciated haemostasis regulator and potential therapeutic agent. 2018, 101, 21-28	22
1362	Computational and biological characterization of fusion proteins of two insecticidal proteins for control of insect pests. 2018 , 8, 4837	5
1361	Use of a Tyrosine Analogue To Modulate the Two Activities of a Nonheme Iron Enzyme OvoA in Ovothiol Biosynthesis, Cysteine Oxidation versus Oxidative C-S Bond Formation. 2018 , 140, 4604-4612	29
1360	Use of quercetin in animal feed: effects on the P-gp expression and pharmacokinetics of orally administrated enrofloxacin in chicken. 2018 , 8, 4400	17
1359	Zinc knuckle of TAF1 is a DNA binding module critical for TFIID promoter occupancy. 2018 , 8, 4630	15
1358	CoABind: a novel algorithm for Coenzyme A (CoA)- and CoA derivatives-binding residues prediction. 2018 , 34, 2598-2604	8
1357	Interaction of rs316019 variants of SLC22A2 with metformin and other drugs- an analysis. 2018 , 16, 769-775	8
1356	Analysis of mutations in pncA reveals non-overlapping patterns among various lineages of Mycobacterium tuberculosis. 2018 , 8, 4628	4
1355	Identification of broadly reactive epitopes targeting major glycoproteins of Herpes simplex virus (HSV) 1 and 2 - An immunoinformatics analysis. 2018 , 61, 24-35	6
1354	Organohalide respiratory chains: composition, topology and key enzymes. 2018 , 94,	35
1354 1353	Organohalide respiratory chains: composition, topology and key enzymes. 2018 , 94, Alpha-helical domain from IL-8 of salmonids: Mechanism of action and identification of a novel antimicrobial function. 2018 , 498, 803-809	35 9
1353	Alpha-helical domain from IL-8 of salmonids: Mechanism of action and identification of a novel	
1353	Alpha-helical domain from IL-8 of salmonids: Mechanism of action and identification of a novel antimicrobial function. 2018 , 498, 803-809	9
1353 1352	Alpha-helical domain from IL-8 of salmonids: Mechanism of action and identification of a novel antimicrobial function. 2018 , 498, 803-809 Predicting rates of in vivo degradation of recombinant spider silk proteins. 2018 , 12, e97-e105 Molecular characterization and transcriptional analysis of the female-enriched chondroitin	9
1353 1352 1351	Alpha-helical domain from IL-8 of salmonids: Mechanism of action and identification of a novel antimicrobial function. 2018, 498, 803-809 Predicting rates of in vivo degradation of recombinant spider silk proteins. 2018, 12, e97-e105 Molecular characterization and transcriptional analysis of the female-enriched chondroitin proteoglycan 2 of Toxocara canis. 2018, 92, 154-160	9 14 3
1353 1352 1351 1350	Alpha-helical domain from IL-8 of salmonids: Mechanism of action and identification of a novel antimicrobial function. 2018, 498, 803-809 Predicting rates of in vivo degradation of recombinant spider silk proteins. 2018, 12, e97-e105 Molecular characterization and transcriptional analysis of the female-enriched chondroitin proteoglycan 2 of Toxocara canis. 2018, 92, 154-160 Structural and antigenic properties of thermally treated gluten proteins. 2018, 267, 43-51	9 14 3 25
1353 1352 1351 1350 1349	Alpha-helical domain from IL-8 of salmonids: Mechanism of action and identification of a novel antimicrobial function. 2018, 498, 803-809 Predicting rates of in vivo degradation of recombinant spider silk proteins. 2018, 12, e97-e105 Molecular characterization and transcriptional analysis of the female-enriched chondroitin proteoglycan 2 of Toxocara canis. 2018, 92, 154-160 Structural and antigenic properties of thermally treated gluten proteins. 2018, 267, 43-51 Mutations in ERGIC1 cause Arthrogryposis multiplex congenita, neuropathic type. 2018, 93, 160-163 Molecular Cloning, Identification, and Expression Patterns of Myostatin Gene in Water Buffalo	9143256

1345	Molecular dynamics approach to probe the antigenicity of PagN - an outer membrane protein of Salmonella Typhi. 2018 , 36, 2131-2146	2
1344	The emerging role of NPNT in tissue injury repair and bone homeostasis. 2018 , 233, 1887-1894	15
1343	Incorporation of Solvent Effect into Multi-Objective Evolutionary Algorithm for Improved Protein Structure Prediction. 2018 , 15, 1365-1378	33
1342	Mutation Spectrum and Genotype-Phenotype Analyses in a Pakistani Cohort With Hemophilia B. 2018 , 24, 741-748	3
1341	Mitochondrial dynamics: The dynamin superfamily and execution by collusion. 2018 , 76, 201-212	45
1340	Impact of a CD4 gene haplotype on the immune response in minipigs. 2018 , 70, 209-222	3
1339	DEEPre: sequence-based enzyme EC number prediction by deep learning. 2018, 34, 760-769	106
1338	Bioengineering a non-genotoxic vector for genetic modification of mesenchymal stem cells. 2018 , 152, 1-14	9
1337	Role of extracytoplasmic function sigma factor PG1660 (RpoE) in the oxidative stress resistance regulatory network of Porphyromonas gingivalis. 2018 , 33, 89-104	10
1336	Potassium Channels. 2018 ,	
1335	Assessment of contact predictions in CASP12: Co-evolution and deep learning coming of age. 2018 , 86 Suppl 1, 51-66	126
1335		126
	86 Suppl 1, 51-66	
1334	86 Suppl 1, 51-66 Studying Kv Channels Function using Computational Methods. 2018 , 1684, 321-341	2
1334	86 Suppl 1, 51-66 Studying Kv Channels Function using Computational Methods. 2018, 1684, 321-341 Spider's venom phospholipases D: A structural review. 2018, 107, 1054-1065	9
1334 1333 1332	Studying Kv Channels Function using Computational Methods. 2018, 1684, 321-341 Spider's venom phospholipases D: A structural review. 2018, 107, 1054-1065 Cysteine desulfurase is regulated by phosphorylation of Nfs1 in yeast mitochondria. 2018, 40, 29-41	9
1334 1333 1332	Studying Kv Channels Function using Computational Methods. 2018, 1684, 321-341 Spider's venom phospholipases D: A structural review. 2018, 107, 1054-1065 Cysteine desulfurase is regulated by phosphorylation of Nfs1 in yeast mitochondria. 2018, 40, 29-41 Peptide-based electrochemical biosensor for juvenile idiopathic arthritis detection. 2018, 100, 577-582 Finding the needle in the haystack: towards solving the protein-folding problem computationally.	29626

1327	Phospho-mimicking Atf1 mutants bypass the transcription activating function of the MAP kinase Sty1 of fission yeast. 2018 , 64, 97-102	8
1326	Activity of 2-(quinolin-4-yloxy)acetamides in Mycobacterium tuberculosis clinical isolates and identification of their molecular target by whole-genome sequencing. 2018 , 51, 378-384	13
1325	Cloning, expression, purification and bioactivity evaluation of a thrombin-like enzyme from Deinagkistrodon acutus venom gland library. 2018 , 40, 93-102	5
1324	Association Between Germline Mutations in BRF1, a Subunit of the RNA Polymerase III Transcription Complex, and Hereditary Colorectal Cancer. 2018 , 154, 181-194.e20	25
1323	Structural Dynamics of the GW182 Silencing Domain Including its RNA Recognition motif (RRM) Revealed by Hydrogen-Deuterium Exchange Mass Spectrometry. 2018 , 29, 158-173	4
1322	Structural characterization of the catalytic hand regulatory hubunits of phosphorylase kinase in the context of the hexadecameric enzyme complex. 2018 , 27, 485-497	3
1321	Methods for Virtual Screening of GPCR Targets: Approaches and Challenges. 2018 , 1705, 233-264	2
1320	Direct Substrate Identification with an Analog Sensitive (AS) Viral Cyclin-Dependent Kinase (v-Cdk). 2018 , 13, 189-199	4
1319	Comparative genomics reveals the presence of putative toxin-antitoxin system in Wolbachia genomes. 2018 , 293, 525-540	7
1318	Protein Structure Modeling. 2018 , 113-127	
1318	Protein Structure Modeling. 2018, 113-127 Molecular characterization, tissue distribution and differential nutritional regulation of putative Elovl5 elongase in silver barb (Puntius gonionotus). 2018, 217, 27-39	10
1317	Molecular characterization, tissue distribution and differential nutritional regulation of putative	10
1317	Molecular characterization, tissue distribution and differential nutritional regulation of putative Elovl5 elongase in silver barb (Puntius gonionotus). 2018 , 217, 27-39	
1317 1316	Molecular characterization, tissue distribution and differential nutritional regulation of putative Elovl5 elongase in silver barb (Puntius gonionotus). 2018 , 217, 27-39 Shared CaM- and S100A1-binding epitopes in the distal TRPM4 N terminus. 2018 , 285, 599-613 Structure-function analysis of ferroportin defines the binding site and an alternative mechanism of	9
1317 1316 1315	Molecular characterization, tissue distribution and differential nutritional regulation of putative Elovl5 elongase in silver barb (Puntius gonionotus). 2018, 217, 27-39 Shared CaM- and S100A1-binding epitopes in the distal TRPM4 N terminus. 2018, 285, 599-613 Structure-function analysis of ferroportin defines the binding site and an alternative mechanism of action of hepcidin. 2018, 131, 899-910 Identification and target-modifications of temporin-PE: A novel antimicrobial peptide in the	9
1317 1316 1315 1314	Molecular characterization, tissue distribution and differential nutritional regulation of putative ElovI5 elongase in silver barb (Puntius gonionotus). 2018, 217, 27-39 Shared CaM- and S100A1-binding epitopes in the distal TRPM4 N terminus. 2018, 285, 599-613 Structure-function analysis of ferroportin defines the binding site and an alternative mechanism of action of hepcidin. 2018, 131, 899-910 Identification and target-modifications of temporin-PE: A novel antimicrobial peptide in the defensive skin secretions of the edible frog, Pelophylax kl. esculentus. 2018, 495, 2539-2546	9 142 9
1317 1316 1315 1314	Molecular characterization, tissue distribution and differential nutritional regulation of putative ElovI5 elongase in silver barb (Puntius gonionotus). 2018, 217, 27-39 Shared CaM- and S100A1-binding epitopes in the distal TRPM4 N terminus. 2018, 285, 599-613 Structure-function analysis of ferroportin defines the binding site and an alternative mechanism of action of hepcidin. 2018, 131, 899-910 Identification and target-modifications of temporin-PE: A novel antimicrobial peptide in the defensive skin secretions of the edible frog, Pelophylax kl. esculentus. 2018, 495, 2539-2546 Cryo-EM structures of the human INO80 chromatin-remodeling complex. 2018, 25, 37-44 A bifunctional cellulase-xylanase of a new Chryseobacterium strain isolated from the dung of a	9 142 9 38

1309	The structure of the large regulatory Bubunit of phosphorylase kinase examined by modeling and hydrogen-deuterium exchange. 2018 , 27, 472-484	1
1308	An ultraprocessive, accurate reverse transcriptase encoded by a metazoan group II intron. 2018 , 24, 183-195	33
1307	Template-based and free modeling of I-TASSER and QUARK pipelines using predicted contact maps in CASP12. 2018 , 86 Suppl 1, 136-151	58
1306	Whole exome sequencing reveals a mutation in ARMC9 as a cause of mental retardation, ptosis, and polydactyly. 2018 , 176, 34-40	7
1305	Constructing novel chimeric DNA vaccine against Salmonella enterica based on SopB and GroEL proteins: an in silico approach. 2018 , 48, 639-655	6
1304	Evaluation of the genetic variability found in Brazilian commercial vaccines for infectious bronchitis virus. 2018 , 54, 77-85	2
1303	Structure analysis of capsid protein of Porcine circovirus type 2 from pigs with systemic disease. 2018 , 49, 351-357	7
1302	Familial choreoathetosis due to novel heterozygous mutation in PDE10A. 2018 , 176, 146-150	9
1301	Generation and testing anti-influenza human monoclonal antibodies in a new humanized mouse model (DRAGA: HLA-A2. HLA-DR4. Rag1 KO. IL-2RE KO. NOD). 2018 , 14, 345-360	16
1300	Novel frame shift mutation in ERCC6 leads to a severe form of Cockayne syndrome with postnatal growth failure and early death: A case report and brief literature review. 2018 , 97, e11636	5
1299	Reframing gene essentiality in terms of adaptive flexibility. 2018 , 12, 143	9
1298	Expression of a novel surfactant protein gene is associated with sites of extrapulmonary respiration in a lungless salamander. 2018 , 285,	2
1297	Tissue-specific alternative splicing of pentatricopeptide repeat (PPR) family genes in Arabidopsis thaliana. 2019 , 12, 569-579	3
1296	Increasing the Capping Efficiency of the Sindbis Virus nsP1 Protein Negatively Affects Viral Infection. 2018 , 9,	9
1295	Expansion and Functional Divergence of the SHORT VEGETATIVE PHASE (SVP) Genes in Eudicots. 2018 , 10, 3026-3037	13
1294	An in silico approach for construction of a chimeric protein, targeting virulence factors of Shigella spp 2018 , 11, 310	4
1293	The Proteomic Analysis of Pancreatic Exocrine Insufficiency Protein Marker in Type 2 Diabetes Mellitus Patients. 2018 , 299, 012021	
1292	Protein Design Assisted Residue Conservation and Functional Stability Analysis for Bacterial Chemotaxis. 2018 ,	

1291	Newly Identified Essential Amino Acids Affecting DGAT1 Function Revealed by Site-Directed Mutagenesis. 2018 , 19,	1
1290	Controlling SpyTag/SpyCatcher Reactivity via Redox-Gated Conformational Restriction. 2018 , 7, 1388-1393	5
1289	Evolution and functional characterization of pectate lyase PEL12, a member of a highly expanded Clonostachys rosea polysaccharide lyase 1 family. 2018 , 18, 178	13
1288	ChiE1 from Coprinopsis cinerea is Characterized as a Processive Exochitinase and Revealed to Have a Significant Synergistic Action with Endochitinase Chilll on Chitin Degradation. 2018 , 66, 12773-12782	9
1287	Characterizing the Binding Interactions between DNA-Binding Proteins, XPA and XPE: A Molecular Dynamics Approach. 2018 , 3, 15442-15454	2
1286	Efficient and robust proteome-wide approaches for cross-linking mass spectrometry. 2018 , 13, 2964-2990	77
1285	Analysis of Two New Arabinosyltransferases Belonging to the Carbohydrate-Active Enzyme (CAZY) Glycosyl Transferase Family1 Provides Insights into Disease Resistance and Sugar Donor Specificity. 2018 , 30, 3038-3057	26
1284	Molecular pathogenesis of human CD59 deficiency. 2018 , 4, e280	8
1283	An aromatic amino acid and associated helix in the C-terminus of the potato leafroll virus minor capsid protein regulate systemic infection and symptom expression. 2018 , 14, e1007451	9
1282	Extender Unit Promiscuity and Orthogonal Protein Interactions of an Aminomalonyl-ACP Utilizing Trans-Acyltransferase from Zwittermicin Biosynthesis. 2018 , 13, 3361-3373	7
1281	Phage Mu Gam protein promotes NHEJ in concert with ligase. 2018, 115, E11614-E11622	16
1280	Combining bioinformatics, cheminformatics, functional genomics and whole organism approaches for identifying epigenetic drug targets in Schistosoma mansoni. 2018 , 8, 559-570	19
1279	Comparative evolutionary histories of fungal proteases reveal gene gains in the mycoparasitic and nematode-parasitic fungus Clonostachys rosea. 2018 , 18, 171	12
1278	Phosphate Lock Residues of Acidothermus cellulolyticus Cas9 Are Critical to Its Substrate Specificity. 2018 , 7, 2908-2917	3
1277	Distinct control of PERIOD2 degradation and circadian rhythms by the oncoprotein and ubiquitin ligase MDM2. 2018 , 11,	22
1276	Novel Ethanol- and 5-Hydroxymethyl Furfural-Stimulated EGlucosidase Retrieved From a Brazilian Secondary Atlantic Forest Soil Metagenome. 2018 , 9, 2556	7
1275	Novel Findings of Anti-Filarial Drug Target and Structure-Based Virtual Screening for Drug Discovery. 2018 , 19,	5
1274	Health improvement of human hair and their reshaping using recombinant keratin K31. 2018 , 20, e00288	6

1273	Atomistic Details of Chymotrypsin Conformational Changes upon Adsorption on Silica. 2018 , 4, 4036-4050	9
1272	A novel PNPLA6 compound heterozygous mutation identified in a Chinese patient with Boucher-Neuhliser syndrome. 2018 , 18, 261-267	9
1271	Selecting near-native protein structures from ab initio models using ensemble clustering. 2018 , 6, 307-312	0
1270	Biochemical and Biophysical Roles of Cell Surface Molecules. 2018,	1
1269	F-type Lectin Domains: Provenance, Prevalence, Properties, Peculiarities, and Potential. 2018 , 1112, 345-363	1
1268	A Network Pharmacology-Based Approach to Investigate the Novel TCM Formula against Huntington's Disease and Validated by Support Vector Machine Model. 2018 , 2018, 6020197	4
1267	Molecular Mechanisms of and Mammalian Erythrocyte Interactions: A Review. 2018 , 8, 431	15
1266	Novel Mutation in a Patient With APLAID and Cutis Laxa. 2018 , 9, 2863	32
1265	Unveiling the Enigmatic Structure of TdCMO Transcripts in Durum Wheat. 2018 , 8, 270	3
1264	Biallelic mutations in nucleoporin NUP88 cause lethal fetal akinesia deformation sequence. 2018 , 14, e1007845	13
1263	Motif-Based Prediction of Plant Tubulin Phosphorylation Sites Associated with Calcium-Dependent Protein Kinases in Arabidopsis thaliana. 2018 , 52, 428-439	2
1262	Cryo-EM Structures of Eastern Equine Encephalitis Virus Reveal Mechanisms of Virus Disassembly and Antibody Neutralization. 2018 , 25, 3136-3147.e5	25
1261	Adevonin, a novel synthetic antimicrobial peptide designed from the Adenanthera pavonina trypsin inhibitor (ApTI) sequence. 2018 , 112, 438-447	4
1260	Structure-function analysis of Sedolisins: evolution of tripeptidyl peptidase and endopeptidase subfamilies in fungi. 2018 , 19, 464	O
1259	The extracellular loop of Man-PTS subunit IID is responsible for the sensitivity of Lactococcus garvieae to garvicins A, B and C. 2018 , 8, 15790	18
1258	The inhibition of acetylcholinesterase by a brain-targeting polylysine-ApoE peptide: biochemical and structural characterizations. 2018 , 2018, 155-158	
1257	Evolution of mitochondrial TAT translocases illustrates the loss of bacterial protein transport machines in mitochondria. 2018 , 16, 141	15
1256	The evolution of ependymin-related proteins. 2018 , 18, 182	4

1255	Analysis of novel domain-specific mutations in the zebrafish ndr2/cyclops gene generated using CRISPR-Cas9 RNPs. 2018 , 97, 1315-1325	9
1254	Interactive online application for the prediction, ranking and prioritisation of drug targets in Schistosoma haematobium. 2018 , 11, 605	
1253	The Widely Conserved Cluster Is Involved in Precursor Transport to the Periplasm during Scytonemin Synthesis in. 2018 , 9,	15
1252	tRNA Translocation by the Eukaryotic 80S Ribosome and the Impact of GTP Hydrolysis. 2018 , 25, 2676-2688.e	7 25
1251	Aggregation of Influenza A Virus Nuclear Export Protein. 2018 , 83, 1411-1421	2
1250	Photoinactivation of the Staphylococcus aureus Lactose-Specific EIICB Phosphotransferase Component with p-azidophenyl-ED-Galactoside and Phosphorylation of the Covalently Bound Substrate. 2018 , 28, 147-158	2
1249	The diverse role of TIGAR in cellular homeostasis and cancer. 2018 , 52, 1240-1249	23
1248	Molecular dynamics and structure function analysis show that substrate binding and specificity are major forces in the functional diversification of Eqolisins. 2018 , 19, 338	1
1247	Lanthanides-based catalysis in eukaryotes. 2018 , 70, 1067-1075	3
1246	Structure and Protein Interaction-Based Gene Ontology Annotations Reveal Likely Functions of Uncharacterized Proteins on Human Chromosome 17. 2018 , 17, 4186-4196	20
1245	Global Profiling of Lysine Acetylation in B31 Reveals Its Role in Central Metabolism. 2018 , 9, 2036	13
1244	AntiTbPdb: a knowledgebase of anti-tubercular peptides. 2018 , 2018,	26
1243	Template-Guided Protein Structure Prediction and Refinement Using Optimized Folding Landscape Force Fields. 2018 , 14, 6102-6116	10
1242	New Insights Into Sunflower (L.) FatA and FatB Thioesterases, Their Regulation, Structure and Distribution. 2018 , 9, 1496	7
1241	CRISPR-Cas9-mediated base-editing screening in mice identifies DND1 amino acids that are critical for primordial germ cell development. 2018 , 20, 1315-1325	36
1240	Computational design of chemogenetic and optogenetic split proteins. 2018 , 9, 4042	49
1239	Soil Viruses Are Underexplored Players in Ecosystem Carbon Processing. 2018 , 3,	99
1238	Conserved epitopes in variants of amastin protein of Trypanosoma cruzi for vaccine design: A bioinformatics approach. 2018 , 125, 423-430	2

1237	Can the Fact That Myelin Proteins Are Old and Break down Explain the Origin of Multiple Sclerosis in Some People?. 2018 , 7,	2
1236	Structural modulation of a periplasmic sugar-binding protein probes into its evolutionary ancestry. 2018 , 204, 498-506	
1235	Filamentous Aggregates of Tau Proteins Fulfil Standard Amyloid Criteria Provided by the Fuzzy Oil Drop (FOD) Model. 2018 , 19,	19
1234	Computational prediction of nsSNPs effects on protein function and structure, a prioritization approach for further in vitro studies applied to bovine GSTP1. 2018 , 129, 486-491	2
1233	Identification of SLAC1 anion channel residues required for CO/bicarbonate sensing and regulation of stomatal movements. 2018 , 115, 11129-11137	32
1232	Protein Dynamics in Solution by Quantitative Crosslinking/Mass Spectrometry. 2018 , 43, 908-920	34
1231	Characteristics of the essential pathogenicity factor Rv1828, a MerR family transcription regulator from Mycobacterium tuberculosis. 2018 , 285, 4424-4444	2
1230	Exploring NS3/4A, NS5A and NS5B proteins to design conserved subunit multi-epitope vaccine against HCV utilizing immunoinformatics approaches. 2018 , 8, 16107	57
1229	A Virus in American Blackcurrant () with Distinct Genome Features Reshapes Classification in the. 2018 , 10,	5
1228	Functional characterization of natural variants found on the major stress inducible 70-kDa heat shock gene, HSPA1A, in humans. 2018 , 506, 799-804	8
1227	Production and Transduction of a Human Recombinant EGlobin Chain into Proerythroid K-562 Cells To Replace Missing Endogenous EGlobin. 2018 , 15, 5665-5677	5
1226	Developing a circularly permuted variant of Renilla luciferase as a bioluminescent sensor for measuring Caspase-9 activity in the cell-free and cell-based systems. 2018 , 506, 1032-1039	2
1225	Quaternary Structure, Salt Sensitivity, and Allosteric Regulation of EAMYLASE2 From. 2018, 9, 1176	5
1224	PR/SET Domain Family and Cancer: Novel Insights from the Cancer Genome Atlas. 2018 , 19,	17
1223	An electron transfer path connects subunits of a mycobacterial respiratory supercomplex. 2018 , 362,	76
1222	Structural modeling and mRNA expression of epididymal Edefensins in GnRH immunized boars: A model for secondary hypogonadism in man. 2018 , 85, 921-933	2
1221	Large-scale whole-exome sequencing association studies identify rare functional variants influencing serum urate levels. 2018 , 9, 4228	31
1220	acl Actinobacteria Assemble a Functional Actinorhodopsin with Natively Synthesized Retinal. 2018 , 84,	6

1219	Three Antifungal Proteins From: Different Patterns of Production and Antifungal Activity. 2018 , 9, 2370	36
1218	Cytoplasmic p21 Mediates 5-Fluorouracil Resistance by Inhibiting Pro-Apoptotic Chk2. 2018 , 10,	11
1217	Application of molecular dynamics simulations to design a dual-purpose oligopeptide linker sequence for fusion proteins. 2018 , 24, 313	11
1216	In-Silico Prediction and Modeling of the Quorum Sensing LuxS Protein and Inhibition of AI-2 Biosynthesis in. 2018 , 23,	11
1215	S-Locus F-Box Proteins Are Solely Responsible for S-RNase-Based Self-Incompatibility of Pollen. 2018 , 30, 2959-2972	15
1214	Characterization of a New Glyoxal Oxidase from the Thermophilic Fungus Myceliophthora thermophila M77: Hydrogen Peroxide Production Retained in 5-Hydroxymethylfurfural Oxidation. 2018 , 8, 476	12
1213	Programmed Secretion Arrest and Receptor-Triggered Toxin Export during Antibacterial Contact-Dependent Growth Inhibition. 2018 , 175, 921-933.e14	39
1212	Machine learning and structural analysis of Mycobacterium tuberculosis pan-genome identifies genetic signatures of antibiotic resistance. 2018 , 9, 4306	73
1211	Protease inhibitors broadly effective against feline, ferret and mink coronaviruses. 2018, 160, 79-86	20
1210	High-Throughput Sequencing and the Viromic Study of Grapevine Leaves: From the Detection of Grapevine-Infecting Viruses to the Description of a New Environmental Member. 2018 , 9, 1782	24
1209	Bacterial flagellar switching: a molecular mechanism directed by the logic of an electric motor. 2018 , 24, 280	1
1208	Structure of the membrane-assembled retromer coat determined by cryo-electron tomography. 2018 , 561, 561-564	104
1207	Interaction of Haloarchaeal Gas Vesicle Proteins Determined by Split-GFP. 2018 , 9, 1897	12
1206	Analysis of structure-function relationship in porcine rotavirus A enterotoxin gene. 2018 , 19, 35-43	3
1205	Adenylate kinase potentiates the capsular polysaccharide by modulating Cps2D in Streptococcus pneumoniae D39. 2018 , 50, 1-14	4
1204	Variability of defensin genes from a Mexican endemic Triatominae: (Hemiptera: Reduviidae). 2018 , 38,	7
1203	RNA-Binding Protein RBP-P Is Required for Glutelin and Prolamine mRNA Localization in Rice Endosperm Cells. 2018 , 30, 2529-2552	22
1202	Identification of a perchloric acid-soluble protein (PSP)-like ribonuclease from Trichomonas vaginalis. 2018 , 117, 3639-3652	1

1201	Structural Prediction and Mutational Analysis of Rv3906c Gene of HRv to Determine Its Essentiality in Survival. 2018 , 2018, 6152014	23
1200	A paratransgenic strategy to block transmission of Xylella fastidiosa from the glassy-winged sharpshooter Homalodisca vitripennis. 2018 , 18, 50	11
1199	Complete genome sequence of a novel sea otterpox virus. 2018 , 54, 756-767	4
1198	Dissecting MMP P' and P' subsite sequence preferences, utilizing a positional scanning, combinatorial triple-helical peptide library. 2018 , 293, 16661-16676	1
1197	Application of alignment-free bioinformatics methods to identify an oomycete protein with structural and functional similarity to the bacterial AvrE effector protein. 2018 , 13, e0195559	6
1196	Plasmodium vivax Pv12 B-cell epitopes and HLA-DRII*-dependent T-cell epitopes in vitro antigenicity. 2018 , 13, e0203715	O
1195	Positive selection drives the evolution of endocrine regulatory bone morphogenetic protein system in mammals. 2018 , 9, 18435-18445	13
1194	Adoption of an improved PSO to explore a compound multi-objective energy function in protein structure prediction. 2018 , 72, 539-551	14
1193	Molecular characterization and expression of TLR7 and TLR8 in barbel chub (Squaliobarbus curriculus): Responses to stimulation of grass carp reovirus and lipopolysaccharide. 2018 , 83, 292-307	5
1192	Taxonomic Landscape of the Dark Proteomes: Whole-Proteome Scale Interplay Between Structural Darkness, Intrinsic Disorder, and Crystallization Propensity. 2018 , 18, e1800243	23
1191	Molecular Basis for Immunity Protein Recognition of a Type VII Secretion System Exported Antibacterial Toxin. 2018 , 430, 4344-4358	10
1190	CRISPR-Induced Deletion with SaCas9 Restores Dystrophin Expression in Dystrophic Models In Vitro and In Vivo. 2018 , 26, 2604-2616	39
1189	Biological Databases for Medicinal Plant Research. 2018 , 655-665	О
1188	Transcriptome profiling uncovers Egalactosidases of diverse domain classes influencing hypocotyl development in jute (Corchorus capsularis L.). 2018 , 156, 20-32	8
1187	Evolutionary Algorithms for the Inverse Protein Folding Problem. 2018 , 999-1023	
1186	Biochemical and Structural Characterization of TtnD, a Prenylated FMN-Dependent Decarboxylase from the Tautomycetin Biosynthetic Pathway. 2018 , 13, 2728-2738	14
1185	Identification and characterization of a novel KG42 xylanase (GH10 family) isolated from the black goat rumen-derived metagenomic library. 2018 , 469, 1-9	10
1184	Immunoinformatics-aided design of a potential multi-epitope peptide vaccine against Leishmania infantum. 2018 , 120, 1127-1139	34

1183	Modeling, dynamics and phosphoinositide binding of the pleckstrin homology domain of two novel PLCs: ¶ and ¶. 2018, 85, 130-144	О
1182	Effective in Vivo Targeting of Influenza Virus through a Cell-Penetrating/Fusion Inhibitor Tandem Peptide Anchored to the Plasma Membrane. 2018 , 29, 3362-3376	19
1181	Whole grain intake associated molecule 5-aminovaleric acid betaine decreases Ebxidation of fatty acids in mouse cardiomyocytes. 2018 , 8, 13036	18
1180	The major nectar protein of Brassica rapa is a non-specific lipid transfer protein, BrLTP2.1, with strong antifungal activity. 2018 , 69, 5587-5597	16
1179	Selection of cytochrome B mutants by putative PfNDH2 inhibitors. 2018 , 115, 6285-6290	14
1178	Signatures of diversifying selection and convergence acting on passerine Toll-like receptor 4 in an evolutionary context. 2018 , 27, 2871-2883	4
1177	The Bicarbonate Transporter SLC4A7 Plays a Key Role in Macrophage Phagosome Acidification. 2018 , 23, 766-774.e5	33
1176	Anti-haemostatic compounds from the vampire snail Cumia reticulata: Molecular cloning and in-silico structure-function analysis. 2018 , 75, 168-177	3
1175	Investigation of Solvent Hydron Exchange in the Reaction Catalyzed by the Antibiotic Resistance Protein Cfr. 2018 , 57, 4431-4439	4
1174	The unequivocal preponderance of biocomputation in clinical virology 2018 , 8, 17334-17345	2
1173	HotSpot Wizard 3.0: web server for automated design of mutations and smart libraries based on sequence input information. 2018 , 46, W356-W362	76
1172	Crystal structure and substrate specificity of ExoY, a unique T3SS mediated secreted nucleotidyl cyclase toxin from Pseudomonas aeruginosa. 2018 , 1862, 2090-2103	11
1171	Coupling Drosophila melanogaster Cryptochrome Light Activation and Oxidation of the Kv Subunit Hyperkinetic NADPH Cofactor. 2018 , 122, 6503-6510	4
1170	A nuclease-toxin and immunity system for kin discrimination in Myxococcus xanthus. 2018 , 20, 2552-2567	14
1169	Role of the Histone Acetyltransferase Rtt109 in Development and Pathogenicity of the Rice Blast Fungus. 2018 , 31, 1200-1210	12
1168	Structure of a volume-regulated anion channel of the LRRC8 family. 2018 , 558, 254-259	108
1167	Heterologous expression and enhanced production of 日,4-glucanase of Bacillus halodurans C-125 in Escherichia coli. 2018 , 34, 29-36	3
1166	Conservation and variation of the hepatitis E virus ORF2 capsid protein. 2018 , 675, 157-164	6

Computational Methods Applicable to the Discovery of Small-Molecule Inhibitors of 1165 Protein-Protein Interactions. 2018, 73-94 A Novel Heterozygous Missense Mutation in Leads to Autosomal Dominant Riggs Type of 1164 Congenital Stationary Night Blindness. 2018, 2018, 7694801 1163 A Computational Approach Using Bioinformatics to Screening Drug Targets for Species. 2018, 2018, 6813467 6 1162 Comment on 'YcgC represents a new protein deacetylase family in prokaryotes'. 2018, 7, 7 Pirin: A novel redox-sensitive modulator of primary and secondary metabolism in Streptomyces. 1161 15 2018, 48, 254-268 The Hyr1 protein from the fungus Candida albicans is a cross kingdom immunotherapeutic target 1160 19 for Acinetobacter bacterial infection. 2018, 14, e1007056 Expression, functional analysis and mutation of a novel neutral zearalenone-degrading enzyme. 1159 15 **2018**, 118, 1284-1292 Intrinsically disordered N-terminal domain of the Helicoverpa armigera Ultraspiracle stabilizes the 1158 3 dimeric form via a scorpion-like structure. 2018, 183, 167-183 1157 Optimal protein structure extraction with clustering algorithm. 2018, IL-1RA VNTR and IL-1#845G>T polymorphisms and risk of idiopathic male infertility in Iranian 21 men: A case-control study and an in silico analysis. 2018, 50, e13081 MR-REX: molecular replacement by cooperative conformational search and occupancy optimization 1155 1 on low-accuracy protein models. 2018, 74, 606-620 1154 Thymol Induces Conidial Apoptosis in Aspergillus flavus via Stimulating K Eruption. 2018, 66, 8530-8536 14 Sensitivity of the C-Terminal Nuclease Domain of Kaposi's Sarcoma-Associated Herpesvirus ORF29 7 to Two Classes of Active-Site Ligands. 2018, 62, Characterization of a novel secretory spherical body protein in Babesia orientalis and Babesia orientalis-infected erythrocytes. 2018, 11, 433 1151 Site-specific PEGylation of Human Growth Hormone by Mutated Sortase A. 2018, 34, 428-433 6 Complex Evolutionary History of Translation Elongation Factor 2 and Diphthamide Biosynthesis in 1150 24 Archaea and Parabasalids. 2018, 10, 2380-2393 COACH-D: improved protein-ligand binding sites prediction with refined ligand-binding poses 1149 77 through molecular docking. 2018, 46, W438-W442 1148 Identification of a diphtheria toxin-like gene family beyond the Corynebacterium genus. 2018, 592, 2693-2705 10

1147	Directly light-regulated binding of RGS-LOV photoreceptors to anionic membrane phospholipids. 2018 , 115, E7720-E7727	31
1146	Metagenomic Mining and Functional Characterization of a Novel KG51 Bifunctional Cellulase/Hemicellulase from Black Goat Rumen. 2018 , 66, 9034-9041	21
1145	Binding Specificity of Two PBPs in the Yellow Peach Moth (Guen E). 2018, 9, 308	7
1144	Characterization of an Atypical Metalloproteinase Inhibitors Like Protein (Sbp8-1) From Scallop Byssus. 2018 , 9, 597	9
1143	Biodegradation of lignin by Pseudomonas sp. Q18 and the characterization of a novel bacterial DyP-type peroxidase. 2018 , 45, 913-927	22
1142	small basic protein (Sbp) forms amyloid fibrils, consistent with its function as a scaffolding protein in biofilms. 2018 , 293, 14296-14311	13
1141	Sequence-based prediction of physicochemical interactions at protein functional sites using a function-and-interaction-annotated domain profile database. 2018 , 19, 204	2
1140	The phenotypic spectrum of germline variants: from isolated sideroblastic anemia to mitochondrial myopathy, lactic acidosis and sideroblastic anemia 2. 2018 , 103, 2008-2015	14
1139	Genomic screening of new putative antiviral lectins from Amazonian cyanobacteria based on a bioinformatics approach. 2018 , 86, 1047-1054	5
1138	MmpL3 as a Target for the Treatment of Drug-Resistant Nontuberculous Mycobacterial Infections. 2018 , 9, 1547	26
1137	Tachykinin-3 Genes and Peptides Characterized in a Basal Teleost, the European Eel: Evolutionary Perspective and Pituitary Role. 2018 , 9, 304	10
1136	Computational Protein Phenotype Characterization of IL10RA Mutations Causative to Early Onset Inflammatory Bowel Disease (IBD). 2018 , 9, 146	11
1135	Identification of DEAD-Box RNA Helicase DDX41 as a Trafficking Protein That Involves in Multiple Innate Immune Signaling Pathways in a Zebrafish Model. 2018 , 9, 1327	18
1134	Discovery of Distinctin-Like-Peptide-PH (DLP-PH) From the Skin Secretion of , a Prototype of a Novel Family of Antimicrobial Peptide. 2018 , 9, 541	8
1133	A Carbohydrate Moiety of Secreted Stage-Specific Glycoprotein 4 Participates in Host Cell Invasion by Extracellular Amastigotes. 2018 , 9, 693	10
1132	Charge and Polarity Preferences for -Glycosylation: A Genome-Wide Study and Its Implications Regarding Constitutive Proliferation and Adhesion of Carcinoma Cells. 2018 , 8, 29	5
1131	Fungal Screening on Olive Oil for Extracellular Triacylglycerol Lipases: Selection of a Trichoderma harzianum Strain and Genome Wide Search for the Genes. 2018 , 9,	4
1130	Differential Enzymatic Activity of Rat ADAR2 Splicing Variants Is Due to Altered Capability to Interact with RNA in the Deaminase Domain. 2018 , 9,	7

1129	Genome-Wide Identification of the Alba Gene Family in Plants and Stress-Responsive Expression of the Rice Alba Genes. 2018 , 9,	12
1128	Production of Plant Secondary Metabolites: Examples, Tips and Suggestions for Biotechnologists. 2018 , 9,	116
1127	EpsN from Bacillus subtilis 168 has UDP-2,6-dideoxy 2-acetamido 4-keto glucose aminotransferase activity in vitro. 2018 , 28, 802-812	6
1126	Strand-Specific Dual RNA Sequencing of Bronchial Epithelial Cells Infected with Influenza A/H3N2 Viruses Reveals Splicing of Gene Segment 6 and Novel Host-Virus Interactions. 2018 , 92,	18
1125	A Comparative Study of Modern Homology Modeling Algorithms for Rhodopsin Structure Prediction. 2018 , 3, 7555-7566	29
1124	Structure-Activity Relationships of Thiazolyl Resorcinols, Potent and Selective Inhibitors of Human Tyrosinase. 2018 , 19,	23
1123	CD9 and CD81 Interactions and Their Structural Modelling in Sperm Prior to Fertilization. 2018 , 19,	14
1122	Molecular Evolution and Expression Divergence of Gene Family in Plants. 2018, 19,	5
1121	Novel Insights from Comparative In Silico Analysis of Green Microalgal Cellulases. 2018, 19,	5
1120	The Cyanobacterial Ribosomal-Associated Protein LrtA from sp. PCC 6803 Is an Oligomeric Protein in Solution with Chameleonic Sequence Properties. 2018 , 19,	4
1119	Characterization of Human Type C Enterotoxin Produced by Clinical S. epidermidis Isolates. 2018 , 10,	4
1118	Antimicrobial and Chemotactic Activity of Scorpion-Derived Peptide, ToAP2, against. 2018, 10,	11
1117	Tick-Borne Encephalitis Virus: A Structural View. 2018 , 10,	31
1116	Genome-Wide Identification and Analysis of Sodium Proton Antiporter (NHX) and Human Sodium Proton Exchanger (NHE) Homologs in. 2018 , 9,	21
1115	Convergent evolution of unusual complex I homologs with increased proton pumping capacity: energetic and ecological implications. 2018 , 12, 2668-2680	20
1114	Prespliceosome structure provides insights into spliceosome assembly and regulation. 2018 , 559, 419-422	65
1113	In vitro genomic and proteomic evidence of a type IV pili-like structure in the fish pathogen Piscirickettsia salmonis. 2018 , 365,	8
1112	Type-3 von Willebrand disease in India-Clinical spectrum and molecular profile. 2018 , 24, 930-940	6

1111	Genome-wide association studies and expression-based quantitative trait loci analyses reveal roles of HCT2 in caffeoylquinic acid biosynthesis and its regulation by defense-responsive transcription factors in Populus. 2018 , 220, 502-516	51
1110	In silico prediction, phylogenetic and bioinformatic analysis of SoPCS gene, survey of its protein characterization and gene expression in response to cadmium in Saccharum officinarum. 2018 , 163, 7-18	8
1109	Effects of substrate binding site residue substitutions of xynA from Bacillus amyloliquefaciens on substrate specificity. 2018 , 18, 9	8
1108	Insight into vitamin B -dependent epilepsy due to PLPBP (previously PROSC) missense mutations. 2018 , 39, 1002-1013	17
1107	Selenoprotein W as a molecular target of d-amino acid oxidase is regulated by d-amino acid in chicken neurons. 2018 , 10, 751-758	8
1106	Overexpressed HDAC8 in cervical cancer cells shows functional redundancy of tubulin deacetylation with HDAC6. 2018 , 16, 20	31
1105	Structure of an Ancient Respiratory System. 2018 , 173, 1636-1649.e16	61
1104	Dual binding in cohesin-dockerin complexes: the energy landscape and the role of short, terminal segments of the dockerin module. 2018 , 8, 5051	4
1103	Three-dimensional spatial analysis of missense variants in RTEL1 identifies pathogenic variants in patients with Familial Interstitial Pneumonia. 2018 , 19, 18	6
1102	Towards a more predictable plant breeding pipeline with CRISPR/Cas-induced allelic series to optimize quantitative and qualitative traits. 2018 , 45, 218-225	29
1101	Unraveling the mechanism of the cadherin-catenin-actin catch bond. 2018 , 14, e1006399	9
1100	A novel glycosyltransferase catalyses the transfer of glucose to glucosylated anthocyanins in purple sweet potato. 2018 , 69, 5444-5459	16
1099	Domains with highest heparan sulfate-binding affinity reside at opposite ends in BMP2/4 BMP5/6/7: Implications for function. 2018 , 293, 14371-14383	21
1098	Pattern Formation in the Longevity-Related Expression of Heat Shock Protein-16.2 in Caenorhabditis elegans. 2018 , 80, 2669-2697	4
1097	Natural and targeted isovariants of the rice actin depolymerizing factor 2 can alter its functional and regulatory binding properties. 2018 , 503, 1516-1523	O
1096	Molecular characterization of a novel ovodefensin gene in chickens. 2018 , 678, 233-240	14
1095	B-cell and T-cell epitope identification with stability analysis of AI-2 import ATP-binding cassette LsrA from S. typhiIn silico approach. 2018 , 123, 487-495	2
1094	Divergent genes of teleosts and mammals share conserved roles in erythropoiesis: analysis using transgenic and mutant zebrafish. 2018 , 7,	5

1093 Ceruloplasmin, a moonlighting protein in fish. 2018 , 82, 460-468	11
A seven-helix protein constitutes stress granules crucial for regulating translation during human-to-mosquito transmission of Plasmodium falciparum. 2018 , 14, e1007249	13
The crystal structure of KSHV ORF57 reveals dimeric active sites important for protein stability and function. 2018 , 14, e1007232	10
Procyanidin B2 ameliorates free fatty acids-induced hepatic steatosis through regulating TFEB-mediated lysosomal pathway and redox state. 2018 , 126, 269-286	72
Defining Dynamics of Membrane-Bound Pyrophosphatases by Experimental and Computational Single-Molecule FRET. 2018 , 607, 93-130	2
HDV Can Constrain HBV Genetic Evolution in HBsAg: Implications for the Identification of Innovative Pharmacological Targets. 2018 , 10,	3
1087 Electrostatic Potential in the tRNA Binding Evolution of Dihydrouridine Synthases. 2018 , 57, 5407-5416	4 4
1086 PvaxDB: a comprehensive structural repository of Plasmodium vivax proteome. 2018 , 2018,	2
A Leishmania-specific gene upregulated at the amastigote stage is crucial for parasite survival. 2018 , 117, 3215-3228	2
CD19 Alterations Emerging after CD19-Directed Immunotherapy Cause Retention of the Misfolded Protein in the Endoplasmic Reticulum. 2018 , 38,	38
The Expression Pattern of PLIN2 in Differentiated Adipocytes from Qinchuan Cattle Analysis of Its Protein Structure and Interaction with CGI-58. 2018 , 19,	10
Characterization of biochemical properties of an apurinic/apyrimidinic endonuclease from Helicobacter pylori. 2018 , 13, e0202232	3
Severe Osteomalacia with Dent Disease Caused by a Novel Intronic Mutation of the CLCN5 gene. 2018 , 57, 3603-3610	4
Combined proteomic and functional analysis reveals rich sources of protein diversity in skin mucus and venom from the Scorpaena plumieri fish. 2018 , 187, 200-211	12
Persulfide Dioxygenase From : Variable Roles of Cysteine Residues and Hydrogen Bond Networks of the Active Site. 2018 , 9, 1610	2
Teleost-specific TLR25 identified from Schizothorax prenanti may recognize bacterial/viral components and activate NF- B and type I IFNs signaling pathways. 2018 , 82, 361-370	12
The myosin light-chain kinase MLCK-1 relocalizes during Caenorhabditis elegans ovulation to promote actomyosin bundle assembly and drive contraction. 2018 , 29, 1975-1991	7
Protein folding prediction in the HP model using ions motion optimization with a greedy algorithm. 2018 , 11, 17	10

1075	Structure of the human PKD1-PKD2 complex. 2018 , 361,	93
1074	MMB triazole analogs are potent NF- B inhibitors and anti-cancer agents against both hematological and solid tumor cells. 2018 , 157, 562-581	18
1073	Characterization of Gonadotropin-Releasing Hormone (GnRH) Genes From Cartilaginous Fish: Evolutionary Perspectives. 2018 , 12, 607	11
1072	Structural Studies of Predicted Ligand Binding Sites and Molecular Docking Analysis of Slc2a4 as a Therapeutic Target for the Treatment of Cancer. 2018 , 19,	23
1071	Phage display-derived antibody fragments against conserved regions of VacA toxin of Helicobacter pylori. 2018 , 102, 6899-6913	13
1070	Mammalian Solute Carrier (SLC)-like transporters of Legionella pneumophila. 2018 , 8, 8352	4
1069	NtTPN1: a RPP8-like R gene required for Potato virus Y-induced veinal necrosis in tobacco. 2018 , 95, 700	13
1068	Rht23 (5Dq') likely encodes a Q homeologue with pleiotropic effects on plant height and spike compactness. 2018 , 131, 1825-1834	8
1067	EcXyl43 Ekylosidase: molecular modeling, activity on natural and artificial substrates, and synergism with endoxylanases for lignocellulose deconstruction. 2018 , 102, 6959-6971	3
1066	The functions of caspase in whitefly Bemisia tabaci apoptosis in response to ultraviolet irradiation. 2018 , 27, 739-751	13
1065	Protein Complexes and Virus-Like Particle Technology. 2018 , 88, 379-405	7
1064	Identification and validation of a novel panel of Plasmodium knowlesi biomarkers of serological exposure. 2018 , 12, e0006457	18
1063	Biotic and Abiotic Stress Tolerance in Plants. 2018,	6
1062	Action mechanism of melittin-derived antimicrobial peptides, MDP1 and MDP2, de novo designed against multidrug resistant bacteria. 2018 , 50, 1231-1243	23
1061	Improving Sequence-Based Prediction of Protein-Peptide Binding Residues by Introducing Intrinsic Disorder and a Consensus Method. 2018 , 58, 1459-1468	14
1060	Identification and in silico analysis of functional SNPs of human TAGAP protein: A comprehensive study. 2018 , 13, e0188143	42
1059	Bioinformatics Resources for the Stress Biology of Plants. 2018 , 367-386	3
1058	Molecular basis of dimer formation during the biosynthesis of benzofluorene-containing atypical angucyclines. 2018 , 9, 2088	37

1057	Immunity to LuloHya and Lundep, the salivary spreading factors from Lutzomyia longipalpis, protects against Leishmania major infection. 2018 , 14, e1007006	19
1056	Protein Structure Databases. 2019 , 460-471	
1055	Hemizygous UBA5 missense mutation unmasks recessive disorder in a patient with infantile-onset encephalopathy, acquired microcephaly, small cerebellum, movement disorder and severe neurodevelopmental delay. 2019 , 62, 97-102	5
1054	Toward a better understanding of the interaction between somatostatin receptor 2 and its ligands: a structural characterization study using molecular dynamics and conceptual density functional theory. 2019 , 37, 3081-3102	4
1053	A dedicated glyceraldehyde-3-phosphate dehydrogenase is involved in the biosynthesis of volatile sesquiterpenes in Trichoderma virens-evidence for the role of a fungal GAPDH in secondary metabolism. 2019 , 65, 243-252	9
1052	Protein Structural Bioinformatics: An Overview. 2019 , 445-459	9
1051	Ab initio Protein Structure Prediction. 2019 , 62-76	
1050	Protocol for Protein Structure Modelling. 2019 , 252-272	6
1049	An 18 bps in-frame deletion mutation in RUNX2 gene is a population polymorphism rather than a pathogenic variant. 2019 , 62, 124-128	7
1048	Genome Analysis Ildentification of Genes Involved in Host-Pathogen Protein-Protein Interaction Networks. 2019 , 410-424	
1047	Dissecting mRNA decay and translation inhibition during iron deficiency. 2019 , 65, 139-145	7
1046	Characterization of the gene encoding 4-coumarate:CoA ligase in Coleus forskohlii. 2019 , 28, 203-210	6
1045	The activity and action mechanism of novel short selective LL-37-derived anticancer peptides against clinical isolates of Escherichia coli. 2019 , 93, 75-83	16
1044	Identification of UAP1L1 as a critical factor for protein O-GlcNAcylation and cell proliferation in human hepatoma cells. 2019 , 38, 317-331	13
1043	Synthetic cementum protein 1-derived peptide regulates mineralization in vitro and promotes bone regeneration in vivo. 2019 , 33, 1167-1178	9
1042	Molecular cloning and characterization of a lipid transfer protein gene (PsLTP1) from Pinus sylvestris (L.). 2019 , 30, 1149-1158	
1041	Designing a Novel Multi-epitope Peptide Vaccine Against Pathogenic Shigella spp. Based Immunoinformatics Approaches. 2019 , 25, 541-553	9
1040	Cloning and identification of Bartonella & enolase as a plasminogen-binding protein. 2019, 135, 103651	1

1039	Characterization of Female Reproductive Proteases in a Butterfly from Functional and Evolutionary Perspectives. 2019 , 92, 579-590	5
1038	Convergent evolution in the mechanisms of ACBD3 recruitment to picornavirus replication sites. 2019 , 15, e1007962	13
1037	Cloning, expression and characterization of a novel fructosyltransferase from and its application in the synthesis of fructooligosaccharides 2019 , 9, 23856-23863	5
1036	Family of hereditary fibrosing poikiloderma with tendon contractures, myopathy and pulmonary fibrosis caused by a novel FAM111B mutation. 2019 , 46, 1014-1018	1
1035	Flavonoid Versus Artemisinin Anti-malarial Activity in Whole-Leaf Extracts. 2019, 10, 984	14
1034	Synthesis, Biological Evaluation and In Silico Computational Studies of 7-Chloro-4-(1-1,2,3-triazol-1-yl)quinoline Derivatives: Search for New Controlling Agents against (Lepidoptera: Noctuidae) Larvae. 2019 , 67, 9210-9219	7
1033	Differential homotypic and heterotypic interactions of antigen 43 (Ag43) variants in autotransporter-mediated bacterial autoaggregation. 2019 , 9, 11100	7
1032	Changes on the viral capsid surface during the evolution of porcine circovirus type 2 (PCV2) from 2009 till 2018 may lead to a better receptor binding. 2019 , 5, vez026	10
1031	Expression in eukaryotic cells and purification of synthetic gene encoding enterocin P: a bacteriocin with broad antimicrobial spectrum. 2019 , 9, 6	7
1030	Structural and Functional Properties of the Capsid Protein of Dengue and Related. 2019 , 20,	14
1029	Biochemical characterization and low-resolution SAXS shape of a novel GH11 exo-1,4-Ekylanase identified in a microbial consortium. 2019 , 103, 8035-8049	6
1028	DeepGOPlus: improved protein function prediction from sequence. 2020 , 36, 422-429	70
1027	The predominance of nucleotidyl activation in bacterial phosphonate biosynthesis. 2019, 10, 3698	5
1026	Analysis of Vibrio cholerae genomes identifies new type VI secretion system gene clusters. 2019 , 20, 163	16
1025	Advances in protein structure prediction and design. 2019 , 20, 681-697	215
1024	The ghrelin -acyltransferase structure reveals a catalytic channel for transmembrane hormone acylation. 2019 , 294, 14166-14174	14
1023	Molecular cloning and expression pattern of IGFBP-2a in black porgy (Acanthopagrus schlegelii) and evolutionary analysis of IGFBP-2s in the species of Perciformes. 2019 , 45, 1731-1745	2
1022	Structural determination of the large photosystem II-light-harvesting complex II supercomplex of using nonionic amphipol. 2019 , 294, 15003-15013	23

Deciphering the Molecular Recognition Mechanism of Multidrug Resistance NorA Efflux Pump Using a Supervised Molecular Dynamics Approach. 2019 , 20,	9
1020 Structural Mapping of Missense Mutations in the Pex1/Pex6 Complex. 2019 , 20,	9
Identification of a prosurvival neuroprotective mitochondrial peptide in a mammalian hibernator. 2019 , 37, 494-503	6
Improving the specific activity and pH stability of xylanase XynHBN188A by directed evolution. 2019, 6,	8
Improved fragment sampling for ab initio protein structure prediction using deep neural networks. 2019 , 1, 347-355	15
1016 A novel thermostable GH5 Ekylosidase from Thermogemmatispora sp. T81. 2019 , 53, 57-64	7
High Functioning Autism with Missense Mutations in Synaptotagmin-Like Protein 4 (SYTL4) and Transmembrane Protein 187 (TMEM187) Genes: SYTL4- Protein Modeling, Protein-Protein Interaction, Expression Profiling and MicroRNA Studies. 2019 , 20,	10
A novel peptide-based sensor platform for detection of anti-Toxoplasma gondii immunoglobulins. 2019, 175, 112778	5
Human Corneal Expression of SLC4A11, a Gene Mutated in Endothelial Corneal Dystrophies. 2019 , 9, 9681	13
1012 PgFur Is a Member of a Novel Fur Subfamily With Non-canonical Function. 2019 , 9, 233	7
Enhancing -cedrol production in by fusion expression of farnesyl pyrophosphate synthase and -cedrol synthase. 2019 , 19, 606-616	3
Enzyme activity and structural features of three single-domain phloem cyclophilins from Brassica napus. 2019 , 9, 9368	2
1009 Screening of Aptamers Configuration against Hepatitis B Surface Antigen. 2019 , 2019, 6912914	14
Identification and Characterization of a Thermotolerant TILLING Allele of Heat Shock Binding Protein 1 in Tomato. 2019 , 10,	8
Characterisation of a niche-specific excretory-secretory peroxiredoxin from the parasitic nematode Teladorsagia circumcincta. 2019 , 12, 339	4
Identification of a crucial amino acid implicated in the hydroxylation/desaturation ratio of CpFAH12 bifunctional hydroxylase. 2019 , 116, 2451-2462	6
Protein structure prediction using sparse NOE and RDC restraints with Rosetta in CASP13. 2019 , 87, 1341-1350	4
One Aeromonas salmonicida subsp. salmonicida isolate with a pAsa5 variant bearing antibiotic resistance and a pRAS3 variant making a link with a swine pathogen. 2019 , 690, 313-320	15

1003	Lamin A molecular compression and sliding as mechanisms behind nucleoskeleton elasticity. 2019 , 10, 3056	27
1002	Phage N15 protelomerase resolves its tos recognition site into hairpin telomeres within mammalian cells. 2019 , 583, 113361	3
1001	The Med31 Conserved Component of the Divergent Mediator Complex in Tetrahymena thermophila Participates in Developmental Regulation. 2019 , 29, 2371-2379.e6	7
1000	The COOH-Terminal Proline-Rich Region of GRP78 Is a Key Regulator of Its Cell Surface Expression and Viability of Tamoxifen-Resistant Breast Cancer Cells. 2019 , 21, 837-848	14
999	A Structural Model of the Inactivation Gate of Voltage-Activated Potassium Channels. 2019, 117, 377-387	3
998	Structural analysis of the A[11-42) amyloid fibril based on hydrophobicity distribution. 2019 , 33, 665-675	6
997	An extracellular acidic cleft confers profound H-sensitivity to epithelial sodium channels containing the Bubunit in. 2019 , 294, 12507-12520	5
996	Alternative Functional Paralogs in. 2019 , 10, 1370	O
995	Genomic diversity and novel genome-wide association with fruit morphology in Capsicum, from 746k polymorphic sites. 2019 , 9, 10067	25
994	Assembling multidomain protein structures through analogous global structural alignments. 2019 , 116, 15930-15938	30
993	Dafachronic acid promotes larval development in Haemonchus contortus by modulating dauer signalling and lipid metabolism. 2019 , 15, e1007960	19
992	Structure-based rational design of a novel chimeric PD1-NKG2D receptor for natural killer cells. 2019 , 114, 108-113	20
991	Epitope-based immunoinformatics study of a novel Hla-MntC-SACOL0723 fusion protein from Staphylococcus aureus: Induction of multi-pattern immune responses. 2019 , 114, 88-99	8
990	Hotspots of Sequence Variability in Gut Microbial Genes Encoding Pro-Inflammatory Factors Revealed by Oligotyping. 2019 , 10, 631	
989	Deep-learning contact-map guided protein structure prediction in CASP13. 2019 , 87, 1149-1164	108
988	Genotype-phenotype correlation of gangliosidosis mutations using in silico tools and homology modeling. 2019 , 20, 100495	8
987	Identification of most damaging nsSNPs in human CCR6 gene: In silico analyses. 2019 , 46, 459-471	10
986	Predicting Specificities Under the Non-self Gametophytic Self-Incompatibility Recognition Model. 2019 , 10, 879	3

985	Unexpected host dependency of Antarctic Nanohaloarchaeota. 2019 , 116, 14661-14670	69
984	Assessing the development and treatment of rheumatoid arthritis using multiparametric photoacoustic and ultrasound imaging. 2019 , 12, e201900127	8
983	Muskox myoglobin: purification, characterization and kinetics studies compared with cattle and water buffalo myoglobins. 2019 , 99, 6278-6286	7
982	In silico analysis of missense mutations in exons 1-5 of the F9 gene that cause hemophilia B. 2019 , 20, 363	2
981	Next Generation Techniques for Determination of Protein-Protein Interactions: Beyond the Crystal Structure. 2019 , 7, 61-71	2
980	The Use of Diffusion Calculations and Monte Carlo Simulations to Understand the Behavior of Cells in Communities. 2019 , 17, 684-688	1
979	Impact of hepatitis B virus genotype F on in vitro diagnosis: detection efficiency of HBsAg from Amerindian subgenotypes F1b and F4. 2019 , 164, 2297-2307	3
978	AhlX, an -acylhomoserine Lactonase with Unique Properties. 2019 , 17,	3
977	PhyreRisk: A Dynamic Web Application to Bridge Genomics, Proteomics and 3D Structural Data to Guide Interpretation of Human Genetic Variants. 2019 , 431, 2460-2466	13
976	Production and characterization of monoclonal antibodies against the DNA binding domain of the RE1-silencing transcription factor. 2019 , 166, 393-402	3
975	A novel thermostable and halophilic thioredoxin reductase from the Red Sea Atlantis II hot brine pool. 2019 , 14, e0217565	6
974	A theoretical and experimental approach to evaluate zein-calcium interaction in nixtamalization process. 2019 , 297, 124995	3
973	DNA processing by the MOBH family relaxase Tral encoded within the gonococcal genetic island. 2019 , 47, 8136-8153	O
972	Human single-chain antibodies that neutralize Pseudomonas aeruginosa-exotoxin A-mediated cellular apoptosis. 2019 , 9, 14928	8
971	Highly ABA-Induced 1 (HAI1)-Interacting protein HIN1 and drought acclimation-enhanced splicing efficiency at intron retention sites. 2019 , 116, 22376-22385	12
970	Sequence specificity despite intrinsic disorder: How a disease-associated Val/Met polymorphism rearranges tertiary interactions in a long disordered protein. 2019 , 15, e1007390	7
969	Quantitative Proteomics Reveals a Role for SERINE/ARGININE-Rich 45 in Regulating RNA Metabolism and Modulating Transcriptional Suppression the ASAP Complex in. 2019 , 10, 1116	4
968	A TiN Nanorod Array 3D Hierarchical Composite Electrode for Ultrahigh-Power-Density Bromine-Based Flow Batteries. 2019 , 31, e1904690	23

967	Characterization of a novel glycosylated glutathione transferase of , closest relative of the human river blindness parasite. 2019 , 146, 1773-1784	1
966	Molecular dynamics and docking reveal the potency of novel GTP derivatives against RNA dependent RNA polymerase of genotype 4a HCV. 2019 , 238, 116958	30
965	Guanylin, Uroguanylin and Guanylate Cyclase-C Are Expressed in the Gastrointestinal Tract of Horses. 2019 , 10, 1237	1
964	Essentials of Bioinformatics, Volume II. 2019 ,	1
963	Detecting distant-homology protein structures by aligning deep neural-network based contact maps. 2019 , 15, e1007411	25
962	Butyrophilin-like 3 Directly Binds a Human VI T Cell Receptor Using a Modality Distinct from Clonally-Restricted Antigen. 2019 , 51, 813-825.e4	56
961	Vigilin protein Vgl1 is required for heterochromatin-mediated gene silencing in. 2019, 294, 18029-18040	6
960	Targeting of copper-trafficking chaperones causes gene-specific systemic pathology in : prospective expansion of mutational landscapes that regulate tumor resistance to cisplatin. 2019 , 8,	4
959	Identification of a Killer Toxin from with EGlucanase Activity. 2019, 11,	6
958	Highly conserved intracellular H208 residue influences agonist selectivity in bitter taste receptor T2R14. 2019 , 1861, 183057	2
957	Achillin Increases Chemosensitivity to Paclitaxel, Overcoming Resistance and Enhancing Apoptosis in Human Hepatocellular Carcinoma Cell Line Resistant to Paclitaxel (Hep3B/PTX). 2019 , 11,	7
956	Switching the Post-translational Modification of Translation Elongation Factor EF-P. 2019 , 10, 1148	10
955	In silico structural and functional characterization and phylogenetic study of alkaline phosphatase in bacterium, Rhizobium leguminosarum (Frank 1879). 2019 , 83, 107142	1
954	Effect of Euphorbia factor L1 on intestinal barrier impairment and defecation dysfunction in Caenorhabditis elegans. 2019 , 65, 153102	3
953	Contribution of SLC22A12 on hypouricemia and its clinical significance for screening purposes. 2019 , 9, 14360	5
952	IPANDA. 2019 ,	2
951	Both gain-of-function and loss-of-function de novo CACNA1A mutations cause severe developmental epileptic encephalopathies in the spectrum of Lennox-Gastaut syndrome. 2019 , 60, 1881-189	4 34
950	GLTSCR1 Negatively Regulates BRD4-Dependent Transcription Elongation and Inhibits CRC Metastasis. 2019 , 6, 1901114	4

949	A novel LAMP2 p.G93R mutation associated with mild Danon disease presenting with familial hypertrophic cardiomyopathy. 2019 , 7, e00941	4
948	A theoretical and experimental investigation of the effect of sodium dodecyl sulfate on the structural and conformational properties of bovine Lasein. 2019 , 15, 1551-1561	8
947	The chloramphenicol/H+ antiporter CraA of Acinetobacter baumannii AYE reveals a broad substrate specificity. 2019 , 74, 1192-1201	6
946	Synapsins are expressed at neuronal and non-neuronal locations in Octopus vulgaris. 2019 , 9, 15430	3
945	Atomic Structure of the Francisella T6SS Central Spike Reveals a Unique Helical Lid and a Putative Cargo. 2019 , 27, 1811-1819.e6	2
944	Low Frequency of MKRN3 and DLK1 Variants in Chinese Children with Central Precocious Puberty. 2019 , 2019, 9879367	7
943	NFE2L3 Controls Colon Cancer Cell Growth through Regulation of DUX4, a CDK1 Inhibitor. 2019 , 29, 1469-1481.e9	30
942	Intelligent Design of 14-3-3 Docking Proteins Utilizing Synthetic Evolution Artificial Intelligence (SYN-AI). 2019 , 4, 18948-18960	1
941	Interaction of ArmZ with the DNA-binding domain of MexZ induces expression of multidrug efflux pump genes and antimicrobial resistance in. 2019 ,	6
940	Differences in protein structural regions that impact functional specificity in GT2 family Eglucan synthases. 2019 , 14, e0224442	5
939	Molecular dynamics investigations for the prediction of molecular interaction of cauliflower mosaic virus transmission helper component protein complex with stylet's cuticular protein and its docking studies with annosquamosin-A encapsulated in nano-porous Silica. 2019 , 30, 413-425	1
938	Cryo-EM Structure of the Human FLCN-FNIP2-Rag-Ragulator Complex. 2019 , 179, 1319-1329.e8	51
937	Computational Nanoscopy of Tight Junctions at the Blood-Brain Barrier Interface. 2019 , 20,	11
936	The Rich World of p53 DNA Binding Targets: The Role of DNA Structure. 2019 , 20,	18
935	Molecular Dynamics Study of Binding of Substrates Bearing Two Positively Charged Residues to Oligopeptidase B from Serratia proteamaculans. 2019 , 64, 758-764	3
934	The olfactory secretome varies according to season in female sheep and goat. 2019 , 20, 794	4
933	Molecular evolution of cytochrome C oxidase-I protein of insects living in Saudi Arabia. 2019 , 14, e0224336	2
932	An in silico approach to characterize nonsynonymous SNPs and regulatory SNPs in human TOX3 gene. 2019 , 98, 1	О

931	Opposite Charge Movements Within the Photoactive Site Modulate Two-Step Channel Closing in GtACR1. 2019 , 117, 2034-2040	4
930	Voltage vs. Ligand II: Structural insights of the intrinsic flexibility in cyclic nucleotide-gated channels. 2019 , 13, 382-399	2
929	Characterization of the mutation spectrum in a Pakistani cohort of type 3 von Willebrand disease. 2019 , 25, 1035-1044	3
928	An ensemble of flexible conformations underlies mechanotransduction by the cadherin-catenin adhesion complex. 2019 , 116, 21545-21555	15
927	Distribution of SNSs in Mimivirus Genomes and the Classification of Mimiviruses Isolated from Japan. 2019 , 34, 451-455	1
926	Mutational Landscape of the BAP1 Locus Reveals an Intrinsic Control to Regulate the miRNA Network and the Binding of Protein Complexes in Uveal Melanoma. 2019 , 11,	21
925	Evolved Aliphatic Halogenases Enable Regiocomplementary C-H Functionalization of a Pharmaceutically Relevant Compound. 2019 , 58, 18535-18539	35
924	Differential interaction strategies of hepatitis c virus genotypes during entry - An in silico investigation of envelope glycoprotein E2 - CD81 interaction. 2019 , 69, 48-60	1
923	Remnants of ancestral larval eyes in an eyeless mollusk? Molecular characterization of photoreceptors in the scaphopod. 2019 , 10, 25	O
922	The Klebsiella pneumoniae citrate synthase gene, gltA, influences site specific fitness during infection. 2019 , 15, e1008010	10
921	Specificity of the Redox Complex between Cytochrome P450 24A1 and Adrenodoxin Relies on Carbon-25 Hydroxylation of Vitamin-D Substrate. 2019 , 47, 974-982	9
920	Antimicrobial and Antibiofilm Activities of Helical Antimicrobial Peptide Sequences Incorporating Metal-Binding Motifs. 2019 , 58, 3802-3812	23
919	Structures prediction of Plasmodium Falciparum Signal Peptide Peptidase (PfSPP) and identification of binding Site. 2019 , 299, 012007	
918	Acidic residues and a predicted, highly conserved helix are critical for the endonuclease/strand separation functions of bacteriophage & TerL. 2019 , 112, 1483-1498	2
917	A specific small-molecule inhibitor of protein kinase Clactivity improves metabolic dysfunction in human adipocytes from obese individuals. 2019 , 294, 14896-14910	1
916	Molecular genetic investigations identify new clinical phenotypes associated with BCS1L-related mitochondrial disease. 2019 , 28, 3766-3776	14
915	Effect of terminal arrangement of tryptophan on biological activity of symmetric Helix-forming peptides. 2019 , 94, 2051-2063	5
914	Strain-Dependent Porcine Circovirus Type 2 (PCV2) Entry and Replication in T-Lymphoblasts. 2019 , 11,	3

913	Immunoinformatics: Approaches and Computational Design of a Multi-epitope, Immunogenic Protein. 2019 , 38, 307-322	36
912	Human adenovirus type 26 uses sialic acid-bearing glycans as a primary cell entry receptor. 2019 , 5, eaax3567	39
911	Structure-Guided Approach to Identify Potential Inhibitors of Large Envelope Protein to Prevent Hepatitis B Virus Infection. 2019 , 2019, 1297484	1
910	Characterization of Fully Recombinant Human 20S and 20S-PA200 Proteasome Complexes. 2019 , 76, 138-147.e5	44
909	Determining the pathogenicity of CFTR missense variants: Multiple comparisons of in silico predictors and variant annotation databases. 2019 , 42, 560-570	2
908	Prediction of Structure and Molecular Interaction with DNA of BvrR, a Virulence-Associated Regulatory Protein of. 2019 , 24,	O
907	Biallelic Missense Mutation in the Underlies Distal Arthrogryposis Type 5 (DA5D). 2019 , 7, 343	6
906	Identification and functional characterization of a novel selenocysteine methyltransferase from Brassica juncea L. 2019 , 70, 6401-6416	10
905	Prediction of MAYV peptide antigens for immunodiagnostic tests by immunoinformatics and molecular dynamics simulations. 2019 , 9, 13339	3
904	Development of R7BP inhibitors through cross-linking coupled mass spectrometry and integrated modeling. 2019 , 2, 338	1
903	Identification and characterization of a novel heparan sulfate-binding domain in Activin A longest variants and implications for function. 2019 , 14, e0222784	2
902	Multiple Roles of the Polycistronic Gene Tarsal-less/Mille-Pattes/Polished-Rice During Embryogenesis of the Kissing Bug Rhodnius prolixus. 2019 , 7,	2
901	Improvement in activity of cellulase Cel12A of Thermotoga neapolitana by error prone PCR. 2019 , 306, 118-124	13
900	Investigation of the binding between olfactory receptors and odorant molecules in C. elegans organism. 2019 , 255, 106264	3
899	The Komodo dragon (Varanus komodoensis) genome and identification of innate immunity genes and clusters. 2019 , 20, 684	10
898	Molecular characterization and computational structure prediction of activin receptor type IIB in aseel and broiler chicken. 2019 , 126, 139-149	
897	Multiscale design of a dairy beverage model composed of Candida utilis single cell protein supplemented with oleic acid. 2019 , 102, 9749-9762	5
896	Genome-Wide Analysis and Expression Profiling of Rice Hybrid Proline-Rich Proteins in Response to Biotic and Abiotic Stresses, and Hormone Treatment. 2019 , 8,	5

895	Physiological functions of a methuselah-like G protein coupled receptor in Lymantria dispar Linnaeus. 2019 , 160, 1-10	14
894	Tubulin lattice in cilia is in a stressed form regulated by microtubule inner proteins. 2019 , 116, 19930-19938	29
893	A novel 3'-tRNA-derived fragment acts as a tumor suppressor in breast cancer by targeting nucleolin. 2019 , 33, 13228-13240	25
892	Quantum Mechanical and Molecular Mechanics Modeling of Membrane-Embedded Rhodopsins. 2019 , 252, 425-449	5
891	Structure-function insights into elusive Mycobacterium tuberculosis protein Rv1916. 2019 , 141, 927-936	3
890	Electronic and Functional Structure of Copper in Plant Cu/Zn Superoxide Dismutase with Combined Site-directed Mutagenesis and Electron Paramagnetic Resonance. 2019 , 47, e19021-e19026	
889	Pyridoxamine Supplementation Effectively Reverses the Abnormal Phenotypes of Zebrafish Larvae With PNPO Deficiency. 2019 , 10, 1086	2
888	Major royal-jelly protein 2 and its isoform X1 are two novel safe inhibitors for hepatitis C and B viral entry and replication. 2019 , 141, 1072-1087	9
887	Signal generation and storage in FRET-based nanocommunications. 2019 , 21, 100254	2
886	Segmentation and Comparative Modeling in an 8.6-ICryo-EM Map of the Singapore Grouper Iridovirus. 2019 , 27, 1561-1569.e4	6
885	Sibe: a computation tool to apply protein sequence statistics to predict folding and design in silico. 2019 , 20, 455	4
884	Elastin-like polypeptide fusions for high-level expression and purification of human IFN-IIn Escherichia coli. 2019 , 585, 113401	5
883	New Functional Ingredients Based on Microencapsulation of Aqueous Anthocyanin-Rich Extracts Derived from Black Rice (L.). 2019 , 24,	15
882	A homozygous pathogenic missense variant broadens the phenotypic and mutational spectrum of CREB3L1-related osteogenesis imperfecta. 2019 , 28, 1801-1809	15
881	Structure model of ferrochelatase from Salmonella Typhi elucidating metalation mechanism. 2019 , 127, 585-593	5
880	Encrypted antimicrobial and antitumoral peptides recovered from a protein-rich soybean (Glycine max) by-product. 2019 , 54, 187-198	15
879	Mixed lineage kinase 3 promotes breast tumorigenesis via phosphorylation and activation of p21-activated kinase 1. 2019 , 38, 3569-3584	7
878	Overexpression of a serine hydroxymethyltransferase increases biomass production and reduces recalcitrance in the bioenergy crop Populus. 2019 , 3, 195-207	18

877	Global Analysis of Genes Essential for Francisella tularensis Schu S4 Growth and for Fitness during Competitive Infection of Fischer 344 Rats. 2019 , 201,	10
876	Pseudogene repair driven by selection pressure applied in experimental evolution. 2019 , 4, 386-389	10
875	NMR structure of a non-conjugatable, ADP-ribosylation associated, ubiquitin-like domain from Tetrahymena thermophila polyubiquitin locus. 2019 , 1863, 749-759	1
874	SPINT2 (HAI-2) missense variants identified in congenital sodium diarrhea/tufting enteropathy affect the ability of HAI-2 to inhibit prostasin but not matriptase. 2019 , 28, 828-841	16
873	Fungal Endophytes of Alter Host Phenotype, Gene Expression, and Rhizobiome Composition. 2019 , 32, 853-864	33
872	Opposing reactions in coenzyme A metabolism sensitize to enzyme inhibition. 2019 , 363,	37
871	mlDEEPre: Multi-Functional Enzyme Function Prediction With Hierarchical Multi-Label Deep Learning. 2018 , 9, 714	43
870	Construction of a synthetic protein using PCR with a high essential amino acid content for nutritional purposes. 2019 , 46, 1593-1601	1
869	Computational analyses, molecular dynamics, and mutagenesis studies of unprocessed form of [NiFe] hydrogenase reveal the role of disorder for efficient enzyme maturation. 2019 , 1860, 325-340	4
868	Toxin [Reduces the ATP and Modulates the Uridine Diphosphate-N-acetylglucosamine Pool. 2019 , 11,	4
867	Identification of the Epstein Barr Virus portal. 2019 , 529, 152-159	7
866	Surface Binding Energy Landscapes Affect Phosphodiesterase Isoform-Specific Inhibitor Selectivity. 2019 , 17, 101-109	5
865	Engineering the Substrate Specificity of a Modular Polyketide Synthase for Installation of Consecutive Non-Natural Extender Units. 2019 , 141, 1961-1969	23
864	Novel interactions of Selenium Binding Protein family with the PICOT containing proteins AtGRXS14 and AtGRXS16 in Arabidopsis thaliana. 2019 , 281, 102-112	5
863	Identification and localization of Tospovirus genus-wide conserved residues in 3D models of the nucleocapsid and the silencing suppressor proteins. 2019 , 16, 7	6
862	High temperatures affect the hypersensitive reaction, disease resistance and gene expression induced by a novel harpin HpaG-Xcm. 2019 , 9, 990	4
861	Carbohydrate binding modules enhance cellulose enzymatic hydrolysis by increasing access of cellulases to the substrate. 2019 , 211, 57-68	37
860	Natural Variation in 9-Cis-Epoxycartenoid Dioxygenase 3 and ABA Accumulation. 2019 , 179, 1620-1631	12

859	Designating ligand specificities to metal uptake ABC transporters in Thermus thermophilus HB8. 2019 , 11, 597-612	9
858	Design, synthesis and glycosidase inhibition studies of novel triazole fused iminocyclitol-flactams. 2019 , 17, 1130-1140	13
857	Molecular evolution of the VacA p55 binding domain of in mestizos from a high gastric cancer region of Colombia. 2019 , 7, e6634	
856	Triple-hit therapeutic approach for triple negative breast cancers using docetaxel nanoparticles, EN1-iPeps and RGD peptides. 2019 , 20, 102003	22
855	Isolation and functional characterization of an antifungal hydrophilic peptide, Skh-AMP1, derived from Satureja khuzistanica leaves. 2019 , 164, 136-143	11
854	Functional characterization and mechanistic modeling of the human cytochrome P450 enzyme CYP4A22. 2019 , 593, 2214-2225	13
853	A thermostable GH8 endoglucanase of Enterobacter sp. R1 is suitable for Eglucan deconstruction. 2019 , 298, 124999	12
852	Determining protein structures using deep mutagenesis. 2019 , 51, 1177-1186	65
851	Genome editing to generate nonfoam-forming sake yeast strains. 2019 , 83, 1583-1593	7
850	The SOXE transcription factors-SOX8, SOX9 and SOX10-share a bi-partite transactivation mechanism. 2019 , 47, 6917-6931	20
849	Prioritization of SNPs in y+LAT-1 culpable of Lysinuric protein intolerance and their mutational impacts using protein-protein docking and molecular dynamics simulation studies. 2019 , 120, 18496-18508	6
848	Application of Novel Microbial Consortia for Environmental Site Remediation and Hazardous Waste Management Toward Low- and High-Density Polyethylene and Prioritizing the Cost-Effective, Eco-friendly, and Sustainable Biotechnological Intervention. 2019 , 431-478	
847	Ectopic Expression of Cold Responsive Gene Enhances Cold Stress Tolerance in. 2019 , 10,	6
846	Identification and Functional Analysis of NLP-Encoding Genes from the Postharvest Pathogen. 2019 , 7,	13
845	A genetically encoded fluorescent temperature sensor derived from the photoactive Orange Carotenoid Protein. 2019 , 9, 8937	13
844	Phylogenetic Distribution and Diversity of Bacterial Pseudo-Orthocaspases Underline Their Putative Role in Photosynthesis. 2019 , 10, 293	13
843	Endogenous, cholesterol-activated ATP-dependent transport in membrane vesicles from Spodoptera frugiperda cells. 2019 , 137, 104963	4
842	Computational design of a chimeric epitope-based vaccine to protect against Staphylococcus aureus infections. 2019 , 46, 101414	18

841	A short peptide with selective anti-biofilm activity against Pseudomonas aeruginosa and Klebsiella pneumoniae carbapenemase-producing bacteria. 2019 , 135, 103605	4
840	Studies of the oligomerisation mechanism of a cystatin-based engineered protein scaffold. 2019 , 9, 9067	1
839	Interactome of Glyceraldehyde-3-Phosphate Dehydrogenase Points to the Existence of Metabolons in. 2019 , 10, 1537	10
838	The Four FAD-Dependent Histone Demethylases of Arabidopsis Are Differently Involved in the Control of Flowering Time. 2019 , 10, 669	11
837	Drosophila ZIP13 is posttranslationally regulated by iron-mediated stabilization. 2019 , 1866, 1487-1497	11
836	Conformational proofreading of distant 40S ribosomal subunit maturation events by a long-range communication mechanism. 2019 , 10, 2754	20
835	Caveolin-1 selectively regulates microRNA sorting into microvesicles after noxious stimuli. 2019 , 216, 2202-2220	82
834	Selection and characterization of ultrahigh potency designed ankyrin repeat protein inhibitors of C. difficile toxin B. 2019 , 17, e3000311	14
833	Melatonin receptors in Atlantic salmon stimulate cAMP levels in heterologous cell lines and show season-dependent daily variations in pituitary expression levels. 2019 , 67, e12590	13
832	Programmed -2/-1 Ribosomal Frameshifting in Simarteriviruses: an Evolutionarily Conserved Mechanism. 2019 , 93,	8
831	The antenna-like domain of the cyanobacterial ferrochelatase can bind chlorophyll and carotenoids in an energy-dissipative configuration. 2019 , 294, 11131-11143	13
830	Semi-rational evolution of the 3-(3-hydroxyalkanoyloxy)alkanoate (HAA) synthase RhlA to improve rhamnolipid production in Pseudomonas aeruginosa and Burkholderia glumae. 2019 , 286, 4036-4059	7
829	Expression, purification and characterization of diguanylate cyclase from Rhodococcus ruber. 2019 , 163, 105441	3
828	Molecular dynamics simulations on apo ADP/ATP carrier shed new lights on the featured motif of the mitochondrial carriers. 2019 , 47, 94-102	11
827	Identification of Alzheimer's Disease Autoantibodies and Their Target Biomarkers by Phage Microarrays. 2019 , 18, 2940-2953	24
826	Epinecidin-1, a highly potent marine antimicrobial peptide with anticancer and immunomodulatory activities. 2019 , 20, 33	26
825	The Translational Landscape of the Human Heart. 2019 , 178, 242-260.e29	210
824	The Repurposed Drug Disulfiram Inhibits Urease and Aldehyde Dehydrogenase and Prevents Growth of the Oomycete. 2019 , 63,	5

823	Genome-Wide Identification of Na/H Antiporter (NHX) Genes in Sugar Beet (Beta vulgaris L.) and Their Regulated Expression under Salt Stress. 2019 , 10,	30
822	Transcript expression profiling in two contrasting cultivars and molecular cloning of a SKP-1 like gene, a component of SCF-ubiquitin proteasome system from mungbean Vigna radiate L. 2019 , 9, 8103	4
821	Adaptation of the group A Streptococcus adhesin Scl1 to bind fibronectin type III repeats within wound-associated extracellular matrix: implications for cancer therapy. 2019 , 112, 800-819	4
820	Sarconesin II, a New Antimicrobial Peptide Isolated from Excretions and Secretions. 2019 , 24,	5
819	Exome Sequencing Reveals the POLR3H Gene as a Novel Cause of Primary Ovarian Insufficiency. 2019 , 104, 2827-2841	17
818	Characterization of the GPR1/FUN34/YaaH protein family in the green microalga suggests their role as intracellular membrane acetate channels. 2019 , 3, e00148	7
817	Identification of Ezetimibe and Pranlukast as Pharmacological Chaperones for the Treatment of the Rare Disease Mucopolysaccharidosis Type IVA. 2019 , 62, 6175-6189	13
816	Comparative Study of Two Chondroitin Sulfate/Dermatan Sulfate 4Sulfatases With High Identity. 2019 , 10, 1309	6
815	An Ancient Lineage of Highly Divergent Parvoviruses Infects both Vertebrate and Invertebrate Hosts. 2019 , 11,	39
814	encodes a Golgi-localized UDP-galactose transporter in. 2019 , 146, 1379-1386	1
813	Identification of the aquaporin gene family in Cannabis sativa and evidence for the accumulation of silicon in its tissues. 2019 , 287, 110167	22
812	Three new serine-protease autotransporters of (SPATEs) from extra-intestinal pathogenic and combined role of SPATEs for cytotoxicity and colonization of the mouse kidney. 2019 , 10, 568-587	13
811	Extracellular Albumin and Endosomal Ions Prime Enterovirus Particles for Uncoating That Can Be Prevented by Fatty Acid Saturation. 2019 , 93,	16
810	Altering the Substrate Specificity of Acetyl-CoA Synthetase by Rational Mutagenesis of the Carboxylate Binding Pocket. 2019 , 8, 1325-1336	12
809	AlphaFold at CASP13. 2019 , 35, 4862-4865	106
808	Disrupted apolipoprotein L1-miR193a axis dedifferentiates podocytes through autophagy blockade in an APOL1 risk milieu. 2019 , 317, C209-C225	15
807	A novel mutation in the erythroid transcription factor KLF1 is likely responsible for ameliorating Ethalassemia major. 2019 , 40, 1768-1780	9
806	A critical challenge in the development of antibody: Selecting the appropriate fragment of the target protein as an antigen based on various epitopes or similar structure. 2019 , 111, 128-135	2

805	A Functional Agonist of Insect Olfactory Receptors: Behavior, Physiology and Structure. 2019 , 13, 134	6
804	Involvement of PIN-like domain nucleases in tRNA processing and translation regulation. 2019 , 71, 1117-1125	4
803	Engineering proteins for allosteric control by light or ligands. 2019 , 14, 1863-1883	26
802	A novel small-molecule antagonizes PRMT5-mediated KLF4 methylation for targeted therapy. 2019 , 44, 98-111	13
801	Interaction of Alt a 1 with SLC22A17 in the airway mucosa. 2019 , 74, 2167-2180	8
800	Screening and identification of a human domain antibody against Brucella abortus VirB5. 2019 , 197, 105026	4
799	Mapping the Allosteric Communication Network of Aminodeoxychorismate Synthase. 2019 , 431, 2718-2728	6
798	StackSSSPred: A Stacking-Based Prediction of Supersecondary Structure from Sequence. 2019 , 1958, 101-122	3
797	Evolutionary Divergence of Duplicated Genes in. 2019 , 8,	11
796	Tuscan Varieties of Sweet Cherry Are Rich Sources of Ursolic and Oleanolic Acid: Protein Modeling Coupled to Targeted Gene Expression and Metabolite Analyses. 2019 , 24,	6
795	Characterization and Transcript Expression Analyses of Atlantic Cod. 2019 , 10, 311	10
794	Rational Design of a Chimeric Derivative of PcrV as a Subunit Vaccine Against. 2019 , 10, 781	16
793	Predicting and validating a model of suppressor of IKKepsilon through biophysical characterization. 2019 , 28, 1423-1436	2
792	Characterization of recombinant endo-1,4-Ekylanase of Bacillus halodurans C-125 and rational identification of hot spot amino acid residues responsible for enhancing thermostability by an in-silico approach. 2019 , 46, 3651-3662	3
791	A close look at the structural features and reaction conditions that modulate the synthesis of low and high molecular weight fructans by levansucrases. 2019 , 219, 130-142	22
790	Searching for a Match: Structure, Function and Application of Sequence-Specific RNA-Binding Proteins. 2019 , 60, 1927-1938	10
789	Druggability assessment of mammalian Per-Arnt-Sim [PAS] domains using computational approaches. 2019 , 10, 1126-1137	4
788	In silico and in vitro studies of lupeol and iso-orientin as potential antidiabetic agents in a rat model. 2019 , 13, 1501-1513	11

787	Computational structural enzymology methodologies for the study and engineering of fatty acid synthases, polyketide synthases and nonribosomal peptide synthetases. 2019 , 622, 375-409	5
786	Can Predicted Protein 3D Structures Provide Reliable Insights into whether Missense Variants Are Disease Associated?. 2019 , 431, 2197-2212	138
7 ⁸ 5	In-Silico analysis of missense SNPs in Human HPPD gene associated with Tyrosinemia type III and Hawkinsinuria. 2019 , 80, 284-291	1
7 ⁸ 4	Forging tools for refining predicted protein structures. 2019 , 116, 9400-9409	10
783	Steroidogenic Acute Regulatory Protein: Structure, Functioning, and Regulation. 2019 , 84, S233-S253	10
782	Chicken viperin inhibits Newcastle disease virus infection in vitro: A possible interaction with the viral matrix protein. 2019 , 120, 28-40	12
781	The redox regulator sulfiredoxin forms a complex with thioredoxin domain-containing 5 protein in response to ER stress in lung cancer cells. 2019 , 294, 8991-9006	5
78o	End-to-End Differentiable Learning of Protein Structure. 2019 , 8, 292-301.e3	169
779	Molecular architecture, polar targeting and biogenesis of the Legionella Dot/Icm T4SS. 2019 , 4, 1173-1182	42
778	Dauer signalling pathway model for Haemonchus contortus. 2019 , 12, 187	16
777	A Protochlorophyllide (Pchlide) Oxygenase for Plant Viability. 2019 , 10, 593	5
776	The p53 gene family in vertebrates: Evolutionary considerations. 2019 , 332, 171-178	4
775	Functional identification and subcellular localization of NAD kinase in the protozoan parasite Giardia intestinalis. 2019 , 48, 16-25	1
774	Structural Insights into Bacteriophage GIL01 gp7 Inhibition of Host LexA Repressor. 2019 , 27, 1094-1102.e4	7
773	Structural characterization and heterologous expression of a new cyt gene cloned from Bacillus thuringiensis. 2019 , 25, 136	
772	Three dimensional structure prediction of panomycocin, a novel Exo-日,3-glucanase isolated from Wickerhamomyces anomalus NCYC 434 and the computational site-directed mutagenesis studies to enhance its thermal stability for therapeutic applications. 2019 , 80, 270-277	3
771	Discerning the mechanism of action of HtrA4: a serine protease implicated in the cell death pathway. 2019 , 476, 1445-1463	8
770	I-TASSER gateway: A protein structure and function prediction server powered by XSEDE. 2019 , 99, 73-85	35

769	The role of C-terminal extensions in controlling ECF (Factor activity in the widely conserved groups ECF41 and ECF42. 2019 , 112, 498-514	13
768	Effect of low complexity regions within the PvMSP3 block II on the tertiary structure of the protein and implications to immune escape mechanisms. 2019 , 19, 6	5
767	Phycobilisomes Harbor FNR in Cyanobacteria. 2019 , 10,	17
766	Tmem178 negatively regulates store-operated calcium entry in myeloid cells via association with STIM1. 2019 , 101, 94-108	8
765	Inhibitory Effect of Berberine on Broiler P-glycoprotein Expression and Function: In Situ and In Vitro Studies. 2019 , 20,	10
764	Delineation of crosstalk between HSP27 and MMP-2/MMP-9: A synergistic therapeutic avenue for glioblastoma management. 2019 , 1863, 1196-1209	21
763	Novel mutations in MYBPC1 are associated with myogenic tremor and mild myopathy. 2019 , 86, 129-142	14
762	An Interspecies Analysis Reveals Molecular Construction Principles of Interleukin 27. 2019 , 431, 2383-2393	4
761	Discovery of Quinazolin-4(3 H)-ones as NLRP3 Inflammasome Inhibitors: Computational Design, Metal-Free Synthesis, and in Vitro Biological Evaluation. 2019 , 84, 5129-5140	28
760	Cathelicidins PMAP-36, LL-37 and CATH-2 are similar peptides with different modes of action. 2019 , 9, 4780	40
759	Gram-Positive Bacteria-Like DNA Binding Machineries Involved in Replication Initiation and Termination Mechanisms of Mimivirus. 2019 , 11,	2
758	A novel TUFM homozygous variant in a child with mitochondrial cardiomyopathy expands the phenotype of combined oxidative phosphorylation deficiency 4. 2019 , 64, 589-595	12
757	Does inclusion of residue-residue contact information boost protein threading?. 2019 , 87, 596-606	6
756	Differential gene expression associated with fungal trophic shifts along the senescence gradient of the moss Dicranum scoparium. 2019 , 21, 2273-2289	7
755	Overexpression of Gloverin2 in the Bombyx mori silk gland enhances cocoon/silk antimicrobial activity. 2019 , 98, 6-12	O
754	Overexpression of NHL6 affects seed production in transgenic Arabidopsis plants. 2019 , 88, 41-47	4
753	Cysteine-Rich Antifungal Proteins from Filamentous Fungi are Promising Bioactive Natural Compounds in Anti- Therapy. 2019 , 59, 360-370	8
75 ²	Challenges in Modelling Metalloenzymes. 2019 , 503-525	2

(2020-2019)

751	Addressing the Compartmentalization of Specific Integrin Heterodimers in Mouse Sperm. 2019, 20,	6
750	Biosynthetic bifunctional enzyme complex with high-efficiency luciferin-recycling to enhance the bioluminescence imaging. 2019 , 130, 705-714	1
749	Identification of the laccase-like multicopper oxidase gene family of sweet cherry (Prunus avium L.) and expression analysis in six ancient Tuscan varieties. 2019 , 9, 3557	8
748	An Overview of Computational Methods, Tools, Servers, and Databases for Drug Repurposing. 2019 , 743-780	10
747	Promiscuous terpene synthases from Prunella vulgaris highlight the importance of substrate and compartment switching in terpene synthase evolution. 2019 , 223, 323-335	18
746	The Dynamic Structures of the Type IV Pilus. 2019 , 7,	19
745	Sequence Analysis of the cAMP-Dependent Protein Kinase Regulatory Subunit-Like Protein From Trypanosoma brucei. 2019 , 64, 262-267	3
744	Presentation_1.PDF. 2018,	
743	lmage_1.tiff. 2018 ,	
742	Table_1.docx. 2018 ,	
741	lmage_1.pdf. 2019 ,	
740	Data_Sheet_1.PDF. 2020 ,	
739	Data_Sheet_2.PDF. 2020 ,	
738	Data_Sheet_3.PDF. 2020 ,	
737	Data_Sheet_1.pdf. 2018 ,	
736	Table_1.pdf. 2020 ,	
735	Image_1.pdf. 2020 ,	
734	Image_2.pdf. 2020 ,	



(2020-2020)

DataSheet_1.pdf. 2020, 715 Image_1.jpeg. **2020**, 714 Image_2.jpeg. 2020, 713 Image_3.jpeg. 2020, 712 Image_4.jpeg. 2020, 711 Presentation_1.PDF. 2018, 710 709 Image_1.TIF. 2019, 708 Image_2.TIF. 2019, Image_3.TIF. 2019, 707 706 Image_4.TIF. 2019, Image_1.JPEG. 2019, 705 704 Image_2.TIF. 2019, 703 Image_3.JPEG. 2019, Image_4.JPEG. 2019, 702 Image_5.JPEG. 2019, 701 700 Table_1.DOCX. **2019**, Table_2.XLSX. 2019, 699 698 Data_Sheet_1.PDF. 2020,



(2020-2020)

Image_2.JPEG. 2020, 679 Image_3.JPEG. **2020**, 678 Image_1.JPEG. 2019, 677 Image_2.JPEG. 2019, 676 Table_1.DOCX. 2019, 675 Table_2.DOCX. 2019, 674 673 Table_3.DOCX. 2019, Table_4.DOCX. 2019, 672 Table_5.DOCX. 2019, 671 670 Table_6.DOCX. **2019**, Table_7.DOCX. 2019, 669 668 Data_Sheet_1.doc. 2020, 667 Table_1.DOC. 2020, 666 Table_2.DOC. **2020**, Data_Sheet_1.doc. 2020, 665 664 Data_Sheet_1.pdf. 2018, 663 Data_Sheet_1.docx. 2020, 662 Data_Sheet_1.docx. 2020,



(2019-2018)

Table_1.DOCX. 2018, 643 Table_2.DOCX. **2018**, 642 Table_3.XLSX. 2018, 641 Table_4.DOCX. 2018, 640 Data_Sheet_1.PDF. 2019, 639 638 Data_Sheet_2.PDF. 2019, 637 Data_Sheet_3.PDF. 2019, Table_1.pdf. **2019**, 636 Table_2.pdf. 2019, 635 634 Data_Sheet_1.PDF. 2020, Data_Sheet_2.PDF. 2020, 633 Data_Sheet_3.PDF. 2020, 632 631 Data_Sheet_4.PDF. 2020, Data_Sheet_5.PDF. 2020, 630 Table_1.DOCX. 2020, 629 628 Table_2.DOCX. **2020**, Data_Sheet_1.pdf. 2019, 627 626 Data_Sheet_2.ZIP. 2019,



(2019-2019)

Table_1.xlsx. 2019, 607 Table_2.xlsx. 2019, 606 Table_3.xlsx. 2019, 605 Table_4.xlsx. **2019**, 604 603 Table_5.xlsx. **2019**, Image_1.pdf. **2019**, 602 601 Image_2.png. 2019, Data_Sheet_1.zip. 2019, 600 Table_1.DOCX. 2019, 599 598 Table_1.xlsx. **2019**, Image1.jpg. 2018, 597 Image2.jpg. 2018, 596 Image3.jpg. 2018, 595 Table1.pdf. **2018**, 594 Table2.pdf. 2018, 593 592 DataSheet_1.pdf. 2019, 591 Data_Sheet_1.pdf. 2020, Data_Sheet_1.pdf. 2019, 590

Triclosan is a KCNQ3 potassium channel activator.. **2022**, 1

588	An Approach and Experimental Analysis Combination: Two Strategies for Selecting the third Extracellular Domain (D-EC3) of Human CD133 Marker as a Target for Detection of Cancer Stem Cells 2021 , 20, 80-91	
587	Mislocalization of Cancer-associated Thyroid Hormone Receptor Mutants 2020 , 2020,	
586	Antiviral Strategies Against SARS-CoV-2: A Systems Biology Approach 2022 , 2452, 317-351	1
585	ProTranslator: Zero-Shot Protein Function Prediction Using Textual Description. 2022, 279-294	О
584	3D Structure Elucidation and Appraisal of Mode of Action of a Bacteriocin BaCf3 with Anticancer Potential Produced by Marine Bacillus amyloliquefaciens BTSS3. 2022 , 2, 45-56	O
583	Machine Learning in the Study of Animal Health and Veterinary Sciences. 2022 , 251-259	O
582	Mutations of the brpR and brpS genes affect biofilm formation in Staphylococcus aureus. 2022 , 12, 20-32	
581	Novel Disease-Associated Missense Single-Nucleotide Polymorphisms Variants Predication by Algorithms Tools and Molecular Dynamics Simulation of Human TCIRG1 Gene Causing Congenital Neutropenia and Osteopetrosis 2022 , 9, 879875	0
580	Drugsniffer: An Open Source Workflow for Virtually Screening Billions of Molecules for Binding Affinity to Protein Targets 2022 , 13, 874746	O
579	Evolutionary analysis of p38 stress-activated kinases in unicellular relatives of animals suggests an ancestral function in osmotic stress.	1
578	Identification of a new splice-acceptor mutation in HFM1 and functional analysis through molecular docking in nonobstructive azoospermia 2022 , 39, 1195	1
577	Design of D-Amino Acids SARS-CoV-2 Main Protease Inhibitors Using the Cationic Peptide from Rattlesnake Venom as a Scaffold. 2022 , 15, 540	0
576	Case Report: Biallelic Variant in the tRNA Methyltransferase Domain of the AlkB Homolog 8 Causes Syndromic Intellectual Disability 2022 , 13, 878274	1
575	The disordered N-terminus of McdB modulates phase separation via pH-sensitive hydration and folds upon interaction with McdA.	0
574	Characterisation of ascocorynin biosynthesis in the purple jellydisc fungus Ascocoryne sarcoides 2022 , 9, 8	O
573	Disulfide Bond Engineering for Enhancing the Thermostability of the Maltotetraose-Forming Amylase from STB07 2022 , 11,	О
57 ²	Control of carbon monoxide dehydrogenase orientation by site-specific immobilization enables direct electrical contact between enzyme cofactor and solid surface 2022 , 5, 390	2

571	The Conformation of the N-Terminal Tails of Dps Is Modulated by the Ionic Strength 2022, 23,	1
570	nurP28, a New-to-Nature Zein-Derived Peptide, Enhances the Therapeutic Effect of Docetaxel in Breast Cancer Monolayers and Spheroids 2022 , 27,	1
569	Adsorption of Pulmonary and Exogeneous Surfactants on SARS-CoV-2 Spike Protein 2022,	
568	Quercetin: a silent retarder of fatty acid oxidation in breast cancer metastasis through steering of mitochondrial CPT1 2022 , 1	O
567	TULP3 NLS inhibition: an study to hamper cargo transport to nucleus 2022, 1-9	
566	Ivermectin-induced gene expression changes in adult Parascaris univalens and Caenorhabditis elegans: a comparative approach to study anthelminthic metabolism and resistance in vitro 2022 , 15, 158	0
565	Report of three patients, including monozygotic twins and review of clinical and mutation profiles 2022 , 104521	
564	CrowdGO: Machine learning and semantic similarity guided consensus Gene Ontology annotation 2022 , 18, e1010075	O
563	Designing a novel multi-epitope vaccine against Ebola virus using reverse vaccinology approach 2022 , 12, 7757	1
562	In silico study predicts a key role of RNA-binding domains 3 and 4 in nucleolin-miRNA interactions 2022 ,	O
561	Germline mutations in mitochondrial complex I reveal genetic and targetable vulnerability in IDH1-mutant acute myeloid leukaemia 2022 , 13, 2614	O
560	In Silico Analysis Revealed Five Novel High-Risk Single-Nucleotide Polymorphisms (rs200384291, rs201163886, rs193141883, rs201139487, and rs201723157) in Gene Causing Autosomal Dominant Severe Congenital Neutropenia 1 and Cyclic Hematopoiesis 2022 , 2022, 3356835	
559	Recognizing Protein-metal Ion Ligands Binding Residues by Random Forest Algorithm with Adding Orthogonal Properties. 2022 , 107693	
558	DEMO2: Assemble multi-domain protein structures by coupling analogous template alignments with deep-learning inter-domain restraint prediction 2022 ,	1
557	Molecular dynamics, MMGBSA, and docking studies of natural products conjugated to tumor-targeted peptide for targeting BRAF V600E and MERTK receptors 2022 , 1	
556	The effects of cardiolipin on the structural dynamics of the mitochondrial ADP/ATP carrier in its cytosol-open state 2022 , 100227	1
555	Leu22_Leu23 Duplication at the Signal Peptide of PCSK9 Promotes Intracellular Degradation of LDLr and Autosomal Dominant Hypercholesterolemia 2022 , 101161ATVBAHA122315499	0
554	The GDSL-Lipolytic Enzyme Lip1 Is Required for Full Virulence of the Cucurbit Pathogenic Bacterium Acidovorax citrulli. 2022 , 10, 1016	0

553	First report on molecular characterization and in silico analysis of caprine TCIM gene. 2022, 106723	0
552	Spt6 directly interacts with Cdc73 and is required for Paf1C recruitment to active genes.	
551	Proteomic Network Analysis of Bronchoalveolar Lavage Fluid in Ex-Smokers to Discover Implicated Protein Targets and Novel Drug Treatments for Chronic Obstructive Pulmonary Disease. 2022 , 15, 566	1
550	Natural Compound ZINC12899676 Reduces Porcine Epidemic Diarrhea Virus Replication by Inhibiting the Viral NTPase Activity. 2022 , 13,	O
549	Mutations within scavenger receptor cysteine-rich (SRCR) protein domain 5 of porcine CD163 involved in infection with porcine reproductive and respiratory syndrome virus (PRRS) 2022 , 103,	О
548	Multi-State Modeling of G-protein Coupled Receptors at Experimental Accuracy 2022,	5
547	Novel fold of rotavirus glycan-binding domain predicted by AlphaFold2 and determined by X-ray crystallography 2022 , 5, 419	1
546	Rare Variant Analysis and Molecular Dynamics Simulation in Alzheimer Disease Identifies Exonic Variants in FLG. 2022 , 13, 838	O
545	Structural basis of sodium-dependent bile salt uptake into the liver 2022,	1
544	Novel amikacin resistance genes identified from human gut microbiota by functional metagenomics 2022 ,	
543	In silico approaches to develop herbal acaricides against R. (Boophilus) Microplus and In vitro Anti-Tick activities of selected medicinal plants. 2022 , 29, 103302	1
542	Cell membrane enolase of Aedes albopictus C6/36 cells is involved in the entrance mechanism of dengue virus (DENV). 2022 , 25, 101924	
541	Prediction and characterization of a novel hemoglobin-derived mutant peptide (mTgHbP7) from Tegillarca granosa 2022 , 125, 84-89	0
540	Correlating in silico elucidation of interactions between hydroxybenzoic acids and casein with in vitro release kinetics for designing food packaging. 2022 , 32, 100859	O
539	Direct electrical contact of NAD+/NADH-dependent dehydrogenase on electrode surface enabled by non-native solid-binding peptide as a molecular binder. 2022 , 421, 140480	1
538	Progressive assembly of multi-domain protein structures from cryo-EM density maps. 2022 , 2, 265-275	O
537	Structure-Based Binding Pocket Detection and Druggability Assessment. 2022 , 83-97	
536	T-cell epitope-based vaccine prediction against Aspergillus fumigatus: a harmful causative agent of aspergillosis 2022 , 20, 72	

535	Plasticity in structure and assembly of SARS-CoV-2 nucleocapsid protein.	3
534	System-Wide Analysis of the GATC-Binding Nucleoid-Associated Protein Gbn and Its Impact on Development 2022 , e0006122	
533	Novel role of the synaptic scaffold protein Dlgap4 in ventricular surface integrity and neuronal migration during cortical development 2022 , 13, 2746	О
532	Ex silico engineering of cystine-dense peptides yielding a potent bispecific T cell engager 2022 , 14, eabn0402	
531	Exploring the antihyperglycemic potential of tetrapeptides devised from AdMc1 different receptor proteins inhibition using in silico approaches 2022 , 36, 3946320221103120	3
530	Unravelling the mechanisms of adaptation to high pressure in proteins.	1
529	An ancient function of PGR5 in iron delivery?. 2022,	О
528	Innovative in Silico Approaches for Characterization of Genes and Proteins. 2022 , 13,	1
527	Cryo-EM structure of the agonist-bound Hsp90-XAP2-AHR complex.	О
526	Hydrogen-Bonds Mediated Nanomedicine: Design, Synthesis and Applications. 2200168	
525	An integrated approach reveals how lipo-chitooligosaccharides interact with the lysin motif receptor-like kinase MtLYR3. 2022 , 31,	0
524	Structural insights into bacterial sterol transport.	
523	On the interplay between lipids and asymmetric dynamics of an NBS degenerate ABC transporter.	О
522	Topological dynamics of an intrinsically disordered N-terminal domain of the human androgen receptor. 2022 , 31,	2
521	One-step purification and regulation of fructose 1,6-bisphosphatase from the liver of the freeze-tolerant wood frog, Rana sylvatica.	
520	De Novo Protein Fold Design Through Sequence-Independent Fragment Assembly Simulations.	O
519	Syndromic Hearing Loss in Moroccan families is associated to homozygous missense variants in COL4A3 and MASP1. 2022 , 201053	
518	InvL, an Invasin-Like Adhesin, Is a Type II Secretion System Substrate Required for Acinetobacter baumannii Uropathogenesis.	2

517	Substantiation of propitious EnzybioticlFrom two novel bacteriophages isolated from a wastewater treatment plant in Qatar. 2022 , 12,	0
516	Glutamine 666 renders murine ADAM10 an inefficient S. aureus £oxin receptor.	
515	A conserved subunit vaccine designed against SARS-CoV-2 variants showed evidence in neutralizing the virus.	1
514	Identification of branching order within the kingdom Bamfordvirae.	
513	Sesquiterpene from Polygonum barbatum disrupts mitochondrial membrane potential to induce apoptosis and inhibits metastasis by downregulating matrix metalloproteinase and osteopontin in NCI-H460 cells.	
512	In-silico design and assessment of OprD based multi-epitope vaccine against Acinetobacter baumannii.	
511	Molecular dynamics simulations reveal membrane lipid interactions of the full-length lymphocyte specific kinase Lck.	
510	A requirement for Krppel-Like Factor-4 in the maintenance of endothelial cell quiescence.	
509	Characterization and computational simulation of human Syx, a RhoGEF implicated in glioblastoma. 2022 , 36,	
508	The Influence of Short Motifs on the Anticancer Activity of HB43 Peptide. 2022 , 14, 1089	2
507	Deep learning geometrical potential for high-accuracy ab initio protein structure prediction. 2022 , 25, 104425	0
506	Effect of irrigation regimes on starch biosynthesis pathway, cotton (Gossypium hirsutum) yield and in silico analysis of ADP-glucose-pyrophosphorylase.	
505	Novel Variation in Acyl-CoA Synthetase Long Chain Family Member 6 (ACSL6) Results in Protein	
	Structural Modification and Multiple Non-Related Neoplasia in a 46-Year-Old: Case Report. 12,	
504	Structural Modification and Multiple Non-Related Neoplasia in a 46-Year-Old: Case Report. 12, Iron Deprivation Modulates the Exoproteome in Paracoccidioides brasiliensis. 2022, 12,	1
		0
504	Iron Deprivation Modulates the Exoproteome in Paracoccidioides brasiliensis. 2022 , 12,	
504	Iron Deprivation Modulates the Exoproteome in Paracoccidioides brasiliensis. 2022 , 12, The Impact of RNA-DNA Hybrids on Genome Integrity in Bacteria. 2022 , 76,	

499	Additive genetic effect of GCKR, G6PC2, and SLC30A8 variants on fasting glucose levels and risk of type 2 diabetes. 2022 , 17, e0269378	О
498	Learning Strategies in Protein Directed Evolution. 2022 , 225-275	1
497	Identification of 且-fucosidase (ALFuc) of Blastocystis sp. subtypes ST1, ST2 and ST3. 64,	О
496	Execution and Design of an Anti HPIV-1 Vaccine with Multiple Epitopes Triggering Innate and Adaptive Immune Responses: An Immunoinformatic Approach. 2022 , 10, 869	2
495	Targeted gene sequencing of FYCO1 identified a novel mutation in a Pakistani family for autosomal recessive congenital cataract.	0
494	Phylogenetic and Mutation Analysis of the Venezuelan Equine Encephalitis Virus Sequence Isolated in Costa Rica from a Mare with Encephalitis. 2022 , 9, 258	
493	Engineering of triterpene metabolism and overexpression of the lignin biosynthesis gene PAL promotes ginsenoside Rg 3 accumulation in ginseng plant chassis.	1
492	Functional Micropeptides Encoded by Long Non-Coding RNAs: A Comprehensive Review. 9,	1
491	Protein structural bioinformatics: An overview. 2022 , 105695	О
490	Identification of dual active sites in Caenorhabditis elegans GANA-1 protein: an ortholog of the human EGAL a and ENAGA enzymes. 1-16	1
489	A Teleost CXCL10 Is Both an Immunoregulator and an Antimicrobial. 13,	О
488	Keap1-resistant N-Nrf2 isoform does not translocate to the nucleus upon electrophilic stress.	
487	Key Glycosyltransferase Genes of Panax notoginseng: Identification and Engineering Yeast Construction of Rare Ginsenosides.	0
486	Lipidomic Analysis of Arabidopsis T-DNA Insertion Lines Leads to Identification and Characterization of C-Terminal Alterations in FATTY ACID DESATURASE 6.	Ο
485	Machine learning/molecular dynamic protein structure prediction approach to investigate the protein conformational ensemble. 2022 , 12,	1
484	The Indole-3-Acetamide-Induced Arabidopsis Transcription Factor MYB74 Decreases Plant Growth and Contributes to the Control of Osmotic Stress Responses. 13,	1
483	Studies on the antiviral activity of chebulinic acid against dengue and chikungunya viruses and in silico investigation of its mechanism of inhibition. 2022 , 12,	
482	Case Report: A Novel Splice-Site Mutation in DNAJB6 Associated With Juvenile-Onset Proximal D istal Myopathy in a Chinese Patient. 13,	1

481	Schistosoma mansoni Fibroblast Growth Factor Receptor A Orchestrates Multiple Functions in Schistosome Biology and in the Host-Parasite Interplay. 13,	0
480	Homology Modeling and Molecular Docking Approaches for the Proposal of Novel Insecticides against the African Malaria Mosquito (Anopheles gambiae). 2022 , 27, 3846	
479	Artificial metalloenzymes based on protein assembly. 2022 , 214593	1
478	Identification of Novel Circular RNAs of the Human Protein Arginine Methyltransferase 1 (PRMT1) Gene, Expressed in Breast Cancer Cells. 2022 , 13, 1133	O
477	Comparative transcriptomics reveals the molecular toolkit used by an algivorous protist for cell wall perforation. 2022 ,	0
476	Reference-aided full-length transcript assembly, cDNA cloning, and molecular characterization of coronatine-insensitive 1b (COI1b) gene in coconut (Cocos nucifera L.).	
475	Biochemical characterization of a novel oxidatively stable, halotolerant and high-alkaline subtilisin from Alkalihalobacillus okhensis Kh10-101 T .	o
474	Structure-Functional Characteristics of the Svx ProteinThe Virulence Factor of the Phytopathogenic Bacterium Pectobacterium atrosepticum. 2022 , 23, 6914	О
473	The structure of the humanised A33 Fab C226S variant, an immunotherapy candidate for colorectal cancer.	
472	Functional Role of YnfA, an Efflux Transporter in Resistance to Antimicrobial Agents in Shigella flexneri.	o
471	Screening Novel Vaccine Candidates for Leishmania Donovani by Combining Differential Proteomics and Immunoinformatics Analysis. 13,	
470	Translocating Peptides of Biomedical Interest Obtained from the Spike (S) Glycoprotein of the SARS-CoV-2. 2022 , 12, 600	o
469	Potential linear B-cells epitope change to a helix structure in the spike of Omicron 21L or BA.2 predicts increased SARS-CoV-2 antibodies evasion. 2022 , 573, 84-95	0
468	First clinical description of letermovir resistance mutation in cytomegalovirus UL51 gene and potential impact on the terminase complex structure. 2022 , 204, 105361	O
467	A structural vaccinology approach for in silico designing of a potential self-assembled nanovaccine against Leishmania infantum. 2022 , 239, 108295	0
466	Membrane Protein Production in Insect Cells. 2022 , 223-240	1
465	Immunological investigation of a multiepitope peptide vaccine candidate based on main proteins of SARS-CoV-2 pathogen. 2022 , 17, e0268251	2
464	An essential role for tungsten in the ecology and evolution of a previously uncultivated lineage of anaerobic, thermophilic Archaea. 2022 , 13,	2

463	Genome Wide Identification and Annotation of NGATHA Transcription Factor Family in Crop Plants. 2022 , 23, 7063	1
462	Exploring the alternative conformation of a known protein structure based on contact map prediction.	O
461	The evolution of vitamin C biosynthesis and transport in animals. 2022 , 22,	О
460	Glial Fibrillary Acidic Protein: A Biomarker and Drug Target for Alzheimer Disease. 2022, 14, 1354	1
459	Nicotiana tabaccum L. katalaz proteininin in siliko analizi.	
458	In silico Analysis of Peptide-Based Biomarkers for the Diagnosis and Prevention of Latent Tuberculosis Infection. 13,	1
457	The Multistage Antimalarial Compound Calxinin Perturbates P. falciparum Ca2+ Homeostasis by Targeting a Unique Ion Channel. 2022 , 14, 1371	Ο
456	The essential Rhodobacter sphaeroides CenKR two-component system regulates cell division and envelope biosynthesis. 2022 , 18, e1010270	O
455	Molecular characterization and expression analysis of two type I interferons from Asian Seabass (Lates calcarifer) during nervous necrosis virus infection.	
454	Novel In Silico Insights into Rv1417 and Rv2617c as Potential Protein Targets: The Importance of the Medium on the Structural Interactions with Exported Repetitive Protein (Erp) of Mycobacterium tuberculosis. 2022 , 14, 2577	1
453	Molecular Modeling of ABHD5 Structure and Ligand Recognition. 9,	Ο
452	Application of Mathematical Modeling and Computational Tools in the Modern Drug Design and Development Process. 2022 , 27, 4169	1
451	Molecular evolution of the ependymin-related gene epdl2 in African weakly electric fish.	
450	Structure Prediction, Evaluation, and Validation of GPR18 Lipid Receptor Using Free Programs. 2022 , 23, 7917	
449	Thermostability engineering of industrial enzymes through structure modification.	Ο
448	Unravelling rutin content of tartary buckwheat of north western Himalayas and insights into nucleotide polymorphisms in PAL gene to infer the associations with rutin biosynthesis. 2022 , 12,	
447	Biallelic variants in WARS1 cause a highly variable neurodevelopmental syndrome and implicate a critical exon for normal auditory function.	
446	Whole-cell FRET monitoring of transcription factor activities enables functional annotation of signal transduction systems in living bacteria. 2022 , 102258	0

445	In Silico Conformation of the Drug Colchicine into Tubulin Models and Acute Phytotoxic Activity on Cucumis sativus Radicles. 2022 , 11, 1805	
444	The Qc5 Allele Increases Wheat Bread-Making Quality by Regulating SPA and SPR. 2022 , 23, 7581	O
443	In silico structural and functional characterization of Antheraea mylitta cocoonase. 2022 , 20,	O
442	Generation of a live attenuated influenza A vaccine by proteolysis targeting.	2
441	A versatile design platform for glycoengineering therapeutic antibodies. 2022, 14,	
440	Discovery of archaeal fusexins homologous to eukaryotic HAP2/GCS1 gamete fusion proteins. 2022 , 13,	1
439	A fatal case of dengue hemorrhagic fever associated with dengue virus 4 (DENV-4) in Brazil: genomic and histopathological findings.	2
438	Necroptosis-Mediated eCIRP Release in Sepsis. Volume 15, 4047-4059	
437	Structural Bioinformatics and Deep Learning of Metalloproteins: Recent Advances and Applications. 2022 , 23, 7684	O
436	Immunoinformatic Approach to Contrive a Next Generation Multi-Epitope Vaccine Against Achromobacter xylosoxidans Infections. 9,	
435	Redclaw crayfish (Cherax quadricarinatus) responds to Vibrio parahaemolyticus infection by activating toll and immune deficiency signaling pathways and transcription of associated immune response genes. 2022 , 127, 611-622	0
434	Designing a novel fusion protein from Streptococcus agalactiae with apoptosis induction effects on cervical cancer cells. 2022 , 169, 105670	O
433	Mechanism insights into liquid polarity regulation for enhanced dewatering of waste-activated sludge: Specifically focusing on the solid-liquid affinity reduction depending on phase-transfer and conformational features of amphiphilic protein. 2022 , 221, 118793	O
432	Mutational dynamics across VOCs in International travellers and Community transmission underscores importance of Spike-ACE2 interaction. 2022 , 262, 127099	O
431	C. elegans ribosomal protein S3 protects against H2O2-induced DNA damage and suppresses spontaneous mutations in yeast. 2022 , 117, 103359	
430	Molecular simulation -based research on antifreeze peptides: advances and perspectives. 2022 , 2, 203-212	O
429	Structure and host specificity of Staphylococcus epidermidis bacteriophage Andhra.	
428	Predictive Models of within- and between-Species SARS-CoV-2 Transmissibility. 2022 , 14, 1565	

427	Best templates outperform homology models in predicting the impact of mutations on protein stability.	О
426	Combining segments 9 and 10 in DNA and recombinant protein vaccines conferred superior protection against tilapia lake virus in hybrid red tilapia (oreochromis sp.) compared to single segment vaccines. 13,	1
425	Molecular Characterization, Evolutionary and Phylogenetic Analyses of Rice ACT/BAT-type Amino Acid Transporters. 2022 , 107745	
424	Catalytic cycling of human mitochondrial Lon protease. 2022 ,	1
423	CXCL20a, a bactericidal chemokine, consists of four structural fragments with potent bactericidal activity. 2022 , 561, 738633	O
422	Interaction of the gas vesicle proteins GvpA, GvpC, GvpN, and GvpO of Halobacterium salinarum. 13,	1
421	Residues 318 and 323 in capsid protein are involved in immune circumvention of the atypical epizootic infection of infectious bursal disease virus. 13,	O
420	The protein organization of a red blood cell. 2022 , 40, 111103	1
419	Designing Next-Generation Vaccines Against Common Pan-Allergens Using In Silico Approaches.	
418	Human Coronavirus Spike Protein Based Multi-Epitope Vaccine against COVID-19 and Potential Future Zoonotic Coronaviruses by Using Immunoinformatic Approaches. 2022 , 10, 1150	
417	A ricin-based peptide BRIP from Hordeum vulgare inhibits Mpro of SARS-CoV-2. 2022 , 12,	2
416	Is the Glycoprotein Responsible for the Differences in Dispersal Rates between Lettuce Necrotic Yellows Virus Subgroups?. 2022 , 14, 1574	
415	Mutations in SORL1 and MTHFDL1 possibly contribute to the development of Alzheimer disease in a multigenerational Colombian Family. 2022 , 17, e0269955	
4 ¹ 4	Characterization of Treponema denticola Major Surface Protein (Msp) by Deletion Analysis and Advanced Molecular Modeling.	
413	Biochemical Evolution of a Potent Target of Mosquito Larvicide, 3-Hydroxykynurenine Transaminase. 2022 , 27, 4929	1
412	In silico design of a multi-epitope vaccine against HPV16/18. 2022 , 23,	O
411	On the Rapid Calculation of Binding Affinities for Antigen and Antibody Design and Affinity Maturation Simulations. 2022 , 11, 51	1
410	In silico based multi-epitope vaccine design against norovirus. 1-11	O

409	Chikungunya Virus E2 Structural Protein B-Cell Epitopes Analysis. 2022 , 14, 1839	
408	Early Stages of RNA-Mediated Conversion of Human Prions. 2022 , 126, 6221-6230	
407	Genome-Wide Identification of the BvCBL Genes in Sugar Beet (Beta vulgaris L.) and Their Expression Under Salt and Drought Conditions.	
406	Characterization of the chemosensory protein EforCSP3 and its potential involvement in host location by Encarsia formosa. 2022 ,	0
405	Molecular evolutionary analysis of the SHI/STY gene family in land plants: A focus on the Brassica species. 13,	O
404	Subcellular localization of the enterobacterial common antigen GT-E- like glycosyltransferase, WecG.	
403	Identification of key amino acid residues toward improving the catalytic activity and substrate specificity of plant-derived cytochrome P450 monooxygenases CYP716A subfamily enzyme for triterpenoid production in Saccharomyces cerevisiae. 10,	O
402	Glycosylation of a key cubilin Asn residue results in reduced binding to albumin. 2022, 102371	
401	A novel, non-GMO surface display in Limosilactobacillus fermentum mediated by cell surface hydrolase without anchor motif. 2022 , 22,	
400	Tools in the Era of Multidrug Resistance in Bacteria: Applications for New Antimicrobial Peptides Discovery. 2022 , 28,	2
399	Make it double: identification and characterization of a Tandem-Hirudin from the Asian medicinal leech Hirudinaria manillensis.	
398	In silico structural homology modeling and functional characterization of Mycoplasma gallisepticum variable lipoprotein hemagglutin proteins. 9,	
397	Codon-optimized FAM132b gene therapy prevents dietary obesity by blockading adrenergic response and insulin action.	1
396	PIF4 enhances DNA binding of CDF2 to co-regulate target gene expression and promote Arabidopsis hypocotyl cell elongation.	O
395	ppdx: Automated modeling of proteinprotein interaction descriptors for use with machine learning. 2022 , 43, 1747-1757	

Modeling protein structure as a stable static equilibrium. 2022, 106,

Riboflavin salvage by Borrelia burgdorferi supports carbon metabolism and is essential for survival

Identification of novel genes by targeted exome sequencing in Retinoblastoma. 1-18

104

394

393

392

in the tick vector.

391	I-TASSER-MTD: a deep-learning-based platform for multi-domain protein structure and function prediction.	2
390	Structure of Mycobacterium tuberculosis Cya, an evolutionary ancestor of the mammalian membrane adenylyl cyclases. 11,	O
389	Identification of Estradiol Benzoate as an Inhibitor of HBx Using Inducible Stably Transfected HepG2 Cells Expressing HiBiT Tagged HBx. 2022 , 27, 5000	1
388	A novel causative functional mutation in GATA6 gene is responsible for familial dilated cardiomyopathy as supported by in silico functional analysis. 2022 , 12,	
387	New strategies for identifying and masking the bitter taste in traditional herbal medicines: The example of Huanglian Jiedu Decoction. 13,	
386	The START domain mediates Arabidopsis GLABRA2 dimerization and turnover independently of homeodomain DNA binding.	1
385	Sustained deep-tissue voltage recording using a fast indicator evolved for two-photon microscopy. 2022 ,	1
384	A conformational switch controlling the toxicity of the prion protein. 2022 , 29, 831-840	1
383	Functional Analysis of Conserved Hypothetical Proteins from the Antarctic Bacterium, Pedobacter cryoconitis Strain BG5 Reveals Protein Cold Adaptation and Thermal Tolerance Strategies. 2022 , 10, 1654	
382	Optimal COVID-19 therapeutic candidate discovery using the CANDO platform. 13,	Ο
381	Inhibition of Hepatitis E Virus Replication by Novel Inhibitor Targeting Methyltransferase. 2022 , 14, 1778	
380	Clinical characteristics of high myopia in female carriers of pathogenic RPGR mutations: a case series and review of the literature. 1-9	
379	Ab initio modelling of an essential mammalian protein: Transcription Termination Factor 1 (TTF1). 1-10	1
379 378	Ab initio modelling of an essential mammalian protein: Transcription Termination Factor 1 (TTF1). 1-10 Hybrid antigens expressing surface loops of BauA from Acinetobacter baumannii are capable of inducing protection against infection. 13,	0
	Hybrid antigens expressing surface loops of BauA from Acinetobacter baumannii are capable of	
378	Hybrid antigens expressing surface loops of BauA from Acinetobacter baumannii are capable of inducing protection against infection. 13, The Plasmodium falciparum Nuclear Protein Phosphatase NIF4 Is Required for Efficient Merozoite	
378 377	Hybrid antigens expressing surface loops of BauA from Acinetobacter baumannii are capable of inducing protection against infection. 13, The Plasmodium falciparum Nuclear Protein Phosphatase NIF4 Is Required for Efficient Merozoite Invasion and Regulates Artemisinin Sensitivity. Resistance screening and in-silico characterization of cloned novel RGA from multi race resistant	

373	Structure-activity relationships among mono- and dihydroxy flavones as aryl hydrocarbon receptor (AhR) agonists or antagonists in CACO2 cells. 2022 , 365, 110067	Ο
372	Molecular characterization and phylogenetic relationships among Rhynchophorus sp. haplotypes in Makkah Al-Mukarramah Region-KSA. 2022 , 29, 103388	
371	Protocol to identify host-viral protein interactions between coagulation-related proteins and their genetic variants with SARS-CoV-2 proteins. 2022 , 3, 101648	
370	Serum-isolated exosomes from Piscirickettsia salmonis-infected Salmo salar specimens enclose bacterial DnaK, DnaJ and GrpE chaperones. 2022 , 59, 83-93	
369	Evaluation of novel L-histidine-based Schiff base derivatives as microbial-HO inhibitors and their antimicrobial and molecular docking studies. 2022 , 1270, 133890	
368	In silico study on miRNA regulation and NSs protein interactome characterization of the SFTS virus. 2022 , 117, 108291	
367	StarMap: a user-friendly workflow for Rosetta-driven molecular structure refinement.	0
366	Bovine viral diarrhea virus in China: A comparative genomic and phylogenetic analysis with complete genome sequences. 9,	O
365	Virtual Screening in the Identification of Sirtuins (Activity Modulators. 2022 , 27, 5641	0
364	Txp40, an insecticidal toxin protein from Xenorhabdus nematophila: Purification, toxicity assessment and biophysical characterization. 2022 , 218, 40-46	O
363	Mycobacterium tuberculosis dormancy regulon proteins Rv2627c and Rv2628 as Toll like receptor agonist and as potential adjuvant. 2022 , 112, 109238	0
362	Integrating in silico and in vivo approach for investigating the role of polyherbal oil in prevention and treatment of COVID-19 infection. 2022 , 367, 110179	1
361	Mechanisms of deformation and drug release of targeting polypeptides based on fibronectin induction. 2022 , 219, 112836	0
360	Cloning and characterization of the major AP endonuclease from Staphylococcus aureus. 2022 , 119, 103390	O
359	Ferrous sulfate efficiently kills Vibrio parahaemolyticus and protects salmon sashimi from its contamination. 2022 , 382, 109929	0
358	MALDI-TOF-MS and in-depth dynamic simulations on the molecular forces determining the stability of the 4-hydroxybenzoic acid ECasein complex following UHT-like treatment. 2023 , 400, 134047	O
357	Computational Methods for Peptide Macrocycle Drug Design. 2022 , 79-161	0
356	Computational design and characterization of a multiepitope vaccine against carbapenemase-producing Klebsiella pneumoniae strains, derived from antigens identified through reverse vaccinology. 2022 , 20, 4446-4463	1

355	COMPUTATIONAL IDENTIFICATION VALIDATION AND STRUCTURAL CHARACTERIZATION OF SOME POTENTIAL CANDIDATE GENES FOR DIABETES MELLITUS.	0
354	Golgi localized Arl15 regulates cargo transport, cell adhesion and motility.	Ο
353	Evolution of a chordate-specific mechanism for myoblast fusion. 2022, 8,	0
352	In silico designing of a novel epitope-based candidate vaccine against Streptococcus pneumoniae with introduction of a new domain of PepO as adjuvant. 2022 , 20,	O
351	A GFET Nitrile Sensor Using a Graphene-Binding Fusion Protein. 2207669	1
350	Genome mining of Fusarium reveals structural and functional diversity of pectin lyases: a bioinformatics approach. 2022 , 12,	Ο
349	Effective drug combinations targeting driver KRAS mutations in non-small cell lung cancer.	O
348	A heterozygous LAMA5 variant may contribute to slowly progressive, vinculin-enhanced familial FSGS and pulmonary defects.	Ο
347	Design of a multi-epitope vaccine against the pathogenic fungi Candida tropicalis using an in silico approach. 2022 , 20,	2
346	Stitched peptides as potential cell permeable inhibitors of oncogenic DAXX protein.	Ο
345	CryoBlectron microscopy unveils unique structural features of the human Kir2.1 channel. 2022 , 8,	2
344	Spns1 is a lysophospholipid transporter mediating lysosomal phospholipid salvage. 2022 , 119,	2
343	The non-glycosylated protein of Toxocara canis MUC-1 interacts with proteins of murine macrophages. 2022 , 16, e0010734	O
342	In silico prediction, characterization, docking studies and molecular dynamics simulation of human p97 in complex with p37 cofactor. 2022 , 23,	O
341	Genetic Testing for a Patient with Suspected 3 Beta-Hydroxysteroid Dehydrogenase Deficiency: A Case of Unreported Genetic Variants. 2022 , 11, 5767	O
340	Giardia duodenalis: Flavohemoglobin is involved in drug biotransformation and resistance to albendazole. 2022 , 18, e1010840	O
339	Inhibitors targeting the autophosphorylation of serine/threonine kinase of Streptococcus suis show potent antimicrobial activity. 13,	0
338	Functional comparison of phosphomimetic S15D and T160D mutants of myosin regulatory light chain exchanged in cardiac muscle preparations of HCM and WT mice. 9,	O

337	Function-Related Asymmetry of the Interactions between Matrix Loops and Conserved Sequence Motifs in the Mitochondrial ADP/ATP Carrier. 2022 , 23, 10877	1
336	Sequence-Dependent Backbone Dynamics of Intrinsically Disordered Proteins.	Ο
335	In-silico comparative modeling and interaction studies of PRSV proteins - Accelerated towards dissection of structure based evolutionary divergence and functional interaction of virus within the host.	O
334	Fast and accurate Ab Initio Protein structure prediction using deep learning potentials. 2022 , 18, e1010539	O
333	Homology modeling of Forkhead box protein C2: identification of potential inhibitors using ligand and structure-based virtual screening.	O
332	Electrostatics in Computational Biophysics and Its Implications for Disease Effects. 2022 , 23, 10347	О
331	Designing multi-epitope based peptide vaccine targeting spike protein SARS-CoV-2 B1.1.529 (Omicron) variant using computational approaches.	1
330	Mechanism of enhanced sensitivity of mutated Endrenergic-like octopamine receptor to amitraz in honeybee Apis mellifera: An insight from MD simulations.	О
329	Biomimetic Bacteriophage-Like Particles Formed from Probiotic Extracts and NO Donors for Eradicating Multidrug-Resistant Staphylococcus aureus. 2206134	2
328	Suitability of potyviral recombinant virus-like particles bearing a complete food allergen for immunotherapy vaccines. 13,	1
327	MAIA, Fc receptorlike 3, supersedes JUNO as IZUMO1 receptor during human fertilization. 2022 , 8,	1
326	A filarial parasite-encoded human IL-10 receptor antagonist reveals a novel strategy to modulate host responses.	O
325	The TOG protein Stu2 is regulated by acetylation. 2022 , 18, e1010358	0
324	The PROSCOOP10 gene encodes two extracellular hydroxylated peptides and impacts flowering time in Arabidopsis.	O
323	Phylogeny and adaptative evolution to chemosynthetic habitat in barnacle (Cirripedia: Thoracica) revealed by mitogenomes. 9,	0
322	Lumateperone Interact with S-Protein of Ebola Virus and TIM-1 of Human Cell Membrane: Insights from Computational Studies. 2022 , 12, 8820	O
321	Naturally occurring Neisseria gonorrhoeae can have large deletions in housekeeping gene abcZ, making them untypable with multilocus sequence typing. 2022 , 8,	0
320	Characterization of TelE, an LXG effector of Streptococcus gallolyticus, antagonized by a non-canonical immunity protein.	O

319	Multi-spectroscopic, molecular docking and molecular dynamic simulation evaluation of hydroxychloroquine sulfate interaction with caseins and whey proteins. 2022 , 120460	О
318	Homology Modeling Epitopes of Kirsten Rat Sarcoma (KRAS) G12D, G12V and G12R as Pancreatic Ductal Adenocarcinoma Vaccine Candidates.	O
317	Peptides derived from hookworm anti-inflammatory proteins suppress inducible colitis in mice and inflammatory cytokine production by human cells. 9,	О
316	Two novel mutations in ALDH18A1 and SPG11 gene found by whole-exome sequencing in spastic paraplegia disease patients in Iran. 2022 , 20, e30	O
315	Two cooperative binding sites sensitize PI(4,5)P 2 recognition by the tubby domain. 2022, 8,	О
314	Insilico Analysis of pathogenic genes as a major rescue of Candida albicans.	O
313	The design of cell-selective tryptophan and arginine-rich antimicrobial peptides by introducing hydrophilic uncharged residues. 2022 ,	2
312	Bioinformatics Analysis to Designing a Multi-epitope-based Peptide Vaccine Combat Leishmania major. 2022 , 16, 430-446	O
311	Sirtuin Evolution at the Dawn of Animal Life. 2022 , 39,	2
310	Simulated Docking Predicts Putative Channels for the Transport of Long-Chain Fatty Acids in Vibrio cholerae. 2022 , 12, 1269	Ο
309	First generation of multifunctional peptides derived from latarcin-3a from Lachesana tarabaevi spider toxin. 13,	0
308	In silico analyses of Wnt1 nsSNPs reveal structurally destabilizing variants, altered interactions with Frizzled receptors and its deregulation in tumorigenesis. 2022 , 12,	0
307	Cation ATPase (ATP4) Orthologue Replacement in the Malaria Parasite Plasmodium knowlesi Reveals Species-Specific Responses to ATP4-Targeting Drugs.	1
306	Germline gain-of-function MMP11 variant results in an aggressive form of colorectal cancer.	O
305	Sappanone A ameliorates acetaminophen-induced acute liver injury in mice. 2022, 480, 153336	1
304	Opposing regulation of METTL11A by its family members METTL11B and METTL13.	1
303	Computational modeling of TP63-TP53 interaction and rational design of inhibitors: Implications for therapeutics.	О
302	Machine learning-assisted elucidation of CD81-CD44 interactions in promoting cancer stemness and extracellular vesicle integrity. 11,	1

301	Potential antiviral peptides against the nucleoprotein of SARS-CoV-2.	0
300	A SPX domain vacuolar transporter links phosphate sensing to homeostasis in Arabidopsis. 2022 , 15, 1590-1601	O
299	NHA1 is a cation/proton antiporter essential for the water-conserving functions of the rectal complex in Tribolium castaneum.	О
298	Evaluating the role of trypsin in silk degumming: An in silico approach. 2022 , 359, 35-47	1
297	Data analysis and modeling of small-angle neutron scattering data with contrast variation from bio-macromolecular complexes. 2022 ,	О
296	In silico investigation of the role of vitamins in cancer therapy through inhibition of MCM7 oncoprotein. 2022 , 12, 31004-31015	O
295	Directed Evolution of Laccase for Improved Thermal Stability Facilitated by Droplet-Based Microfluidic Screening System. 2022 , 70, 13700-13708	1
294	Acetylenotrophic and Diazotrophic Bradyrhizobium sp. Strain I71 from TCE-Contaminated Soils.	Ο
293	AgeMTPT, a Catalyst for Peptide N-Terminal Modification.	0
292	Genomic distribution of signal transducer and activator of transcription (STAT) family in colorectal cancer.	0
291	Herpes simplex virus 1 protein pUL21 alters ceramide metabolism by activating the inter-organelle transport protein CERT. 2022 , 102589	1
2 90	Identification and molecular evolution of the La and LARP genes in 16 plant species: A focus on the Gossypium hirsutum. 2022 ,	O
289	Bee-safe peptidomimetic acaricides achieved by comparative genomics. 2022 , 12,	О
288	A Missense Variant in COMT Associated with Hearing Loss among Young Adults: The National Longitudinal Study of Adolescent to Adult Health (Add Health). 2022 , 10, 2756	O
287	Broad Antiviral Effects of Echinacea purpurea against SARS-CoV-2 Variants of Concern and Potential Mechanism of Action. 2022 , 10, 2145	1
286	The RNA repair proteins RtcAB regulate transcription activator RtcR via its CRISPR-associated Rossmann fold domain 2022 , 105425	O
285	Genetic diversity in the transmission-blocking vaccine candidate Plasmodium vivax gametocyte protein Pvs230 from the ChinaMyanmar border area and central Myanmar. 2022 , 15,	О
284	From Genome Mining to Protein Engineering: A Structural Bioinformatics Route. 2023 , 79-94	O

283	Role of NS2 specific RNA binding and phosphorylation in liquid I quid phase separation and virus assembly.	1
282	Genomic landscape of drug response reveals mediators of anthelmintic resistance. 2022 , 41, 111522	O
281	Leptospira borgpetersenii Leucine-Rich Repeat Proteins and Derived Peptides in an Indirect ELISA Development for the Diagnosis of Canine Leptospiral Infections. 2022 , 7, 311	O
280	Comprehensive Genome-Wide Analysis and Expression Pattern Profiling of the SlHVA22 Gene Family Unravels Their Likely Involvement in the Abiotic Stress Adaptation of Tomato. 2022 , 23, 12222	1
279	A Non-Canonical Teleost NK-Lysin: Antimicrobial Activity via Multiple Mechanisms. 2022, 23, 12722	O
278	Dp71 Point Mutations Induce Protein Aggregation, Loss of Nuclear Lamina Integrity and Impaired Braf35 and Ibraf Function in Neuronal Cells. 2022 , 23, 11876	O
277	Immunoinformatics-Based Identification of B and T Cell Epitopes in RNA-Dependent RNA Polymerase of SARS-CoV-2. 2022 , 10, 1660	1
276	Amino acid substitution in CAPRICE (CPC) protein affects its cell-to-cell movement in the root epidermis of Arabidopsis thaliana.	1
275	In silico detection of Cucurbitacin-E on antioxidant enzymes of model organism Galleria mellonella L. (Lepidoptera: Pyralidae) and variation of antioxidant enzyme activities and lipid peroxidation in treated larvae. 2022 , 11,	1
274	Tick-borne encephalitis virus capsid protein induces translational shut-off as revealed by its structural-biological analysis. 2022 , 102585	O
273	Paraquat is an agonist of STIM1 and increases intracellular calcium levels. 2022, 5,	O
272	An inducible amphipathic Helix mediates subcellular targeting and membrane binding of RPE65. 2023 , 6, e202201546	О
271	Molecular characteristics of a coxsackievirus A12 strain in Zhejiang of China, 2019. 2022 , 19,	o
270	Evaluation of a Novel Synthetic Peptide Derived from Cytolytic Mycotoxin Candidalysin. 2022 , 14, 696	O
269	The antimicrobial peptide Magainin-2 interacts with BamA impairing folding of E. coli membrane proteins. 10,	0
268	Thoroughly review the recent progresses in improving O/W interfacial properties of proteins through various strategies. 9,	O
267	Identification and characterization of alternative sites and molecular probes for SARS-CoV-2 target proteins. 10,	0
266	Study on internal structure of casein micelles in reconstituted skim milk powder. 2022,	O

265	Proteins from Thermophilic Thermus thermophilus Often Do Not Fold Correctly in a Mesophilic Expression System Such as Escherichia coli. 2022 , 7, 37797-37806	О
264	KIF1A novel frameshift variant p.(Ser887Profs*64) exhibits clinical heterogeneity in a Pakistani family with Hereditary Sensory and Autonomic Neuropathy Type IIC. 1-17	O
263	The enzymatic and neurochemical outcomes of a mutation in Mexican cavefish MAO reveal teleost-specific aspects of brain monoamine homeostasis.	О
262	Exome sequencing identified five novel USH2A variants in Korean patients with retinitis pigmentosa. 1-8	O
261	Crystal Structure and Biochemical Analysis of a Cytochrome P450 CYP101D5 from Sphingomonas echinoides. 2022 , 23, 13317	0
2 60	Emulation of the structure of the Saposin protein fold by a lung surfactant peptide construct of surfactant Protein B. 2022 , 17, e0276787	О
259	BefA, a microbiota-secreted membrane disrupter, disseminates to the pancreas and increases Itell mass. 2022 , 34, 1779-1791.e9	0
258	Sequence driven interaction of amino acids in de-novo designed peptides determines c-Myc G-quadruplex unfolding inducing apoptosis in cancer cells. 2022 , 130267	О
257	Full opening of helix bundle crossing does not lead to NaK channel activation. 2022, 154,	1
256	The interplay between MMP-12 and t-PA in the brain after ischemic stroke. 2022 , 161, 105436	О
255	Comprehensive in silico analysis of Phospholipase D gene family in economically important orchids. 2022 , 151, 655-666	0
254	Integration of spectroscopic and computational data to analyze protein structure, function, folding, and dynamics. 2023 , 483-502	О
253	Combining enhanced sampling and deep learning dimensionality reduction for the study of the heat shock protein B8 and its pathological mutant K141E. 2022 , 12, 31996-32011	0
252	In-silico designing of an inhibitor against mTOR FRB domain: Therapeutic implications against breast cancer. 2022 , 10, 1016-1023	О
251	Functional Characterization and Development of Novel Human Kinase Insert Domain Receptor Chimeric Antigen Receptor T-cells for Immunotherapy of Non-Small Cell Lung Cancer. 2022 , 106331	0
250	A requirement for Krppel Like Factor-4 in the maintenance of endothelial cell quiescence. 10,	О
249	Targeting Acanthamoeba proteins interaction with flavonoids of Propolis extract by in vitro and in silico studies for promising therapeutic effects. 11, 1274	О
248	Towards developing resistance to chickpea chlorotic dwarf virus through CRISPR/Cas9-mediated gene editing using multiplexed gRNAs.	1

247	In silico analyses and design of chimeric proteins containing epitopes of Bartonella henselae antigens for the control of cat scratch disease.	0
246	Two new Scianna variants causing loss of high prevalence antigens: ERMAP ´model and 3D analysis of the antigens.	O
245	Cyclin Dependent kinase 5 regulates cPLA2 activity and neuroinflammation in Parkinson disease. ENE	URO.0180-22.202
244	CRISPR/Cas-mediated knockdown of vacuolar invertase gene expression lowers the cold-induced sweetening in potatoes. 2022 , 256,	O
243	Cryo-EM structure of the agonist-bound Hsp90-XAP2-AHR cytosolic complex. 2022, 13,	1
242	Computer-Aided Multi-Epitope based Vaccine Design against Monkeypox Virus Surface Protein A30L: An Immunoinformatics Approach.	o
241	Identification of nuclear pore complexes (NPCs) and revealed outer-ring component BnHOS1 related to cold tolerance in B. napus. 2022 ,	0
240	An Integrated Protein Structure Fitness Scoring Approach for Identifying Native-Like Model Structures. 2022 ,	O
239	Comprehensive Genome-Wide Analysis and Expression Pattern Profiling of PLATZ Gene Family Members in Solanum Lycopersicum L. under Multiple Abiotic Stresses. 2022 , 11, 3112	О
238	Comparative computational study to augment UbiA prenyltransferases inherent in purple photosynthetic bacteria cultured from mangrove microbial mats in Qatar for coenzyme Q10 biosynthesis 2022 , 36, e00775	O
237	Pathogenic variants of the GNAS gene introduce an abnormal amino acid sequence in the B strand/B helix of GsAcausing pseudohypoparathyroidism type 1A and pseudopseudohypoparathyroidism in two unrelated Japanese families. 2022 , 17, 101637	0
236	Dissection of Besnoitia besnoiti intermediate host life cycle stages: From morphology to gene expression. 2022 , 18, e1010955	1
235	Transcriptional analysis in bacteriophage Fc02 of Pseudomonas aeruginosa revealed two overlapping genes with exclusion activity.	0
234	A Zika virus-specific IgM elicited in pregnancy exhibits ultrapotent neutralization. 2022,	o
233	An agnostic analysis of the human AlphaFold2 proteome using local protein conformations. 2022,	1
232	Designing multi-epitope monkeypox virus-specific vaccine using immunoinformatics approach. 2023 , 16, 107-116	1
231	Design of a chimeric protein composed of FimH, FyuA and CNF-1 virulence factors from uropathogenic Escherichia coli and evaluation its biological activity and immunogenicity in vitro and in vivo. 2023 , 174, 105920	0
230	Design of robust malate dehydrogenases by assembly of motifs of halophilic and thermophilic enzyme based on interaction network. 2023 , 190, 108758	O

229	SKAP2 Modular Organization Differently Recognizes SRC Kinases Depending on Their Activation Status and Localization. 2023 , 22, 100451	О
228	The prothoracicotropic hormone (PTTH) of Rhodnius prolixus (Hemiptera) is noggin-like: Molecular characterisation, functional analysis and evolutionary implications. 2023 , 332, 114184	O
227	Structure-based virtual screening to identify potential lipase inhibitors to reduce lipid storage in Wolman disorder. 2022 ,	О
226	An amino acid transporter AAT1 plays a pivotal role in chloroquine resistance evolution in malaria parasites.	1
225	Immunophilin CYN28 is required for accumulation of photosystem II and thylakoid FtsH protease in Chlamydomonas.	О
224	The Effect of the Ala16Val Mutation on the Secondary Structure of the Manganese Superoxide Dismutase Mitochondrial Targeting Sequence. 2022 , 11, 2348	O
223	Poly ADP-ribosylation of SET8 leads to aberrant H4K20 methylation in mammalian nuclear genome. 2022 , 5,	О
222	Evolution of Benzimidazole Resistance Caused by Multiple Double Mutations of ETubulin in Corynespora cassiicola. 2022 , 70, 15046-15056	O
221	Anopheles gambiae Trehalase Inhibitors for Malaria Vector Control: A Molecular Docking and Molecular Dynamics Study. 2022 , 13, 1070	О
220	A lysosomal lipid transport pathway that enables cell survival under choline limitation.	1
219	Prognostic correlation of NOTCH1 and SF3B1 mutations with chromosomal abnormalities in chronic lymphocytic leukemia patients.	0
218	The GGDEF-EAL protein CdgB from Azospirillum baldaniorum Sp245, is a dual function enzyme with potential polar localization. 2022 , 17, e0278036	O
217	Inhibiting a promiscuous GPCR: iterative discovery of bitter taste receptor ligands.	О
216	Tcte1knockout influence on energy chain transportation, apoptosis and spermatogenesis $\mbox{\ensuremath{\square}}$ implications for male infertility.	O
215	DeepHomo2.0: improved proteinprotein contact prediction of homodimers by transformer-enhanced deep learning.	О
214	Bacterial production and biophysical characterization of a hard-to-fold scFv against myeloid leukemia cell surface marker, IL-1RAP.	O
213	MeGATAs, functional generalists in interactions between cassava growth and development, and abiotic stresses.	О
212	A likely HOXC4 predisposition variant for Chiari malformations. 2022 , 1-9	1

211	Research progress on unique paratope structure, antigen binding modes, and systematic mutagenesis strategies of single-domain antibodies. 13,	0
210	Classical EhlersDanlos syndrome with severe kyphoscoliosis due to a novel pathogenic variant of COL5A2. 2022 , 10,	O
209	Exploring B and T-cell epitopes for constructing a Novel Multiepitope vaccine to combat emerging Monkeypox infection: A Reverse Vaccinology approach.	0
208	Improving automatic GO annotation with semantic similarity. 2022 , 23,	O
207	ModelCIF: An extension of PDBx/mmCIF data representation for computed structure models.	0
206	SEC14-GOLD protein PATELLIN2 binds IRON-REGULATED TRANSPORTER1 linking root iron uptake to vitamin E.	0
205	Recurrent germline variant in ATM associated with familial myeloproliferative neoplasms.	Ο
204	The Gln15Arg mutation in the transcriptional factor PALM1 produces multifoliate alfalfa.	Ο
203	An Alternative Splicing Variant of the Mixed-Lineage Leukemia 5 Protein Is a Cellular Adhesion Receptor for ScaA of Orientia tsutsugamushi.	0
202	Proteomics approaches: A review regarding an importance of proteome analyses in understanding the pathogens and diseases. 9,	Ο
201	In silico analysis of peroxidase from Luffa acutangula. 2023 , 13,	0
200	Light Boosts the Activity of Novel LPMO from Aspergillus fumigatus Leading to Oxidative Cleavage of Cellulose and Hemicellulose. 2022 , 10, 16969-16984	1
199	A pH-sensitive switch activates virulence inSalmonella.	Ο
198	Customized chitooligosaccharide productionBontrolling their length via engineering of rhizobial chitin synthases and the choice of expression system. 10,	Ο
197	Molecular Analysis and Sex-specific Response of the Hepcidin Gene in Yellow Perch (Perca Flavescens) Following Lipopolysaccharide Challenge.	Ο
196	Iron Acquisition Proteins of Pseudomonas aeruginosa as Potential Vaccine Targets: In Silico Analysis and In Vivo Evaluation of Protective Efficacy of the Hemophore HasAp. 2023 , 11, 28	O
195	Molecular dynamics simulations reveal membrane lipid interactions of the full-length lymphocyte specific kinase (Lck). 2022 , 12,	0
194	A novel peptide isolated from Catla skin collagen acts as a self-assembling scaffold promoting nucleation of calcium-deficient hydroxyapatite nanocrystals.	O

193	Combination of Docking-Based and Pharmacophore-Based Virtual Screening Identifies Novel Agonists That Target the Urotensin Receptor. 2022 , 27, 8692	O
192	An ELF4 hypomorphic variant results in NK cell deficiency. 2022, 7,	O
191	Exploring different computational approaches for effective diagnosis of breast cancer. 2022,	O
190	Cell-Permeable PROTAC Degraders against KEAP1 Efficiently Suppress Hepatic Stellate Cell Activation through the Antioxidant and Anti-Inflammatory Pathway.	O
189	First record of Mordellistena semiferruginea (Coleoptera: Mordellidae) in Italy and analysis of intraspecific variation in the COI gene. 2022 , 1-9	O
188	Expression and functional characterization of odorant-binding protein 2 in the predatory mite Neoseiulus barkeri.	O
187	Identification of antibody against wingless-type MMTV integration site family member 7B as a biliary cancer tumor marker. 2022 , 49,	O
186	The PROSCOOP10 Gene Encodes Two Extracellular Hydroxylated Peptides and Impacts Flowering Time in Arabidopsis. 2022 , 11, 3554	O
185	Genome-wide survey of catalase genes in Brassica rapa, Brassica oleracea, and Brassica napus: identification, characterization, molecular evolution, and expression profiling of BnCATs in response to salt and cadmium stress.	O
184	Human mutations inSLITRK3implicated in GABAergic synapse development in mice.	O
183	A genetic disorder reveals a hematopoietic stem cell regulatory network co-opted in leukemia.	O
182	Correlation analysis of European Sea Bass (Dicentrarchus labrax) Growth Hormone (GH) Gene and Growth Traits.	O
181	Functional Divergence of the N-Lobe and C-Lobe of Transferrin Gene in Pungitius sinensis (Amur Stickleback). 2022 , 12, 3458	O
180	Decreased echinocandin susceptibility in Candida parapsilosis causing candidemia and emergence of a pan-echinocandin resistant case in China. 2023 , 12,	O
179	Structural and functional analyses of GH51 alpha-L-arabinofuranosidase of Geobacillus vulcani GS90 reveal crucial residues for catalytic activity and thermostability.	1
178	Bioinformatic evaluation of the substrate specificity exhibited by the highly thermostable esterase EstDZ3.	O
177	Proteomic profiling reveals the molecular control of oocyte maturation. 2022, 100481	O
176	Characterisation of Macrophage Inhibitory Factor-2 (MIF-2) in Haemonchus contortus and Teladorsagia circumcincta. 2022 , 2, 338-349	1

175	Extracellular CIRP dysregulates macrophage bacterial phagocytosis in sepsis.	0
174	Structure and host specificity of Staphylococcus epidermidis bacteriophage Andhra. 2022, 8,	1
173	An apicomplexan bromodomain, TgBDP1 associates with diverse epigenetic factors to regulate essential transcriptional processes in Toxoplasma gondii	О
172	Molecular evolution of the ependymin-related gene epdl2 in African weakly electric fish.	O
171	New Glycosyltransferases in Panax notoginseng Perfect Main Ginsenosides Biosynthetic Pathways.	О
170	Computational analysis of missense variant CYP4F2*3 (V433M) in association with human CYP4F2 dysfunction: A functional and structural impact.	O
169	Identification and In Silico Analysis of a Homozygous Nonsense Variant in TGM1 Gene Segregating with Congenital Ichthyosis in a Consanguineous Family. 2023 , 59, 103	О
168	A novel consensus-based computational pipeline for screening of antibody therapeutics for efficacy against SARS-CoV-2 variants of concern including Omicron variant.	0
167	In-silico design and evaluation of an epitope-based serotype-independent promising vaccine candidate for highly cross-reactive regions of pneumococcal surface protein A. 2023 , 21,	0
166	In silico design of a promiscuous chimeric multi-epitope vaccine against Mycobacterium tuberculosis. 2023 ,	О
165	Cross-variant proof predictive vaccine design based on SARS-CoV-2 spike protein using immunoinformatics approach. 2023 , 12,	О
164	Identifying and characterising Thrap3, Bclaf1 and Erh interactions using cross-linking mass spectrometry. 6, 260	O
163	Modelling eNvironment for Isoforms (MoNvIso): A general platform to predict structural determinants of protein isoforms in genetic diseases. 10,	0
162	Therapeutic target mapping from the genome of Kingella negevensis and biophysical inhibition assessment through PNP synthase binding with traditional medicinal compounds.	o
161	Probing the Interactions of LRP1 Ectodomain-Derived Peptides with Fibrillar Tau Protein and Its Impact on Cellular Internalization. 2023 , 13, 853	0
160	The N-terminal hydrophobicity modulates a distal structural domain conformation of zearalenone lacton hydrolase and its application in protein engineering. 2023 , 110195	O
159	The DEAD-box protein Dbp6 is an ATPase and RNA annealase interacting with the peptidyl transferase center (PTC) of the ribosome.	О
158	Type I interferons link skin-associated dysbiotic commensal bacteria to pathogenic inflammation and angiogenesis in rosacea.	O

157	Analysis of tafazzin and deoxyribonuclease 1 like 1 transcripts and X chromosome sequencing in the evaluation of the effect of mosaicism in the TAZ gene on phenotypes in a family affected by Barth syndrome. 2023 , 826, 111812	О
156	The Association between Genetic Variations and Morphology-based Brain Networks Changes in Alzheimer's Disease.	O
155	Conformational and mechanical stability of the isolated large subunit of membrane-bound [NiFe]-hydrogenase from Cupriavidus necator. 13,	0
154	Evolutionary analysis of p38 stress-activated kinases in unicellular relatives of animals suggests an ancestral function in osmotic stress. 2023 , 13,	O
153	Resolving the challenge of insoluble production of mature human growth differentiation factor 9 protein (GDF9) in E. coli using bicistronic expression with thioredoxin. 2023 , 123225	О
152	Employing non-targeted interactomics approach and subcellular fractionation to increase our understanding of the ghost proteome. 2023 , 105943	O
151	Proteogenomic Approaches to Understand Gene Mutations and Protein Structural Alterations in Colon Cancer. 2023 , 3, 11-29	О
150	Large-scale analyses of angiosperm Flowering Locus T genes reveal duplication and functional divergence in monocots. 13,	O
149	Developing a multiepitope vaccine for the prevention of SARS-CoV-2 and monkeypox virus co-infection: A reverse vaccinology analysis. 2023 , 115, 109728	1
148	Characterization of a VRC01-like antibody lineage with immature VL from an HIV-1 infected Chinese donor. 2023 , 154, 11-23	O
147	Molecular characterization and functional analysis of interferon regulatory factor-4 in the Red Claw Crayfish (Cherax quadricarinatus). 2023 , 28, 101456	О
146	Trophoblast-specific knockdown of CSPG4 expression causes pregnancy complications with poor placentation in mice. 2023 , 23, 100731	O
145	Effect of tryptophan mutation on the structure of LOV1 domain of phototropin1 protein of Ostreococcus tauri: A combined molecular dynamics simulation and biophysical approach. 2023 , 1867, 130304	О
144	A Novel De Novo Frameshift Pathogenic Variant in the FAM111B Resulting in Progressive Osseous Heteroplasia Phenotype.	O
143	In Silico Structural Analysis Predicting the Pathogenicity of PLP1 Mutations in Multiple Sclerosis. 2023 , 13, 42	1
142	Haploinsufficiency of EXT1 and Heparan Sulphate Deficiency Associated with Hereditary Multiple Exostoses in a Pakistani Family. 2023 , 59, 100	O
141	Comparative genomics and integrated system biology approach unveiled undirected phylogeny patterns, mutational hot spots, functional patterns and molecule repurposing for monkey pox virus.	0
140	Functional, and phylogenetic analysis of maleylacetate reductase of Pseudomonas sp strain PNPG3: An in-silico approach. 2022 , 10, 1331-1343	O

139	Functional Characterization of the Cystine-Rich-Receptor-like Kinases (CRKs) and Their Expression Response to Sclerotinia sclerotiorum and Abiotic Stresses in Brassica napus. 2023 , 24, 511	O
138	Tecovirimat as a Potential Bioavailable inhibitor against MPXVgp158 Established through Molecular Dynamic Simulations and Docking Studies. 2022 , 16, 3168-3178	O
137	Dimerisation of the Yeast K+ Translocation Protein Trk1 Depends on the K+ Concentration. 2023 , 24, 398	0
136	Ancestral reconstruction reveals catalytic inactivation of activation-induced cytidine deaminase concomitant with cold water adaption in the Gadiformes bony fish. 2022 , 20,	O
135	Herbivory-inducible lipid-transfer proteins (LTPs) of Cicer arietinum as potential human allergens. 1-17	0
134	Cell-penetrating porcine single-chain antibodies (transbodies) to nonstructural protein 1[[NSP1]] of PRRSV inhibit the virus replication.	O
133	Improving DNA-Binding Protein Prediction Using Three-Part Sequence-Order Feature Extraction and a Deep Neural Network Algorithm.	0
132	In silico Structure Prediction, Molecular Docking, and Dynamic Simulation of Plasmodium falciparum AP2-I Transcription Factor. 2023 , 17, 117793222211496	O
131	Prediction of the tetramer protein complex interaction based on CNN and SVM. 14,	О
130	pH modulates the role of SP6 RNA polymerase in transcription process: an in silico study. 1-18	O
129	Molecular dynamics simulations depict structural motions of the whole human aryl hydrocarbon receptor influencing its binding of ligands and HSP90. 1-16	0
128	Novel Variants in MPV17, PRX, GJB1, and SACS Cause CharcotMariellooth and Spastic Ataxia of CharlevoixBaguenay Type Diseases. 2023 , 14, 328	O
127	Integrated multi-dimensional analysis highlights DHCR7 mutations involving in cholesterol biosynthesis and contributing therapy of gastric cancer. 2023 , 42,	0
126	The Oxidative Stress-Induced Hypothetical Protein PG_0686 in Porphyromonas gingivalis W83 Is a Novel Diguanylate Cyclase.	O
125	Bioinformatics analysis and consistency verification of a novel tuberculosis vaccine candidate HP13138PB. 14,	1
124	Cytomegalovirus breakthrough and resistance during letermovir prophylaxis.	Ο
123	Protective Efficacy of Anti-Hyr1p Monoclonal Antibody against Systemic Candidiasis Due to Multi-Drug-Resistant Candida auris. 2023 , 9, 103	O
122	Discovery of benzochromene derivatives first example with dual cytotoxic activity against the resistant cancer cell MCF-7/ADR and inhibitory effect of the P-glycoprotein expression levels. 2023 , 38,	1

121	Molecular Interactions of the Copper Chaperone Atx1 of Paracoccidioides brasiliensis with Fungal Proteins Suggest a Crosstalk between Iron and Copper Homeostasis. 2023 , 11, 248	0
120	Genome-Wide Identification of BTB Domain-Containing Gene Family in Grapevine (Vitis vinifera L.). 2023 , 13, 252	O
119	Jewel beetle opsin duplication and divergence is the mechanism for diverse spectral sensitivities.	0
118	State-of-the-art experimental and computational approaches to investigate structure, substrate recognition, and catalytic mechanism of enzymes. 2023 , 75-107	O
117	Crystal structure and biochemical analysis of acetylesterase (LgEstI) from Lactococcus garvieae. 2023 , 18, e0280988	0
116	Chemokine ReceptorsBtructure-Based Virtual Screening Assisted by Machine Learning. 2023, 15, 516	O
115	Prediction and Evaluation of Bioactive Properties of Cowpea Protein Hydrolysates. 2023, 2023, 1-12	0
114	Lymphocyte antigen 6K signaling to aurora kinase promotes advancement of the cell cycle and the growth of cancer cells, which is inhibited by LY6K-NSC243928 interaction. 2023 , 558, 216094	O
113	High-Risk Pedigree Study Identifies LRBA (rs62346982) as a Likely Predisposition Variant for Prostate Cancer. 2023 , 15, 2085	O
112	Orthogonal inducible control of Cas13 circuits enables programmable RNA regulation in mammalian cells.	O
111	In-Depth Occlusion of Dentinal Tubules and Rapid Remineralization of Demineralized Dentin Induced by Polyelectrolyte-Calcium Complexes.	O
110	Molecular Characterization of Dehydrin in Azraq Saltbush among Related Atriplex Species. 2023 , 12, 27	O
109	Antifungal activity of ginsenoside CK against Botrytis cinerea by targeting sterol 14Edemethylase cytochrome P450 (CYP51) and the application on cherry tomato preservation. 2023 , 199, 112294	0
108	Role of calcium sensor protein module CBL-CIPK in abiotic stress and light signaling responses in green algae. 2023 , 237, 124163	O
107	Bioengineering of air-filled protein nanoparticles by genetic and chemical functionalization. 2023 , 21,	O
106	The function of the phytoplasma effector SWP12 depends on the properties of two key amino acids. 2023 , 299, 103052	O
105	Novel pathogenic variants in the androgen receptor gene associated with androgen insensitivity syndrome identified through exome sequencing and in silico analysis. 2023 , 860, 147225	0
104	Chitosan targets PI3K/Akt/FoxO3a axis to up-regulate FAM172A and suppress MAPK/ERK pathway to exert anti-tumor effect in osteosarcoma. 2023 , 373, 110354	O

103	Modelling and Simulation of Proteins. 2021 , 394-411	О
102	Exploring AlphaFold2?s Performance on Predicting Amino Acid Side-Chain Conformations and Its Utility in Crystal Structure Determination of B318L Protein. 2023 , 24, 2740	O
101	Genome-wide analysis of Catalase gene family reveal insights into abiotic stress response mechanism in Brassica juncea and B. rapa 2023 , 330, 111620	O
100	Novel compound heterozygous missense variants in TOE1 gene associated with pontocerebellar hypoplasia type 7. 2023 , 862, 147250	O
99	Suppression of Cancer Cell Stemness and Drug Resistance via MYC Destabilization by Deubiquitinase USP45 Inhibition with a Natural Small Molecule. 2023 , 15, 930	0
98	On the interplay between lipids and asymmetric dynamics of an NBS degenerate ABC transporter. 2023 , 6,	O
97	Transcriptional analysis in bacteriophage Fc02 of Pseudomonas aeruginosa revealed two overlapping genes with exclusion activity. 14,	O
96	Systematic mapping of the conformational landscape and dynamism of soluble fibrinogen. 2023,	O
95	A novel high-prevalence antigen in the Lutheran system, LUGA (LU24), and an updated, full-length 3D BCAM model. 2023 , 63, 798-807	0
94	Identification of potential novel inhibitors against glutamine synthetase enzyme of Leishmania major by using computational tools. 1-9	O
93	Structural Insights into ATP-Sensitive Potassium Channel Mechanics: A Role of Intrinsically Disordered Regions. 2023 , 63, 1806-1818	0
92	Targeting Acanthamoeba proteins interaction with flavonoids of Propolis extract by in vitro and in silico studies for promising therapeutic effects. 11, 1274	O
91	Quality assessment of VHH models. 1-15	0
90	Discovery of a Potential Molluscicide Based on Protein PcRoo in Gill Cilia of Pomacea canaliculata.	O
89	Comprehensive classification of proteins based on structures that engage lipids by COMPOSEL. 2023 , 295, 106971	0
88	Rational design of HJH antimicrobial peptides to improve antimicrobial activity. 2023 , 83, 129176	O
87	In-silico methods for milk-derived bioactive peptide prediction. 2023, 137-162	0
86	In-silico drug design for the novel Karachi-NF001 strain of brain-eating amoeba: Naegleria fowleri. 10,	O

85	Genetic architecture of hippocampus subfields volumes in Alzheimer∃ disease.	0
84	Lipidation Alters the Structure and Hydration of Myristoylated Intrinsically Disordered Proteins. 2023 , 24, 1244-1257	О
83	Deep learning for reconstructing protein structures from cryo-EM density maps: Recent advances and future directions. 2023 , 79, 102536	0
82	Comparative Modeling and Analysis of Extremophilic D-Ala-D-Ala Carboxypeptidases. 2023 , 13, 328	О
81	LCN2-Fungal siderophore-iron binding and uptake leads to oxidative stress and cell death in hepatocellular carcinoma cell line HepG2. 1-20	0
80	Potent transmission-blocking monoclonal antibodies from naturally exposed individuals target a conserved epitope on Plasmodium falciparum Pfs230. 2023 , 56, 420-432.e7	O
79	Determination of protein conformation and orientation at buried solid/liquid interfaces. 2023 , 14, 2999-3009	1
78	Simultaneous membrane and RNA binding by tick-borne encephalitis virus capsid protein. 2023 , 19, e1011125	О
77	Discovery of DNA aptamers targeting SARS-CoV-2 nucleocapsid protein and protein-binding epitopes for label-free COVID-19 diagnostics. 2023 , 31, 731-743	0
76	SNP based analysis depicts phenotypic variability in heme oxygenase-1 protein. 2023,	O
75	Parallel expansion and divergence of an adhesin family in pathogenic yeasts. 2023, 223,	0
74	Structural organization of RDGB (retinal degeneration B), a multi-domain lipid transfer protein: a molecular modelling and simulation based approach. 1-15	O
73	Pyrazolones Potentiate Colistin Activity against MCR-1-Producing Resistant Bacteria: Computational and Microbiological Study. 2023 , 8, 8366-8376	0
72	Production of recombinant proteins including the B-cell epitopes of autolysin A of Staphylococcus aureus isolated from clinical sheep mastitis and their potential for vaccine development.	О
71	Molecular Dynamic Simulations Unravel the Underlying Impact of Missense Mutation in Autoimmunity Gene PTPN22 on Predisposition to Rheumatoid Arthritis. 2023 , 43, 121-132	Ο
70	Dissecting Phenotype from Genotype with Clinical Isolates of SARS-CoV-2 First Wave Variants. 2023 , 15, 611	1
69	ModelCIF: An Extension of PDBx/mmCIF Data Representation for Computed Structure Models. 2023 , 168021	0
68	Machine Learning-based Modeling of Olfactory Receptors in their Inactive State: Human OR51E2 as a Case Study.	O

67	Uncovering the Interaction Interface Between Harpin (Hpa1) and Rice Aquaporin (OsPIP1;3) Through Protein Protein Docking: An In Silico Approach.	Ο
66	Immunoinformatics-aided design of a new multi-epitope vaccine adjuvanted with domain 4 of pneumolysin against Streptococcus pneumoniae strains. 2023 , 24,	O
65	The Mechanism of Action of SAAP-148 Antimicrobial Peptide as Studied with NMR and Molecular Dynamics Simulations. 2023 , 15, 761	0
64	In silico analysis of highly disordered human IRS1 protein 3D structure to uncover new target for Metformin to ameliorate diabetes.	O
63	An investigation of binding interactions of tumor-targeted peptide conjugated polyphenols with the kinase domain of ephrin B4 and B2 receptors.	О
62	Discovery of 2-Aminopyrimidines as Potent Agonists for the Bitter Taste Receptor TAS2R14. 2023 , 66, 3499-3521	Ο
61	The molecular mechanism of Y473 phosphorylation of UGDH relieves the inhibition effect of UDP-glucose on HuR. 2023 , 25, 8714-8724	0
60	MTORC2 is a physiological hydrophobic motif kinase of S6 Kinase 1. 2023 , 1870, 119449	Ο
59	Spinocerebellar ataxia 38: structure-function analysis shows ELOVL5 G230V is proteotoxic, conformationally altered and a mutational hotspot.	0
58	E-2 Glycoprotein Structural Variations Analysed within the CSFV 2.2. Genogroup in a ¶losed Grid Sampling Study from Meghalaya, India. 2023 , 14, 343-354	Ο
57	An X-Domain Phosphoinositide Phospholipase C (PI-PLC-like) of Trypanosoma brucei Has a Surface Localization and Is Essential for Proliferation. 2023 , 12, 386	0
56	Molecular cloning, characterization and expression profile of FLOWERING LOCUS T (FT) gene from Prunus armeniaca L 2023 , 155, 330-339	O
55	Modulated protein-sterol interactions drive oxysterol-induced impaired CXCR4 signalling.	0
54	Exploring microbial functional biodiversity at the protein family level from metagenomic sequence reads to annotated protein clusters. 3,	Ο
53	Urolithin A analog inhibits castration-resistant prostate cancer by targeting the androgen receptor and its variant, androgen receptor-variant 7.14,	0
52	Molecular architecture and dynamics of SARS-CoV-2 envelope by integrative modeling. 2023 , 31, 492-503.e7	0
51	Extracellular vesicles of Euryarchaeida: precursor to eukaryotic membrane trafficking.	0
50	The landscape of m1A modification and its posttranscriptional regulatory functions in primary neurons. 12,	Ο

49	Inferring B-cell derived T-cell receptor induced multi epitope-based vaccine candidate against enterovirus 71 (EV 71): A reverse vaccinology approach.	0
48	Identification and examination of nitrogen metabolic genes in Lelliottia amnigena PTJIIT1005 for their ability to perform nitrate remediation. 2023 , 24,	O
47	Structural and Dynamic Differences between Calreticulin Mutants Associated with Essential Thrombocythemia. 2023 , 13, 509	0
46	QSAR via multisite 时ynamics in the orphaned TSSK1B kinase. 2023 , 32,	Ο
45	Exploring Host-Binding Machineries of Mycobacteriophages with AlphaFold2. 2023, 97,	0
44	The Josephin domain (JD) containing proteins are predicted to bind to the same interactors: Implications for spinocerebellar ataxia type 3 (SCA3) studies using Drosophila melanogaster mutants. 16,	O
43	Lysine Methyltransferase EhPKMT2 Is Involved in the In Vitro Virulence of Entamoeba histolytica. 2023 , 12, 474	O
42	Spt6 directly interacts with Cdc73 and is required for Paf1 complex occupancy at active genes inSaccharomyces cerevisiae.	Ο
41	In silico investigation of a novel anti EGFR Scfv ${\rm I\!L}$ 24 fusion protein induces apoptosis in malignant cells.	0
40	MERS virus spike protein HTL-epitopes selection and multi-epitope vaccine design using computational biology. 1-16	O
39	In Silico Analysis of a Candidate Multi-epitope Peptide Vaccine Against Human Brucellosis.	0
38	Structural analysis and molecular dynamics simulation studies of HIV-1 antisense protein predict its potential role in HIV replication and pathogenesis. 14,	O
37	Screening and Identification of Nanobody against Inhibin	0
36	Evaluation of SNPs from human IGFBP6 associated with gene expression: an in-silico study. 1-13	O
35	Homology Modeling in the Twilight Zone: Improved Accuracy by Sequence Space Analysis. 2023 , 1-23	0
34	Extracellular vesicles of Euryarchaeida: precursor to eukaryotic membrane trafficking.	O
33	Targeting Acanthamoeba proteins interaction with flavonoids of Propolis extract by in vitro and in silico studies for promising therapeutic effects. 11, 1274	0
32	Combining Phage Display Technology with In Silico -Designed Epitope Vaccine to Elicit Robust Antibody Responses against Emerging Pathogen Tilapia Lake Virus.	O

31	Cheminformatics-Based Study Identifies Potential Ebola VP40 Inhibitors. 2023, 24, 6298	1
30	High-level production of nervonic acid in the oleaginous yeastYarrowia lipolyticaby systematic metabolic engineering.	0
29	RND pumps across the genus Acinetobacter: AdelJK is the universal efflux pump. 2023, 9,	0
28	Protein Structure Prediction: Challenges, Advances, and the Shift of Research Paradigms. 2023,	Ο
27	The Trypanosoma brucei MISP family of invariant proteins is co-expressed with BARP as triple helical bundle structures on the surface of salivary gland forms, but is dispensable for parasite development within the tsetse vector. 2023 , 19, e1011269	0
26	Omics-assisted characterization of two-component system genes from Gossypium Raimondii in response to salinity and molecular interaction with abscisic acid. 14,	O
25	Comparative In Silico Analysis and Functional Characterization of TANK-Binding Kinase 1 B inding Protein 1. 2023 , 17, 117793222311648	0
24	Inhibiting a promiscuous GPCR: iterative discovery of bitter taste receptor ligands. 2023, 80,	О
23	Cannabis monoterpene synthases: evaluating structure f unction relationships.	0
22	Intrinsically Disordered Kiwellin Protein-Like Effectors Target Plant Chloroplasts and are Extensively Present in Rust Fungi.	O
21	Circuit Topology Approach for the Comparative Analysis of Intrinsically Disordered Proteins.	О
20	Cell-penetrating porcine single-chain antibodies (transbodies) against nonstructural protein 1 (NSP1 porcine reproductive and respiratory syndrome virus inhibit virus replication. 2023 , 168,	O
19	The IgG4 hinge with CD28 transmembrane domain improves VHH-based CAR T cells targeting a membrane-distal epitope of GPC1 in pancreatic cancer. 2023 , 14,	0
18	The Yeast Permease Agp2 Senses Cycloheximide and Undergoes Degradation That Requires the Small Protein Brp1-Cellular Fate of Agp2 in Response to Cycloheximide. 2023 , 24, 6975	O
17	Enhanced Thermostability and Catalytic Activity of Streptomyces mobaraenesis Transglutaminase by Rationally Engineering Its Flexible Regions.	0
16	Genome-wide identification and expression profiling of snakin/GASA genes under drought stress in barley (Hordeum vulgare L.). 2023 , 13,	О
15	Dimerisation of European robin cryptochrome 4a.	О
14	The role of ETFS amino acids on the stability and inhibition of p53-MDM2 complex of anticancer p53-derivatives peptides: Density functional theory and molecular docking studies. 2023 , 122, 108472	О

13	Genome-wide in silico analysis leads to identification of deleterious L290V mutation in RBBP5 gene in Bos indicus. 1-9	0
12	Elucidating the Potential Inhibitor against Type 2 Diabetes Mellitus Associated Gene of GLUT4. 2023 , 13, 660	O
11	Identification of common candidate genes and pathways for Spina Bifida and Wilm⊞ Tumor using an integrative bioinformatics analysis. 1-16	О
10	Computational Insights on the Impact of Allotypic Variation and Dimerization on Erap1 and Erap2 Structures Running Title: Structural Analysis of Erap1 and Erap2 Allotype Dimers.	O
9	An SPNS1-dependent lysosomal lipid transport pathway that enables cell survival under choline limitation. 2023 , 9,	0
8	Production of recombinant proteins including the B-cell epitopes of autolysin A of Staphylococcus aureus isolated from clinical sheep mastitis and their potential for vaccine development.	O
7	Reinventing Therapeutic Proteins: Mining a Treasure of New Therapies. 2023 , 3, 72-94	0
6	Discovery of a highly efficient TylF methyltransferase via random mutagenesis for improving tylosin production. 2023 ,	O
5	Resistance screening and in silico characterization of cloned novel RGA from multi-race resistant lentil germplasm against Fusarium wilt (Fusarium oxysporum f. sp. lentis). 14,	0
4	Effective holistic characterization of small molecule effects using heterogeneous biological networks. 14,	O
3	A Candidate Antigen of the Recombinant Membrane Protein Derived from the Porcine Deltacoronavirus Synthetic Gene to Detect Seropositive Pigs. 2023 , 15, 1049	0
2	An aquatic virus exploits the IL6-STAT3-HSP90 signaling axis to promote viral entry. 2023 , 19, e1011320	O
1	Anticandidal Activity and Mechanism of Action of Several Cationic Chimeric Antimicrobial Peptides. 2023 , 29,	0